Vol. 58 JULY, 1954 No. 7

THE JOURNAL OF PHYSICAL CHEMISTRY

(Registered in U. S. Patent Office)

SYMPOSIUM ON HYDRATION OF AQUEOUS IONS, LOS ANGELES, CALIF., MARCH, 1953

Wendell M. Latimer: Introductory Remarks: Symposium on Hydration of Aqueous Ions 513
Arthur W. Adamson: Diffusion and Self-diffusion of Electrolytes 514
Henry Taube: Use of Oxygen Isotope Effects in Study of Hydration of Ions 523
R. E. Powell: The Entropies of Aqueous Ions 528

* * * * *

J. S. Stanley: The Effect of Paraffin Chain Salts on the Charge on Textile Fibers 533
Sterling E. Voltz and M. Wesley Rigg: A Dielectric Study of the Autoxidation of Ethyl Sorbate 537
Kōzō Shinoda: The Critical Micelle Concentration of Soap Mixtures (Two-Component Mixture) 541
Aubrey P. Altshuller: The Shapes of Particles from Dielectric Constant Studies of Suspensions 544
H. H. G. Jellinek and J. R. Urwin: Ultraviolet Absorption Spectra and Dissociation Constants of Picolinic, Isonicotinic Acids and their Amides 548
Victor J. Kehrer, Jr., and Henry Leidheiser, Jr.: The Catalytic Decomposition of Carbon Monoxide on Large Metallic Single Crystals 550
O. D. Bonner and Jane C. Moorefield: Ion Exchange in Mixed Solvents 555
W. J. Svirbely: Thermodynamic Data for the Zinc–Indium System Obtained from the Phase Diagram 557
R. M. Barrer and N. Mackenzie: Sorption by Attapulgite. I. Availability of Intracrystalline Channels 560
R. M. Barrer, N. Mackenzie and D. M. MacLeod: Sorption by Attapulgite. II. Selectivity Shown by Attapulgite, Sepiolite and Montmorillonite for *n*-Paraffins 568
NOTE: **Earl E. Bryant:** Potentiometric Determination of Formation Constants of Acetylacetonates by a Displacement Reaction 573
NOTE: **Leonard S. Levitt:** Extreme Pressures. I. A New Pressure-Volume Relationship 573
NOTE: **Alan Dobry:** Solubility of Cupric Stearate in Water and Benzene at 25° 576

The Journal of Physical Chemistry is being published monthly in 1954
Notes and Communications to the Editor will be considered for
publication in THIS JOURNAL

THE JOURNAL OF PHYSICAL CHEMISTRY

(Registered in U. S. Patent Office)

Published monthly by the American Chemical Society at 20th and Northampton Sts., Easton, Pa.

Entered as second-class matter at the Post Office at Easton, Pennsylvania.

The *Journal of Physical Chemistry* is devoted to the publication of selected symposia in the broad field of physical chemistry and to other contributed papers.

Manuscripts originating in the British Isles, Europe and Africa should be sent to F. C. Tompkins, The Faraday Society, 6 Gray's Inn Square, London W. C. 1, England.

Manuscripts originating elsewhere should be sent to W. Albert Noyes, Jr., Department of Chemistry, University of Rochester, Rochester 3, N. Y.

Correspondence regarding accepted copy, proofs and reprints should be directed to Assistant Editor, Allen D. Bliss, Department of Chemistry, Simmons College, 300 The Fenway, Boston 15, Mass.

Business Office: American Chemical Society, 1155 Sixteenth St. N. W., Washington 6, D. C.

Advertising Office: Reinhold Publishing Corporation, 430 Park Avenue, New York 22, N. Y.

Articles must be submitted in duplicate, typed and double spaced. They should have at the beginning a brief Abstract, in no case exceeding 300 words. Original drawings should accompany the manuscript. Lettering at the sides of graphs (black on white or blue) may be pencilled in, and will be typeset. Figures and tables should be held to a minimum consistent with adequate presentation of information. Photographs will not be printed on glossy paper except by special arrangement. All footnotes and references to the literature should be numbered consecutively and placed on the manuscript at the proper places. Initials of authors referred to in citations should be given. Nomenclature should conform to that used in *Chemical Abstracts*, mathematical characters marked for italic, Greek letters carefully made or annotated, and subscripts and superscripts clearly shown. Articles should be written as briefly as possible consistent with clarity and should avoid historical background unnecessary for specialists.

Symposium papers should be sent in all cases to Secretaries of Divisions sponsoring the symposium, who will be responsible for their transmittal to the Editor. The Secretary of the Division by agreement with the Editor will specify a time after which symposium papers cannot be accepted. The Editor reserves the right to refuse to publish symposium articles, for valid scientific reasons. Each symposium paper may not exceed four printed pages (about sixteen double spaced typewritten pages) in length except by prior arrangement with the Editor.

Remittances and orders for subscriptions and for single copies, notices of changes of address and new professional connections, and claims for missing numbers should be sent to the American Chemical Society, 1155 Sixteenth St., N. W., Washington 6, D. C. Changes of address for the *Journal of Physical Chemistry* must be received on or before the 30th of the preceding month.

Claims for missing numbers will not be allowed (1) if received more than sixty days from date of issue (because of delivery hazards, no claims can be honored from subscribers in Central Europe, Asia, or Pacific Islands other than Hawaii), (2), if loss was due to failure of notice of change of address to be received before the date specified in the preceding paragraph, or (3) if the reason for the claim is "missing from files."

Subscription Rates: to members of the American Chemical Society, $8.00 for 1 year, $15.00 for 2 years, $22.00 for 3 years; to nonmembers, $10.00 for 1 year, $18.00 for 2 years, $26.00 for 3 years. Postage free to countries in the Pan American Union; Canada, $0.40; all other countries, $1.20. Single copies, $1.25; foreign postage, $0.15; Canadian postage $0.05. Back issue rates (starting with Vol. 56): nonmember, $1.50 per issue, foreign postage $0.15, Canadian postage $0.05; $12.50 per volume, foreign postage $1.20, Canadian postage $0.40; special rates for A.C.S. members supplied on request.

THE JOURNAL OF
PHYSICAL CHEMISTRY

(Registered in U. S. Patent Office) (Copyright, 1954, by the American Chemical Society)

VOLUME 58 JULY 31, 1954 NUMBER 7

SYMPOSIUM ON HYDRATION OF AQUEOUS IONS. INTRODUCTORY REMARKS

BY WENDELL M. LATIMER

Department of Chemistry, University of California, Berkeley, Calif.

Received April 12, 1954

It is important to take an inventory, from time to time, of our information in a given field and today we are making such an inventory of our information on the nature of the hydration of aqueous ions. The Born cycle has enabled us to calculate the sum of the total hydration energies of pairs of positive and negative gaseous ions and also the differences in the energies of hydration of ions of like charge; but we do not know how to break down these sums and differences into absolute values. At present we can only give approximate answers to this problem.

It would be nice if we could make a theoretical calculation of the energy of interaction between an ion and the solvent water, but we do not know the dielectric constant of the water in the neighborhood of the ion and the calculations are uncertain whether we attempt to use the Born expression for the field energy of a charge in a continuous dielectric medium or attempt to calculate the energy of interaction of the charge with fixed dipoles.

In most cases we do not know how many water molecules are in the first hydration layer and also, how much additional water is held in outer layers. Thus, for example, we have only approximate values for the moles of water which move with an ion in electrical conductance or in diffusion.

In recent years we have obtained considerable information on the entropy changes involved in hydration. Since these entropy terms arise largely from the loss of entropy of the bound water, the values have given us some insight into the nature of the hydration process. We think we know the absolute partial molal entropies of the ions with considerable certainty. Hence in the case of the total entropy of hydration of a pair of positive and negative ions, we do know how the total entropy should be divided between the two ions. From the nature of the hydration process, this suggests that the energies of hydration should be divided in the same ratio as the entropies. At present this must be considered only a tentative theory.

There is one more problem which should be mentioned. When the charge on an ion is suddenly changed, as for example, the ejection of an electron from an iodide by the absorption of a photon, the resulting atom is left in an excited state because the bound water molecules do not have time to reorient themselves. What is the energy of this reorientation or relaxation? In the case of iodide the estimates of this quantity range from 4 to 70 kcal. This relaxation energy appears to be related to the activation energies in exchange reactions involving an electron transfer, as between Fe^{++} and Fe^{+++}. Today we do not have this answer.

In our symposium we are not going to get the answers to all of these problems. However, we are going to have a lot of evidence presented and I hope our discussion will stimulate work which will lead to eventual solutions of many of these problems.

THE DIFFUSION AND SELF-DIFFUSION OF ELECTROLYTES AND HYDRATION EFFECTS[1]

BY ARTHUR W. ADAMSON

Department of Chemistry of the University of Southern California, Los Angeles, Calif.

Received April 12, 1954

The existing theoretical explanations of the concentration dependence of the mean diffusion coefficients of electrolytes and of the self-diffusion coefficients of ions are examined in the light of current data. Inadequacies in the mathematical approximations made in the electrophoretic effect treatment of mean diffusion coefficients are discussed and it is shown that even after allowing for these, agreement with present data is poor. A possible additional effect, arising from the counter diffusion of solvent, is discussed. This second approach yields hydrodynamic radii for electrolytes which are quite large and, in concentrated solutions, tend to approach (as an upper limit) the atmosphere radius. The mathematical basis for the relaxation effect computed for the self-diffusion of ions is outlined. An alternative theory based on the absolute rate treatment of diffusion is presented. It is found, however, that the present self-diffusion data are insufficiently precise for adequate testing of limiting laws, and that in concentrated solutions, systematic differences appear to exist between the various experimental methods employed.

The appearance in recent years of self-diffusion data for ions in aqueous electrolyte solutions has added a new dimension to the field of electrolyte diffusion. In addition, the list of salts whose mean diffusion coefficients are known accurately has been greatly extended. These developments make it desirable to consider critically the bases upon which diffusional behavior may be related to the interaction of ions and solvent.

A certain dualism exists in the treatment of diffusion in binary or higher mixtures and at least two approaches have been used in relating diffusion coefficients to basic physical properties. On the one hand, the phenomenological treatment has been very fruitful. Here, with Einstein,[2] Hartley,[3] and others, one considers that a molecular species will be acted upon by a force equal to the gradient of its chemical potential. In sedimentation equilibrium for example, this force is considered to oppose that of gravity.

In solutions, considered as viscous media, the species is assumed to move at a velocity proportional to the diffusion force

$$v_i = -\omega_i \nabla \mu_i \tag{1}$$

where ω is the mobility or inverse of the friction coefficient. Diffusion velocities customarily are reported in the form of diffusion coefficients, as defined by Fick's first law (for one-dimensional diffusion)

$$P_i = n_i v_i = -\mathfrak{D}_i \frac{dn_i}{dx} \tag{2}$$

where P_i and n_i are the permeation per square centimeter and the molecules per cubic centimeter, respectively. For the general case of a non-ideal solution, it follows from (1) and (2) that

$$\mathfrak{D}_i = \omega_i kT \left(1 + n_i \frac{d \ln y_i}{dn_i}\right) \tag{3}$$

where y is the appropriate activity coefficient, defined by the convention

$$\mu_i = \mu_i^\circ + kT \ln y_i n_i \quad y_i \longrightarrow 1 \text{ as } n_i \longrightarrow 0 \tag{4}$$

For self-diffusion

$$\mathfrak{D}_i^* = \omega_i^* kT \tag{5}$$

on the basis that the activity coefficient of a tagged species does not vary with its concentration; this, in a sense, constitutes a definition of ω_i^* since ω_i^* is not in general equal to ω_i.

For an electrolyte, diffusing across a net concentration gradient, the restriction of electroneutrality is inserted in the form of a diffusion potential that modifies the permeation of each ion appropriately (for an elaboration of diffusion potential effects, see Vinograd and McBain[4]).

$$P_1 = n_1\omega_1(-\nabla\mu_1 + z_1\epsilon) \tag{6}$$

$$P_2 = n_2\omega_2(-\nabla\mu_2 + z_2\epsilon) \tag{7}$$

$$z_1P_1 + z_2P_2 = 0 \tag{8}$$

On elimination of ϵ

$$\mathfrak{D}_\pm = \omega_\pm kT \left(1 + n \frac{d \ln y_\pm}{dn}\right) \tag{9}$$

$$\omega_\pm = \frac{\nu\omega_+ \omega_-}{\nu_-\omega_+ + \nu_+\omega_-} \tag{10}$$

where ν_+ and ν_- denote the number of positive and negative ions per formula of electrolyte, and ν their sum, and $y_\pm$ is the mean activity coefficient.

Mean diffusion coefficients vary with the concentration of electrolyte, and permeations measured experimentally over an appreciable concentration gradient yield average or integral diffusion coefficients.[5] Differential diffusion coefficients, valid for a particular concentration, may in general be obtained from integral ones, however, and in what follows the former only will be referred to.

Phenomenological mobilities vary with concentration, and, unfortunately, the three that pertain to an ion in solution, ω_i^*, ω_i and λ_i, are all different and not easily interrelatable except at infinite dilution. At infinite dilution

$$\omega_i^{*\circ} = \omega_i^\circ = \frac{300\lambda_i^\circ}{e_i \mathfrak{F}} \tag{11}$$

where λ_i^0 is the limiting equivalent conductance of the ion, e_i its charge and $\mathfrak{F}$ its Faraday's number.

The ω^0 value for an ion frequently has been interpreted as the inverse of a Stokes' Law friction coefficient, $\omega^0 = {}^1/_{6\pi r\eta}$, considering the ion to be spherical, and with a surface of shear which may include

---

[1] These investigations were carried out under contract DA-04-495-Ord-364 between the University of Southern California and the Office of Ordnance Research, and were presented in part at the March, 1953, meeting of the American Chemical Society, Los Angeles, California.

[2] A. Einstein, *Ann. Physik*, [4] **17**, 549 (1905).

[3] G. S. Hartley, *Phil. Mag.*, **12**, 473 (1931).

[4] J. R. Vinograd and J. W. McBain, *J. Am. Chem. Soc.*, **63**, 2008 (1941).

[5] R. H. Stokes, *ibid.*, **72**, 763, 2243 (1950).

some water of hydration. A typical comparison of Stokes' Law and crystal radii, from a paper by Darmois,[6] is shown in Fig. 1. Comparison of the Stokes' Law volume with that from the crystal radius is thus an indication of the amount of bound water. Certain difficulties arise, however, such as distortion of the local water structure[7,8] as evidenced by low partial molal volumes, as well as the possibility that slippage may occur at the shear surface.[8] A number of estimates of hydration numbers have been made that include semi-empirical recognition of such factors but resulting in widely differing values for common ions,[6,9,10] of the order of 2 to 10 for monovalent ones. The concern in the present paper is more with those aspects of solvent interaction which play an important role in determining the variation of diffusional mobility with concentration.

Onsager[11] and Onsager and Fuoss[12] have considered the concentration dependence of the mean mobility of an electrolyte as due to a frame of reference effect. The diffusional velocity ordinarily is measured with respect to laboratory coördinates, whereas this quantity as defined in (1) and (2) is with respect to the medium. Since there is no net motion of the system, the volume forces on the ions and on the solvent must cancel on the average, but due to the ion atmosphere there is a local force excess in the vicinity of each ion. Onsager and Fuoss considered that the force excess arising in a given spherical shell imparts a velocity increment to the medium as though the shell were a Stokes' Law sphere. The correction to the diffusional velocity which results is known as the electrophoretic effect. Longsworth[13] strongly supported this treatment although it has been questioned by Van Rysselberghe[14] and, recently, Harned has commented that the theory may be either wrong or incomplete for the higher valence type electrolytes.[15]

A number of semi-empirical equations have been proposed for the concentration dependence of mean diffusion coefficients[14,16-18] which contain such factors as the viscosity, partial molal volume functions and corrections for the amount of bound water per ion.

Turning to the concentration dependence of ion self-diffusion coefficients, Onsager[11] again has been a principal contributor. Here it is argued that in the absence of flow of the electrolyte as a whole there is no electrophoretic effect, but that the labeled species possesses a net velocity. The asymmetry potential arising from the lag of the ion atmosphere is then combined with the diffusion force. This relaxation effect is of reasonable magnitude, but self-diffusion data are not yet accurate enough to permit a quantitative comparison with theory. Gorin[8] and others have felt that ion atmosphere perturbations do not contribute significantly in the analogous case of electrochemical mobilities (at low fields).

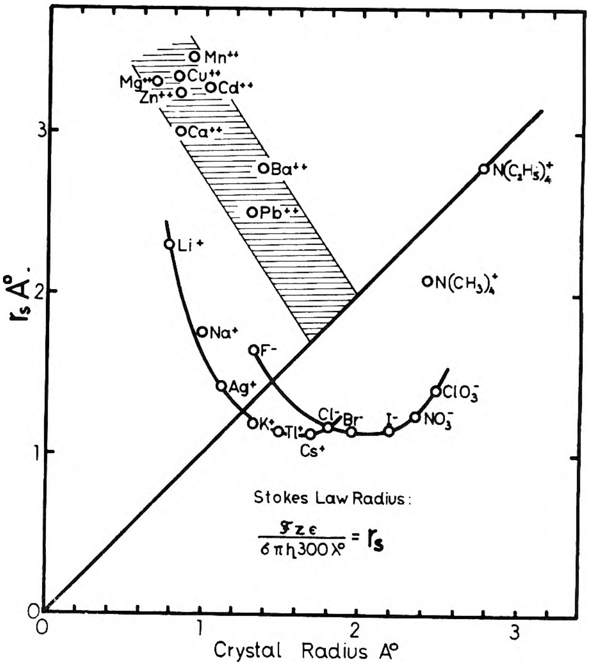

Fig. 1.—Comparison of Stokes law and crystal radii of ions.

The alternative to the phenomenological treatment is to consider the details of the Brownian motion from which diffusional flow arises as a statistical consequence. The classic equation is[2]

$$\mathfrak{D} = \chi^2/2\tau \qquad (12)$$

where χ is the Brownian displacement in time τ. Eyring and co-workers[19] have considered each jump to be an activated process of frequency given the absolute rate theory, and of length related to the size of solvent and solute molecules. The thermodynamic term enters as an increment to the activation energy, and the observed approximate inverse dependence of the diffusion coefficient on the viscosity of the medium, through relating the jump distance to that for viscous flow. An attempt at treating the concentration dependence of self-diffusion coefficients from this point of view will be presented below.

The procedure in what follows will be to consider, in the light of present data, first the case of mean diffusion coefficients, including a critical discussion of the electrophoretic effect and an alternative viewpoint, and then to take up self-diffusion, discuss the relaxation effect, and again consider a possible alternative approach.

Mean Diffusion Coefficients

Electrophoretic Effect.—The electrophoretic ef-

---

(6) E. Darmois, *J. chim. phys.*, **43**, 1 (1946).

(7) J. D. Bernal and R. H. Fowler, *J. Chem. Phys.*, **1**, 515 (1933).

(8) M. H. Gorin, *ibid.*, **7**, 465 (1939).

(9) L. D. Tuck, paper presented at the 118th meeting of the American Chemical Society, Chicago, Illinois.

(10) G. Sutra, *J. chim. phys.*, **43**, 189 (1946).

(11) L. Onsager, *Ann. N. Y. Acad. Sci.*, **46**, 241 (1945).

(12) L. Onsager and R. M. Fuoss, THIS JOURNAL, **36**, 2689 (1932).

(13) L. G. Longsworth, *Ann. N. Y. Acad. Sci.*, **46**, 211 (1945).

(14) P. Van Rysselberghe, *J. Am. Chem. Soc.*, **60**, 2326 (1938).

(15) H. S. Harned and B. B. Owen, "The Physical Chemistry of Electrolyte Solutions," Reinhold Publ. Corp., New York, N. Y., 1950, p. 595.

(16) R. H. Stokes, *J. Am. Chem. Soc.*, **72**, 2243 (1950).

(17) O. Lamm, THIS JOURNAL, **51**, 1063 (1947).

(18) H. R. Gordon, *J. Chem. Phys.*, **5**, 522 (1937).

(19) S. Glasstone, K. J. Laidler and H. Eyring, "The Theory of Rate Processes," McGraw-Hill Book Co., Inc., New York, N. Y., 1941, p. 516f.

fect as treated by Onsager and Fuoss[12] leads to a velocity correction, Δv, given as follows

$$\Delta v_j = \int_{r=a}^{\infty} \mathfrak{F} dr / 6\pi\eta r \tag{13}$$

where

$$\mathfrak{F} dr = 4\pi r^2 \left[\sum_i n_{ji} \mathbf{k}_i - \sum_i n_i \mathbf{k}_i \right] dr \tag{14}$$

since the excess volume force is

$$\sum_i n_{ji} \mathbf{k}_i + n_0 \mathbf{k}_0$$

and (15)

$$\sum_i n_i \mathbf{k}_i + n_0 \mathbf{k}_0 = 0$$

where n_{ji} is the concentration of the ith species near the ion j, $\mathbf{k}_i$ is the force on this species, $\mathbf{k}_0$, that on the solvent, and η is taken to be the viscosity of the pure solvent. From interionic attraction theory

$$n_{ji} = n_i \exp(-e_i \psi_j^0 / kT),\ \psi_j^0 = \frac{e_j}{D} \left[\frac{e^{\kappa a}}{1 + \kappa a} \frac{e^{-\kappa r}}{r} \right] \tag{16}$$

where e_i is the charge on the ith species, D is the dielectric constant (of the pure solvent), a is the Debye–Hückel distance of closest approach, and

$$\kappa^2 = \frac{4\pi}{DkT} \Sigma n_i z_i^2$$

For an electrolyte dissociating into two ions

$$\Delta v_j = \frac{2}{3\eta} [n_1 \mathbf{k}_1 \int [\exp(-e_i \psi_j^0 / kT) - 1] r dr + n_2 k_2 \int [\exp(-e_2 \psi_j^0 / kT) - 1] r dr] \tag{17}$$

This is applied as a velocity correction, giving

$$-\nabla\mu = \nu_1 \rho_1 (v - \Delta v_1) + \nu_2 \rho_2 (v - \Delta v_2) = v\mathbf{f} \tag{18}$$

where

$$\mathbf{f} = \nu_1 \rho_1 + \nu_2 \rho_2 - \nu_1 \rho_1 \frac{\Delta v_1}{v} - \nu_2 \rho_2 \frac{\Delta v_2}{v} \tag{19}$$

$\nabla\mu$ is the chemical potential gradient and $\rho = 1/\omega$. From (18), (1) and (2)

$$\mathfrak{D}\pm = \frac{\nu kT}{\mathbf{f}} \left(1 + c \frac{\mathrm{d} \ln y\pm}{\mathrm{d}c} \right) \tag{20}$$

where c is the concentration in moles per liter. The corrected friction coefficient, $\mathbf{f}$, is obtained from (19) and (17)

$$\mathbf{f} = \nu_1 \rho_1 + \nu_2 \rho_2 - \nu_1 \rho_1 \frac{2a^2}{3\eta} [\eta_1 \rho_1 (\mathrm{I}) + \eta_2 \rho_2 (\mathrm{II})] - \nu_2 \rho_2 \frac{2a^2}{3\eta} (\eta_1 \rho_1 (\mathrm{II}) + \eta_2 \rho_2 (\mathrm{III})] \tag{21}$$

where

$$\begin{aligned} \mathrm{I} &= \int_1^{\infty} \left[\exp\left(\frac{-e_1^2 t}{DakT} \right) - 1 \right] y \mathrm{d}y \\ \mathrm{II} &= \int_1^{\infty} \left[\exp\left(\frac{-e_1 e_2 t}{DakT} \right) - 1 \right] y \mathrm{d}y \qquad t = \frac{e^{\kappa a(1-y)}}{(1 + \kappa a) y} \\ \mathrm{III} &= \int_1^{\infty} \left[\exp\left(\frac{-e_2^2 t}{DakT} \right) - 1 \right] y \mathrm{d}y \qquad y = r/a \end{aligned} \tag{22}$$

The final form obtained by Onsager and Fuoss is given by the first three terms of (27).

It should be noted that in obtaining the above result the following mathematical approximations are made

(a) $\exp(-e_i \psi_j^0 / RT) \cong 1 - e_i \psi_j^0 / kT + {}^1/_2 (e_j \psi_i^0 / RT)^2$ (23)

(b) in equation (17) $k_i \cong v\rho_i$ instead of $\mathbf{k}_i = (v - \Delta v_i) p_i$ (24)

(c) if $f = f^0(1 - \Delta)$ where Δ represents the alteration due to the electrophoretic effect, then $1/f \cong 1/f^0(1 + \Delta)$ (25)

Tests of the Electrophoretic Effect.—Harned and co-workers have obtained during recent years accurate mean diffusion coefficients for a number of electrolytes in dilute solution.[20] If

$$\mathfrak{D}\pm = \mathfrak{D}'\pm \left(1 + c \frac{\mathrm{d} \ln y\pm}{\mathrm{d}c} \right)$$

then (26)

$$\mathfrak{D}'\pm = \mathfrak{D}^0\pm (1 + \Delta)$$

and the departure of $\mathfrak{D}^1\pm$ from $\mathfrak{D}^0\pm$ gives the deviation, Δ, attributed to the electrophoretic effect. For 1–1 electrolytes, the calculated effect is about 0.5%, and agrees with the observed value of Δ to within the experimental error of *ca.* 0.1%, except perhaps for potassium nitrate, for which the data were less precise. Appreciable discrepancies were found for the higher valence types, as shown in Table I.

TABLE I

EXPERIMENTAL TESTS OF THE ELECTROPHORETIC EFFECT

Base line corresponds to the experimental value ○, $\mathfrak{D}\pm$ calculated, including electrophoretic effect ●, $\mathfrak{D}\pm$, calculated, thermodynamic term only

$c \cong 0.004$

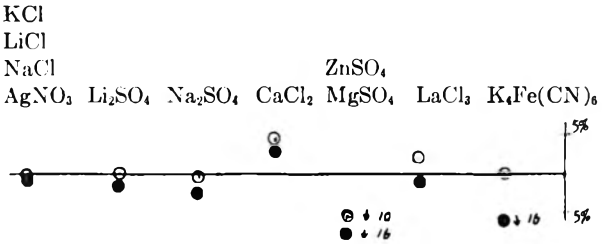

The agreement in the case of potassium ferrocyanide was unbelievably good, and led to the reappraisal of the theory that follows.

An examination of the derivation of the electrophoretic effect indicates that the three approximations (23), (24) and (25) may introduce large errors in the computed effect. Approximations (24) and (25) will be valid in sufficiently dilute solution, but the validity of (23) is more nearly independent of concentration. For 1–1 electrolytes (23) is good, but for higher valence types the arguments of the exponentials in (22) are quite large at small values of r, essentially independently of the magnitude of the concentration. As a first attempt, two additional terms were taken in the expansion (23), leading to the following final equation

---

(20) H. S. Harned and R. L. Nuttall, *J. Am. Chem. Soc.*, **69**, 736 (1947); **71**, 1460 (1949) (KCl); C. A. Blake, Jr., *ibid.*, **73**, 2448 (1951) (Li_2SO_4, Na_2SO_4); **73**, 4255 (1951) ($LaCl_3$); **73**, 5882 (1951) (Cs_2SO_4); A. L. Levy, *ibid.*, **71**, 2781 (1949) ($CaCl_2$); R. M. Hudson, *ibid.*, **73**, 652 (1951) (KNO_3); **73**, 3781 (1951) ($ZnSO_4$); **73**, 5083 (1951) ($K_4Fe(CN)_6$); **73**, 5880 (1951) ($MgSO_4$); C. L. Hildreth, Jr., *ibid.*, **73**, 650 (1951) (LiCl, NaCl); **73**, 3292 (1951) ($AgNO_3$).

$$\mathfrak{D}'_\pm = 3.95 \times 10^{-10}\,\nu T\,\frac{\lambda_1{}^0\lambda_2{}^0}{\nu_1|z_1|\Lambda^0} - 2.58 \times 10^{-8}\,\frac{T}{\eta(DT)^{1/2}}\,\frac{(|z_1|\lambda_2{}^0 - |z_2|\lambda_1{}^0)^2}{|z_1z_2|\ \Lambda^{02}}\,\frac{\Gamma^{1/2}}{1 + \kappa A}$$
$$+ 7.739 \times 10^{-2}\,\frac{\nu T}{\eta(DT)^2}\,\frac{(|z_1|^2\lambda_2{}^0 + |z_2|^2\lambda_1{}^0)^2}{\Lambda^{\circ 2}}\,c\varphi(\kappa a)$$
$$- 4.315 \times 10^{-5}\,\frac{\nu T}{\eta(DT)^3}\,\frac{(|z_1|^3\lambda_2{}^0 - |z_2|^3\lambda_1{}^0)^2}{\Lambda^{\circ 2}}\,c\psi(\kappa a)$$
$$+ 1.800 \times 10^{-8}\,\frac{\nu T}{\eta(DT)^4}\,(|z_1|^4\lambda_2{}^0 + |z_2|^4\lambda_1{}^0)^2\,c\theta(\kappa a) \qquad (27)$$

where

$$\Gamma = \Sigma c_i z_i{}^2 \qquad \varphi(\kappa a) = e^{2\kappa a}Ei(2\kappa a)/(1 + \kappa a)^2$$
$$\psi(\kappa a) = \frac{e^{3\kappa a}}{(1 + \kappa a)^3}\left[\frac{e^{-3\kappa a}}{a} - 3\kappa Ei(3\kappa a)\right]$$
$$\theta(\kappa a) = \frac{e^{4\kappa a}}{(1 + \kappa a)^4}\left[\frac{1}{2}\,\frac{e^{-4\kappa a}}{a^2} - \frac{2\kappa}{a}e^{-4\kappa a} + 8\kappa^2 E_i(4\kappa a)\right]$$
$$E_i(x) = \int_x^\infty e^{-t}\,\frac{dt}{t}$$

For 0.002 *m* potassium ferrocyanide, one obtains

$$\mathfrak{D}'_\pm = 1.48 \times 10^{-5} - 0.229 \times 10^{-6} + 1.667 \times 10^{-6} - 4.365 \times 10^{-6} + 13.47 \times 10^{-6} \qquad (28)$$

Since the fourth term is the largest, it is evident that many more terms would be needed to obtain a convergence. Very recently, Stokes[21] has reported reaching a similar conclusion.

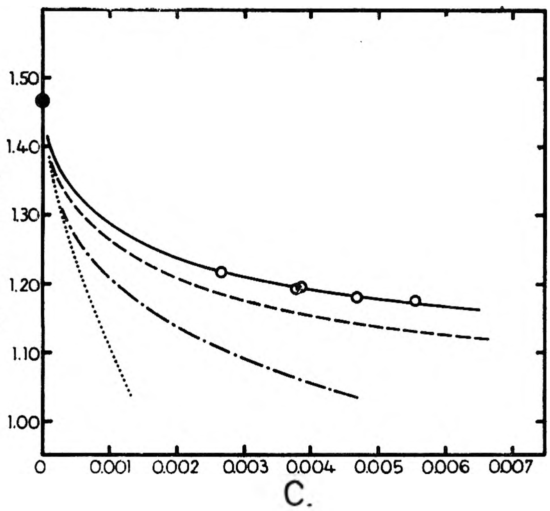

Fig. 2.—$\mathfrak{D}_\pm$ for $K_4Fe(CN)_6$ at 25°; data from Harned and Hudson; calculated $\mathfrak{D}$ values; terms employed: ———, electrophoresis (1st and 2nd) and activity coefficient; - - - - -, electrophoresis (graphical) and activity coefficient; — · —, activity coefficient only; ......, limiting law.

Since the extended equation 27 proved to be inadequate, the integrals (22) were evaluated by graphical integration. Representative values are given in Table II, as compared to those resulting from the use of approximation (23), together with values of Δ and of $\mathfrak{D}_\pm$, calculated and observed. It is seen that quite appreciable discrepancies are present even in the most dilute solutions, except for 1–1 electrolytes. The correct Δ may be either larger or smaller than the one calculated from the customary equation, and their ratio does not necessarily tend toward unity at low concentrations.

In the case of potassium ferrocyanide, the reported agreement is seen to be fortuitous in that the recalculated values of $\mathfrak{D}_\pm$ no longer agree with the observed ones, as shown also in Fig. 2.

The case of magnesium sulfate (and the similarly behaving zinc sulfate) is of some interest because of the extremely large effect of the usual approximations. The recalculated diffusion coefficients are now larger than the experimental ones, as shown also in Fig. 3. Harned and Hudson,[20] attributing the difference between the observed and calculated values of $\mathfrak{D}_\pm$ to ion-pair formation, calculated ion-pair mobilities at the various concentrations. A recalculation of such mobilities would now lead to entirely different results.

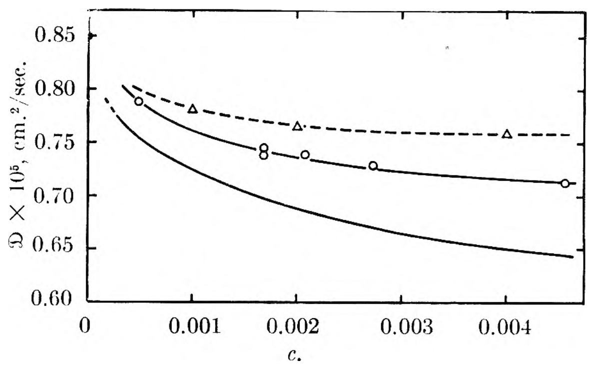

Fig. 3.—Observed and calculated $\mathfrak{D}_\pm$ for $MgSO_4$: △, recalculated values; ⊙, experimental values; solid line, calculated by usual equation.

Except insofar as agreement is brought about through assignment of ion-pair mobilities, it appears that the electrophoretic effect predicts very poorly the experimental values of Δ with the possible exception of 1–1 electrolytes, for which the effect is so small that accurate comparisons are not possible.

Binary *vs.* Intrinsic Diffusion Coefficients.—The above discussion has centered on mathematical inadequacies of certain approximations in the Onsager and Fuoss equation, but since discrepancies with data remain even after accounting for these, it is evident that some further or some different effect must be invoked. Such an effect may be present in the diffusional force arising from the gradient in solvent concentration.

Only a single diffusion coefficient can be obtained from diffusion measurements on a binary system, although there is a concentration gradient in both species (*e.g.*, electrolyte and water) and the measured binary diffusion coefficient must therefore reflect two diffusion processes and two intrinsic diffusion coefficients. The opposing permeations of the two components will in general not cancel and there will be a net volume flow. This effect has been observed in the binary diffusion of metals,[22] as evidenced by the motion of inert markers, and has been treated by Darken for the case of metals of equal atomic volume.

Hartley and Crank,[23] and Lamm[24] have consid-

---

[21] R. H. Stokes, *J. Am. Chem. Soc.*, **75**, 2533 (1953).

[22] L. S. Darken, *Trans. A.I.M.E.*, **175**, 184 (1948).

[23] G. S. Hartley and J. Crank, *Trans. Faraday Soc.*, **45**, 801 (1949).

[24] O. Lamm, THIS JOURNAL, **51**, 1063 (1947).

TABLE II

ELECTROPHORETIC EFFECT CALCULATIONS

(AQUEOUS SOLUTIONS AT 25°)

c, mole/l.	Integrals[a] (eq. 22) I	II	III	Δ[b] (eq. 26)	Δ/Δ'	$\mathfrak{D}_\pm \times 10^5$,[b] cm.²/sec. Calcd.	Exptl.[c]
			$K_4Fe(CN)_6$				
0.001	−8.66	123.6	−74.0	0.056	0.89	1.277	...
	(−8.46)	(58.6)	(162)	(.0625)		(1.285)	
.004	−3.75	57.0	−28.2	.107	.78	1.167	1.194
	(−3.63)	(27.7)	(99.3)	(.136)		(1.198)	
.006	−2.80	42.2	−20.5	.118	.71	1.127	1.175
	(−2.83)	(21.4)	(74.3)	(.165)		(1.174)	
.0085	−2.33	33.8	−16.8	.132	.69	1.095	...
	(−2.24)	(17.5)	(66.9)	(.191)		(1.152)	
			$MgSO_4$				
0.001	−75.6	457	−75.6	0.102	4.6	0.781	0.767
	(−53.9)	(146)	(−53.9)	(.0220)		(.723)	
.002	−47.4	345	−47.4	.152	3.9	.764	.740
	(−29.9)	(103)	(−29.9)	(.0386)		(.687)	
.004	−30.8	254.5	−30.8	.237	3.9	.760	.716
	(−16.7)	(73.3)	(−16.7)	(.0612)		(.651)	
			$CaCl_2$				
0.00247	−26.8	24.6	−8.20	0.0048	0.61	1.240	1.211
	(−20)	(22.2)	(−8.04)	(.0078)		(1.245)	
0.005	−16.9	18.7	−5.40	.0098	0.72	1.219	1.180
	(−12.0)	(15.2)	(−5.29)	(.0135)		(1.224)	
			Na_2SO_4				
0.001	−28.03	89.85	−93.89	0.0098	1.23	1.169	1.174
	(−27.39)	(75.22)	(−69.36)	(.0080)		(1.168)	
0.004	−12.63	47.66	−40.33	.0259	1.17	1.131	1.134
	(−12.31)	(37.94)	(−22.60)	(.0221)		(1.128)	
			NaCl				
0.01	−10.59	14.1	−10.59	0.0043	1.05	1.546	1.547
	(−10.35)	(13.6)	(−10.35)	0.0041)		(1.546)	

[a] Values in parentheses are those obtained using the first two terms of the exponential expansion, equation 23. [b] The values of Δ were obtained without the use of approximations (23), (24) or (25); the values in parentheses are those obtained with the use of these approximations and constitute the electrophoretic correction given by the usual equation of Onsager and Fuoss. The above likewise applies to the calculated values of $\mathfrak{D}_\pm$. [c] The experimental values of $\mathfrak{D}_\pm$ are obtained from the data of Harned and co-workers.

ered the analogous situation for liquid solutions, and obtained relationships similar to the ones developed below. Hall, *et al.*,[25] have employed a modification of Hartley and Crank's equation; no derivation is given, but the equation appears to be semi-empirical. Finally, Onsager and Fuoss[12] have discussed frame of reference effects in general. The following treatment, however, appears to be the best suited to the integration of the various effects observed in electrolyte diffusion. It is assumed throughout that the observed net permeation is with respect to laboratory coördinates, that changes in molar volumes are negligible and that the system is at constant total volume.

Case 1. Binary Solutions of Non-electrolytes.—The following restrictions apply

$$n_1V_1 + n_2V_2 = 1 \tag{29}$$

$$\mathrm{d}n_2/\mathrm{d}x_2 = -\frac{V_1}{V_2}\frac{\mathrm{d}n_1}{\mathrm{d}x} \tag{30}$$

$$P_1V_1 + P_2V_2 = 0 \tag{31}$$

where V_1 and V_2 denote the molal volumes of the two species, and P_1 and P_2, their permeations across unit area fixed in laboratory coördinates. At this point it is assumed that the hydrodynamic and the partial molal volume of a species are identical. As a result of restriction (31), the permeation of a species with respect to the medium, $-\mathfrak{D}_i\mathrm{d}n_i/\mathrm{d}x$, will be altered by a volume flow term $n_i\Delta v$, such that

$$V_1\left(-\mathfrak{D}_1\frac{\mathrm{d}n_1}{\mathrm{d}x} + n_1\Delta v\right) + V_2\left(-\mathfrak{D}_2\frac{\mathrm{d}n_2}{\mathrm{d}x} + n_2\Delta v\right) = 0 \tag{32}$$

hence

$$\Delta v = V_2(\mathfrak{D}_2 - \mathfrak{D}_1)\frac{\mathrm{d}n_2}{\mathrm{d}x} \tag{33}$$

and

$$P_{2\,(\text{apparent})} = -\mathfrak{D}_2\frac{\mathrm{d}n_2}{\mathrm{d}x} + n_2\Delta v = -(F_1\mathfrak{D}_2 + F_2\mathfrak{D}_1)\frac{\mathrm{d}n_2}{\mathrm{d}x} \tag{34}$$

$$\mathfrak{D} = F_1\mathfrak{D}_2 + F_2\mathfrak{D}_1 \tag{35}$$

Equation 35 is symmetrical and there is therefore only one apparent or binary diffusion coefficient, $\mathfrak{D}$; F_1 and F_2 denote the volume fractions occupied by the two species. The quantities $\mathfrak{D}_1$ and $\mathfrak{D}_2$ are

---

[25] J. R. Hall, B. F. Winslow and R. H. Stokes, *J. Am. Chem. Soc.* **75**, 1556 (1953).

not self-diffusion coefficients, but rather the intrinsic differential coefficients that would exist were there no coupling through condition (31); they contain therefore a thermodynamic term which may be abstracted as a separate factor.

$$\mathfrak{D}_1 = \mathfrak{D}_1' \frac{F_2}{N_2}\left(1 + n_1 \frac{\mathrm{d}\ln y_1}{\mathrm{d}n_1}\right) = \mathfrak{D}_1'\left(1 + N_1 \frac{\mathrm{d}\ln f_1}{\mathrm{d}N_1}\right) \tag{36}$$

$$\mathfrak{D}_2 = \mathfrak{D}_2' \frac{F_1}{N_1}\left(1 + n_2 \frac{\mathrm{d}\ln y_2}{\mathrm{d}n_2}\right) = \mathfrak{D}_2'\left(1 + N_2 \frac{\mathrm{d}\ln f_2}{\mathrm{d}N_2}\right) \tag{37}$$

where f is the rational activity coefficient

$$\mu_i = \mu_i^\circ + kT \ln N_i f_i;\ f_i \longrightarrow 1 \text{ as } N_i \longrightarrow 1 \tag{38}$$

$\mathfrak{D}_1'$ and $\mathfrak{D}_2'$ are determined by the intrinsic mobilities of the species, and, to an approximation, can be replaced by the self-diffusion coefficients $\mathfrak{D}_1^*$ and $\mathfrak{D}_2^*$.

From (35), (36), (37) and the Gibbs–Duhem equation, one obtains

$$\mathfrak{D} = (F_2\mathfrak{D}_1^* + F_1\mathfrak{D}_2^*)\left(1 + N\frac{\mathrm{d}\ln f}{\mathrm{d}N}\right) \tag{39}$$

$$\mathfrak{D} = \frac{F_1}{N_1}(F_2\mathfrak{D}_1^* + F_1\mathfrak{D}_2^*)\left(1 + n_2\frac{\mathrm{d}\ln y_2}{\mathrm{d}n_2}\right) \tag{40}$$

Equation 39 reduces to that of Darken[22] in the case of equal molar volumes, and (40) resembles that of Lamm,[24] who did not, however, connect the intrinsic differential coefficients with self-diffusion coefficients. Finally, the behavior predicted by (39) conforms with that observed by Eyring and co-workers[26] for the chloroform–ether system, if the reasonable assumption is made that the self-diffusion coefficients will vary inversely as the viscosity of the medium.

Case 2. Binary Solutions of Non-electrolytes; Hydrodynamic Volumes not Equal to the Partial Molal Volumes.—In liquid solutions solvation effects frequently lead to swelling of solute aggregates, or fixation of solvent by even simple solute molecules, so that the hydrodynamic volumes of the two species may be quite different from the partial molal volumes. The former enter into the flow balance equation 31, while the latter are involved in the thermodynamic relationships (36) and (37). Equation 39 remains unchanged, while (40) becomes

$$\mathfrak{D} = \frac{\bar{F}_1}{N_1}(F_2\mathfrak{D}_1^* + F_1\mathfrak{D}_2^*)\left(1 + n_2\frac{\mathrm{d}\ln y_2}{\mathrm{d}n_2}\right) \tag{41}$$

where $\bar{F}$ denotes the volume fraction based on the partial molal volume.

Case 3. Solutions of an Electrolyte in Water.—For the case of an electrolyte dissociating into two kinds of ions, the restrictions are

$$n_1V_1 + n_2V_2 + n_wV_w = 1 \tag{42}$$

$$P_1Z_1 + P_2Z_2 = 0 \tag{43}$$

$$P_1V_1 + P_2V_2 + P_wV_w = 0 \tag{44}$$

Since the permeations of the ions are separately coupled through (43), the problem reduces to the preceding one through the use of mean diffusion coefficients and mean activity coefficient terms. Thus

$$\Delta v = V_s(\mathfrak{D}_\pm - D_w)\frac{\mathrm{d}n_s}{\mathrm{d}x} \tag{45}$$

where

$$V_s = \nu_1V_1 + \nu_2V_2$$
$$n_s = n_1/\nu_1 = n_2/\nu_2$$

and

$$\mathfrak{D} = (F_w\mathfrak{D}_\pm + F_s\mathfrak{D}_w) \tag{46}$$

$$\mathfrak{D} = \frac{\bar{F}_w}{N_w}(F_s\mathfrak{D}_w^* + F_w\mathfrak{D}_\pm^*)\left(1 + n_s\frac{\mathrm{d}\ln y_\pm}{\mathrm{d}n_s}\right) \tag{47}$$

Here again, the mobilities that enter into $\mathfrak{D}_\pm^*$ may not correspond to the self-diffusional mobilities of the two ions. The quantity $\mathfrak{D}_w^*$ should in general vary considerably with the salt concentration, and the measurement of the self-diffusion of water in electrolyte solutions should yield results of considerable fundamental interest.

For the dilute electrolyte solutions to which the electrophoretic effect has been applied, (47) reduces to

$$\mathfrak{D}_\pm' = F_s\mathfrak{D}_w^{*\circ} + F_w\mathfrak{D}_\pm^\circ \tag{48}$$

where $\mathfrak{D}_\pm'$ and $\mathfrak{D}_\pm^0$ are the quantities defined in (26), and $\mathfrak{D}_\pm^{*0}$ is taken to be the self-diffusion coefficient for pure water, in the absence of values for $\mathfrak{D}_w$. An equation of this type was employed by Nielsen, *et al.*,[27] to explain the upswing in the mean diffusion coefficients of sodium chloride at high concentrations, as compared to the nearly constant values for the self-diffusion coefficients of the ions separately.

An interesting estimate of the hydrodynamic volume of electrolytes can be made if the entire difference between $\mathfrak{D}_\pm'$ and $\mathfrak{D}_\pm^0$ is attributed to the counter flow effect, using (48). Representative results are given in Table III, the diffusion data being taken from the publications of Harned and coworkers,[20] and the self-diffusion coefficient for water as 2.83 × 10^{-5} cm.²/day, from Wang.[28] It is seen that quite large hydrodynamic radii result; they are larger for the more highly charged ions, and tend to approach the values for the Debye–Hückel atmosphere radii in the more concentrated solutions of the polyvalent electrolytes. Hydrodynamic radii of this size are not expected in terms of the Stokes Law interpretation of the limiting mobility values, but do correspond to the degree of long range interaction assumed in the electrophoretic effect. Darmois[6] has discussed other evidence for long range ion–solvent interactions.

TABLE III

HYDRODYNAMIC RADII AS GIVEN BY EQUATION 48

Concentration, M
(Radii in A.)

	0.001		0.002		0.003		0.005		0.010	
Salt	r	$1/\kappa$	r	$1/\kappa$	r	$1/\kappa$	r	$1/\kappa$	r	$1/\kappa$
Li_2SO_4	12.6	56			10.6	32	9.9	25		
Cs_2SO_4	14.1	56	12.5	39	11.5	32				
KNO_3	7.4	96			6.8	56			5.9	31
$LaCl_3$			13.9	28			11.1	18	9.9	12

The approximation (48) is of uncertain accuracy, and it would be desirable to obtain an independent measure of the counter flow effect. This is possible in the case of diffusion in metals, since Δv can be measured directly from the motion of inert makers.[22] A similar determination of the Δv of

---

[26] Reference 19, p. 536.

[27] J. M. Nielsen, A. W. Adamson and J. W. Cobble, *J. Am. Chem. Soc.*, **74**, 446 (1952).

[28] J. H. Wang, *ibid.*, **75**, 468 (1953).

equation 45 should be possible for electrolyte solutions through the use of a third component. The marker component should be a trace species, to avoid interaction with the binary diffusion gradient, neutral, to avoid interaction with the diffusion potential of the electrolyte, and, preferably, of sufficiently low mobility so that its own diffusional motion would be negligible. Occasional reports are found of "anomalous diffusion," presumably due to the volume force effect. Hartley[29] observed the flow of ferric oxide sol due to a water–ether binary gradient, the motion of species such as propyl alcohol, sucrose and carboxylic acids due to a gradient in electrolyte concentration has been reported,[30] and Freundlich and Kruger[31] found that a free diffusion boundary between 1 M potassium chloride and water imposed a rather complex concentration gradient on an initially uniform quinone concentration. None of the above results seemed suited to a quantitative treatment; moreover, the complex effect found by Freundlich and Kruger for a free diffusion system underscores the advantages of employing a steady-state system, such as in the diaphragm cell method.

The combined diffusion and flow effect for a trace marker species can be stated explicitly if steady-state conditions apply so that the binary concentration gradient is essentially constant. The permeation of the marker species will be

$$P_3 = -\mathfrak{D}_3\frac{\mathrm{d}n_3}{\mathrm{d}x} + \Delta v n_3 \qquad (49)$$

This is set equal to zero, and the resulting differential equation solved for n_3

$$\frac{\mathrm{d}^2 n_3}{\mathrm{d}x^2} = \frac{\Delta v}{\mathfrak{D}_3}\frac{\mathrm{d}n_3}{\mathrm{d}x}$$

$$n_3 = \frac{n_3'(e^{\Delta v x/\mathfrak{D}_3} - e^{\Delta v x_0/\mathfrak{D}_3}) + n_3''(1 - e^{\Delta v x/\mathfrak{D}_3})}{1 - e^{\Delta v x_0/\mathfrak{D}_3}} \qquad (50)$$

The concentration of the marker species is n_3' at $x = 0$ and n_3'' at $x = x$. The permeation is then given by (51)

$$P_3 = -\frac{\Delta v(n_3' e^{\Delta v x_0/\mathfrak{D}_3} - n_3'')}{1 - e^{\Delta v x_0/\mathfrak{D}_3}} \qquad (51)$$

which reduces to (52) if $n_3' = n_3''$.

$$P_3 = \Delta v n_3 \qquad (52)$$

Experiments of this type currently are being undertaken at this Laboratory.

Self-diffusion Coefficients

Relaxation Effect.—Onsager[11] has given a limiting law equation for the diffusion of a trace species in the presence of a uniform concentration of a different electrolyte, and this result has been applied to ion self-diffusion by Gosting and Harned.[32] Onsager presented his derivation in rather general terms, in which the limiting law appeared as a special case of the general solution for diffusion in a mixture of electrolytes. A direct derivation will be given here.

The equation is based on the perturbation treatment, whereby due to a net motion (as opposed to individual Brownian displacements) of an ion, its potential is given by the equilibrium value plus the perturbation

$$\psi_j = \psi_j^\circ + \psi_j' \qquad (53)$$

The perturbed potentials are inserted into the continuity equation[33] to give

$$(\nabla\cdot\nabla)^2\psi_j' - \frac{4\pi}{DRT}\sum_{i=1}^{s}\frac{n_i e_i^2\omega_i}{\omega_i + \omega_j}\nabla\cdot\nabla\psi' - \frac{4\pi}{DkT}\sum_{i=1}^{s}\frac{n_i e_i e_j\omega_i}{\omega_i + \omega_j}\nabla\cdot\nabla\psi_i' = \frac{4\pi}{(DkT)^2}\sum_{i=1}^{s}\frac{\omega_i\mathbf{k}_i - \omega_j\mathbf{k}_j}{\omega_i + \omega_j}n_i e_i^2 e_j\frac{\partial}{\partial x}\left(\frac{e^{-kr}}{r}\right) \qquad (54)$$

Case 1. Three Ions, One Present in Trace Amounts.—The assumptions and restrictions are

$$\begin{array}{ll} n_1e_1 + n_2e_2 = 0 & n_3 << n_1 \text{ or } n_2 \\ \omega_1 \neq \omega_2 \neq \omega_3 & \psi_1' = \psi_2' = 0 \\ \mathbf{k}_1 = \mathbf{k}_2 = 0 & \psi_3' \neq 0 \\ \mathbf{k}_3 \neq 0 & \end{array} \qquad (55)$$

Upon insertion of these into (54), one obtains

$$\nabla^2\psi_3' - \frac{4\pi}{DkT}\left[\frac{n_1e_1^2\omega_1}{\omega_1 + \omega_3} + \frac{n_2e_2^2\omega_2}{\omega_2 + \omega_3}\right]\nabla\psi_3' = \frac{4\pi}{(DkT)^2}\left[-\frac{\omega_3\mathbf{k}_3n_1e_1^2e_3}{\omega_1 + \omega_3} - \frac{\omega_3\mathbf{k}_3n_2e_2^2e_3}{\omega_2 + \omega_3}\right]\frac{\partial}{\partial x}\left(\frac{e^{-kr}}{r}\right) \qquad (56)$$

This reduces to

$$\nabla^2\psi_3' - \kappa_1^2\nabla\psi_3' = \Omega\kappa_1^2\frac{\partial}{\partial x}\left(\frac{e^{-kr}}{r}\right) \qquad (57)$$

where

$$\kappa_1^2 = \frac{\kappa^2}{e_1 - e_2}\left[\frac{e_1\omega_1}{\omega_1 + \omega_3} - \frac{e_2\omega_2}{\omega_2 + \omega_3}\right],\ \kappa^2 = \frac{4\pi}{DkT}\Sigma n_ie_i^2 \qquad (58)$$

and

$$\Omega = -\frac{\mathbf{k}_3e_3}{DkT}\frac{\left[\frac{e_1\omega_3}{\omega_1 + \omega_3} - \frac{e_2\omega_3}{\omega_2 + \omega_3}\right]}{\left[\frac{e_1\omega_1}{\omega_1 + \omega_3} - \frac{e_2\omega_2}{\omega_2 + \omega_3}\right]} \qquad (59)$$

The solution to (57) is

$$-\nabla\psi_3'{}_{(r=0)} = \frac{\Omega\kappa_1^2}{3(\kappa + \kappa_1)} = \frac{-\frac{\mathbf{k}_3e_3\kappa}{3DkT}\left[\frac{e_1\omega_3}{\omega_1 + \omega_3} - \frac{e_2\omega_3}{\omega_2 + \omega_3}\right]\frac{1}{(e_1 - e_2)}}{1 + \left[\frac{1}{(e_1 - e_2)}\left[\frac{e_1\omega_1}{\omega_1 + \omega_3} + \frac{e_2\omega_2}{\omega_2 + \omega_3}\right]\right]^{1/2}} \qquad (60)$$

Since

$$v_3 = \mathbf{k}_3\omega_3 - e_3\nabla\psi_3'\omega_3 \qquad (61)$$

then

$$v_3 = \mathbf{k}_3\omega_3\left[1 - \frac{e_3^2\kappa}{3DkT}P\right] \qquad (62)$$

where

$$P = \frac{\frac{1}{(e_1 - e_2)}\left[\frac{e_1\omega_3}{\omega_1 + \omega_3} - \frac{e_2\omega_3\cdot}{\omega_2 + \omega_3}\right]}{1 + \left[\frac{1}{(e_1 - e_2)}\left[\frac{e_1\omega_1}{\omega_1 + \omega_3} - \frac{e_2\omega_2}{\omega_2 + \omega_3}\right]\right]^{1/2}} \qquad (63)$$

Then

$$\mathfrak{D}_3 = \omega_3kT\left[1 - \frac{e_3^2\kappa}{3DkT}P\right] \qquad (64)$$

Equation 64 may be arranged to Onsager's result.

---

[29] G. S. Hartley, *Trans. Faraday Soc.*, **27**, 16 (1931).

[30] T. Erdey-Gruz, A. Hunyar, E. Pogany and A. Vali, *Hung. Acta Chim.*, **1**, No. 3 (1948); *cf.* also A. Hunyar, *J. Am. Chem. Soc.*, **71**, 3552 (1949).

[31] H. Freundlich and D. Kruger, This Journal, **43**, 981 (1939).

[32] L. J. Gosting and H. S. Harned, *J. Am. Chem. Soc.*, **73**, 159 (1951).

[33] Reference 15, p. 81.

Case 2. Two Ions, One Labeled but Not Necessarily a Trace Species.—The assumptions and restrictions are

$$\begin{array}{ll} \omega_1 = \omega_3 \neq \omega_2 & \mathbf{k}_3 = -n_1\mathbf{k}_1/n_3 \\ n_1e_1 + n_2e_2 + n_3e_3 = 0 & \psi_2' = 0 \\ e_1 = e_3 \neq e_2 & n_1\psi_1' + n_3\psi_3' = 0 \quad (65) \\ \mathbf{k}_2 = 0 & \end{array}$$

Upon insertion of these into (54), the same equation results as would be obtained by setting $\omega_1 = \omega_3$, $e_1 = e_3$ in (56), and hence is given by (64), again with the appropriate changes which reduce it to

$$\mathfrak{D}_3 = \omega_3 kT\left(1 - \frac{e_3^2\kappa}{3DkT}\left(1 - \sqrt{\mathrm{d}\omega_j}\right)\right) \quad (66)$$

$$\mathrm{d}\omega_j = \frac{1}{(e_1 - e_2)}\left[\frac{e_1}{2} - \frac{e_2\omega_2}{\omega_2 + \omega_3}\right]$$

These derivations have been presented as being more easily followed than Onsager's matrix algebra, and as an explicit exposition of the assumptions and restrictions employed. Since case 2 was not treated by Onsager, it is noteworthy that the same result obtains whether or not the labeled species is also a trace species. The most interesting assumption is that the net motion of a tracer gives rise to a real perturbation or net bias to the atmosphere potential. In tracer diffusion there is no gradient in total electrolyte concentration, and ordinarily one assumes the atmospheres to be symmetric in such a case, as in the calculation of activity coefficients. Otherwise stated, the diffusion of a tracer is a statistical consequence of its Brownian motion, the quality of which is obviously unaffected by whether or not the ion is considered to be labeled. From this point of view, the perturbation of the atmosphere potential for a tracer appears virtual in character and not easily relatable to the properties of solutions that control the change in quality of Brownian motion with concentration.

Absolute Rate Treatment of Ion Self-diffusion.—It is interesting to consider qualitatively the basis for the relaxation treatment, and to compare it with the situation as viewed by Eyring and coworkers.

Following the presentation in Harned and Owen,[16] the relaxation time of an ion atmosphere, τ, multiplied by the average (*i.e.*, net) diffusion velocity gives a displacement, $\Delta\chi$, which, if taken relative to the atmosphere radius, $1/\kappa$, yields a relative distortion, s. This relative distortion times the total force between the atmosphere and the ion is then approximately the increment in force, $\Delta\mathbf{k}$, due to the relaxation effect. Considering the case of a 0.01 m solution of 1–1 electrolyte, τ is $\sim 10^{-7}$ sec., the mobility is about 10^{-5} cm./sec. per unit diffusion force, and $^1/\kappa$ is 30 Å. Thus the relative distortion is 3×10^{-6}, and this multiplied by the large force between the ion and its atmosphere gives a $\Delta\mathbf{k}$ of a few tenths per unit diffusion force.

If, however, an ion migrates by Brownian jumps of the order of molecular dimensions, the minimum jump velocity will be approximated by $\mathfrak{D}/\lambda$, or about 10^3 cm./sec. The relative distortion is now 300. Thus jumps of this size must occur essentially adiabatically, the ion atmosphere rearranging to new equilibrium during the period between jumps. This reasoning would not apply to electrochemical motion since an external electric field imposes a constant bias or correlation between successive jumps.

On the basis of adiabatic jumps, the ion at the end of each should find itself part way up the potential well of the atmosphere, and the resulting energy increment should appear in the activation energy for self-diffusion. To obtain a specific relationship, the atmosphere potential in the usual form is employed.

$$\psi_{\mathrm{j(atm)}} = \frac{e_j}{Dr}\left[\frac{e^{\kappa a}}{1 + \kappa a}e^{-\kappa r} - 1\right] \quad (67)$$

The increment in energy corresponding to a jump is, approximately

$$\Delta E = -\frac{e_j}{D}\left[\psi_{j(a+\lambda)} - \psi_{j(\lambda)}\right] \cong \frac{\kappa^2\lambda^2}{2D(a + \lambda)(1 + \kappa a)} \quad (68)$$

Writing

$$\mathfrak{D}^* = \lambda^2\mathbf{k},\ \mathbf{k} = \frac{kT}{\eta}\exp\left(-\Delta F^\ddagger/kT\right) \quad (69)$$

and taking the free energy of activation to be $(\Delta F_0^\ddagger + \Delta E)$, one obtains

$$\mathfrak{D}^* = \frac{\lambda^2}{\lambda_0^2}\mathfrak{D}_0^* e^{-\Delta E/kT} \cong \frac{\lambda^2}{\lambda_0^2}\mathfrak{D}_0^*\left[1 - \frac{\kappa^2\lambda^2}{2DkT(a + \lambda)(1 + \kappa a)}\right] \quad (70)$$

For a 1–1 electrolyte in water at 25°, (70) reduces to

$$\mathfrak{D}^* = \frac{\lambda^2}{\lambda_0^2}\mathfrak{D}_0^*\left[1 - \frac{0.386\lambda^{02}}{(\mathring{a} + \lambda^0)(1 + \kappa a)}c\right] \quad (71)$$

taking the dielectric constant to be that of pure water. According to Eyring and co-workers,[20] λ may be related to the viscosity by

$$\lambda^2 = \frac{\lambda_1 kT}{\lambda_2\lambda_3\mathbf{k}'\eta} \quad (72)$$

where $\mathbf{k}'$ is the appropriate specific rate constant. Assuming that λ_1, λ_2, λ_3 and $\mathbf{k}'$ do not vary with concentration, the approximation follows that

$$\mathfrak{D}^* = \frac{\mathfrak{D}^*_0\eta_0}{\eta}\left[1 - \frac{0.386\lambda^{02}}{(\mathring{a} + \lambda^0)(1 + \kappa a)}c\right] \quad (73)$$

Results of Self-diffusion Measurements.—Self-diffusion coefficients in aqueous solutions at 25° have been reported for one or both of the ions of sodium chloride,[27,34–36] sodium iodide,[37] silver nitrate,[38] sodium sulfate[30] and hydrogen, lithium, potassium and rubidium iodides.[39] Values are not available for sufficiently dilute solutions, however, nor of sufficient precision to permit a critical test of limiting laws. This point is illustrated by Figs. 4 and 5 which give the values of the diffusion coefficients for the ions of sodium chloride, plotted against c and against $\sqrt{c}$. For the sequence of iodides, a plot of $\mathfrak{D}_{\mathrm{I}^-}{}^*$ according to equation 73 shows fair agreement, with λ^0 values of about 2, as

---

(34) J. H. Wang and S. Miller, *J. Am. Chem. Soc.*, **74**, 1611 (1952).

(35) J. H. Wang, *ibid.*, **74**, 1612 (1952).

(36) J. E. Burkett and J. W. T. Spinks, *Can. J. Chem.*, **30**, 311 (1952).

(37) J. H. Wang and J. W. Kennedy, *J. Am. Chem. Soc.*, **72**, 2080 (1950).

(38) S. G. Whiteway, D. F. MacLennan and C. C. Coffin, *J. Chem. Phys.*, **18**, 229 (1950).

(39) R. Mills and J. W. Kennedy, *J. Am. Chem. Soc.* **75**, 5696 (1953). The author is indebted for a prepublication communication.

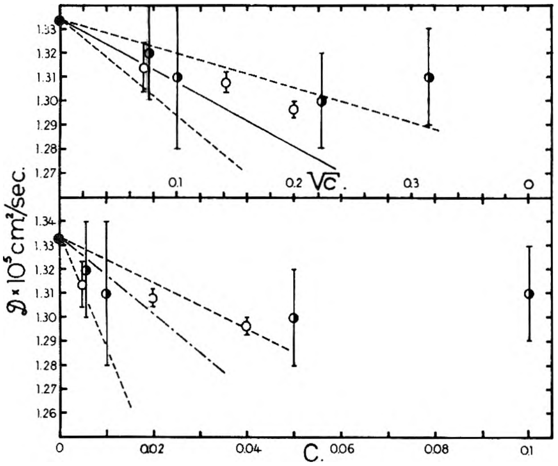

Fig. 4.—Na^+ in NaCl at 25°: - - - - -, possible limiting slopes; ———, Onsager, Gosting and Harned equation; — · —, activated jump λ° = 3 Å.; ●, Nernst value; ◑, Wang; ○, Nielsen, Adamson and Cobble.

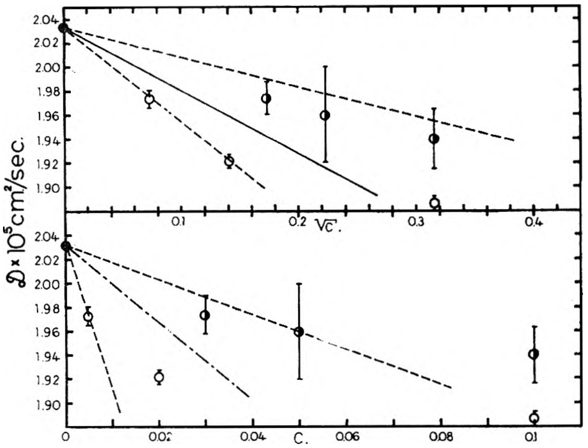

Fig. 5.—Cl^- in NaCl at 25°: ●, Nernst value; ◑, Wang; ○, Nielsen, Adamson and Cobble; - - - - -, possible limiting slopes; ———, Onsager, Gosting and Harned equation; — · —, activated jump λ° = 3 Å.

shown in Fig. 6. Smoothed values of $\mathfrak{D}_{\mathrm{I}^-}^*$ were used in this plot but, as indicated in the figure, the precision was not high enough to justify much confidence in the fit; moreover these data are for sufficiently concentrated solutions that the application of any law involving the Debye–Hückel approximations is questionable. It should be mentioned, however, that in a $\mathfrak{D}_{\mathrm{I}^-}^*$ *vs.* $\sqrt{c}$ plot, extrapolation of the data toward zero concentration gives limiting slopes considerably higher than those predicted by the relaxation effect, whereas the data do extrapolate reasonably according to (73).

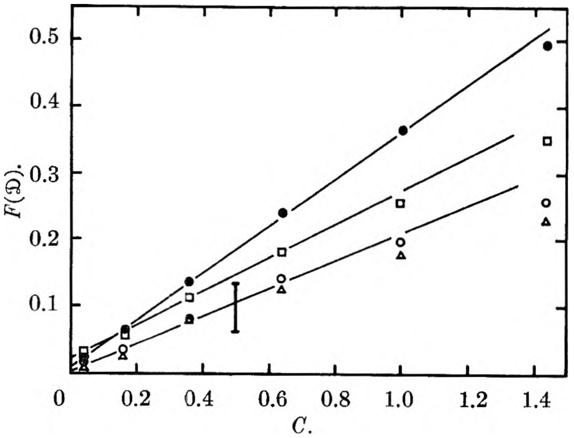

Fig. 6.—$\mathfrak{D}_{\mathrm{I}^-}$ plotted according to (73): ⊙, HI; △, LiI; ⊡, KI; ●, RbI: $F(\mathfrak{D}) = (1 - \mathfrak{D}\eta/\mathfrak{D}_0\eta_0)(1 + \kappa a)$.

Apart from the lack of precision, there appears also to be some systematic differences between the various experimental methods employed. These are the diaphragm cell (I),[27,38] free diffusion (II),[36] free diffusion from an open ended capillary[34,35,39] with stirring (III), and without stirring (IV).[36] Method III tends to give maxima in several tenths molar solutions, which do not appear in the results obtained by (I), (II) and, perhaps, (IV), and to give much lower diffusion coefficients at high concentrations than do (I) and (II). Methods I, II and IV agree in the case of $\mathfrak{D}_{Na^*}$ in sodium iodide. These points are illustrated in Figs. 7 and 8. Wang[40] has attributed the maxima found (by method III) for $\mathfrak{D}_{Na^*}$ in potassium and sodium chloride solutions to an increase in mobility due to a progressive distortion of the water structure, eventually counterbalanced by a relaxation effect.

Currently, work in this Laboratory is being directed toward the elucidation of the causes for these

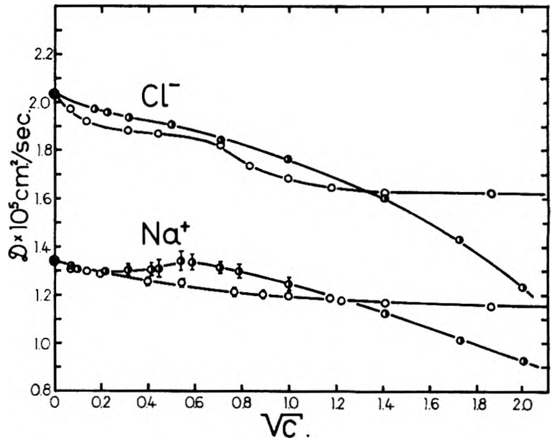

Fig. 7.—Self-diffusion of ions in NaCl at 25°: ●, Nernst value; ○, Nielsen, Adamson and Cobble (diaphragm cell); ◑, Wang (open ended capillary, stirring).

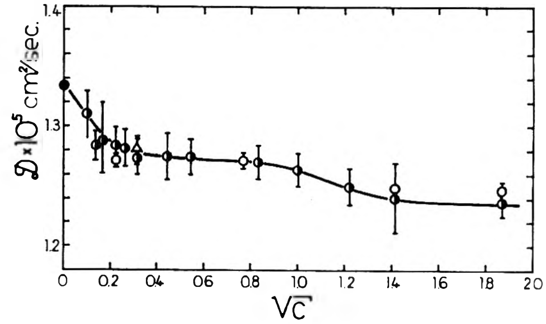

Fig. 8.—Self-diffusion of Na^+ in NaI at 25°: ●, Nernst value; ◑, Wang and Kennedy (free diffusion); ○, Nielsen, Adamson and Cobble (diaphragm cell); △, Burkell and Spinks (open ended capillary, no stirring).

---

[40] J. H. Wang, *J. Am. Chem. Soc.*, **74**, 1182 (1952)

differences. This would seem to be a necessary preliminary to the placing of any confidence in the accuracy of self-diffusion coefficients or in any detailed theoretical explanations.

Acknowledgment.—The author is indebted to Dr. R. Mills and to Mr. G. Appleton for their aid in the calculations on the electrophoretic effect, and to Professor K. Mysels for many helpful discussions.

USE OF OXYGEN ISOTOPE EFFECTS IN THE STUDY OF HYDRATION OF IONS

By Henry Taube

George Herbert Jones Laboratory, University of Chicago, Chicago, Illinois

Received April 12, 1954

This paper is a review of the work of John P. Hunt, Aaron C. Rutenberg, Robert A. Plane and Harold M. Feder, which has been devoted to a study of hydration of ions using isotope effects for oxygen as a tool. An explicit goal in the research is to characterize the species which result on the interaction of the solvent water and the ions contained therein, it being supposed that for some ions at least, a sharp distinction between water in the first sphere and water in outer spheres will be possible. The most direct attack is to use a kinetic method, depending on the difference in rate of exchange with solvent which may exist for water held in the first sphere as against water contained in outer spheres. Some results obtained in these studies have been published.[4,6,9] They are reviewed briefly, and the limitations of this method and the extension of the studies are discussed. A less direct approach but one which can be given great power when developed, is an equilibrium method, the measurement of the effect that salts exert on the activity ratio of H_2O^{18} compared to H_2O^{16} in the liquid. The results of this study have been published only in part and are presented and discussed more fully here.

In this paper is reviewed the use which has been made of isotopic tracer and fractionation effects in the study of hydration of ions. Work on these methods is still in progress, and further experiments are planned. In order to give a more complete account of what is possible with the isotopic methods, the description is not limited to experiments already completed, but some features of interest in present and projected work are also discussed.

As the results will show, oxygen isotope effects are especially suited to the study of hydration of cations. The point of view which has guided the work is this: cations, perhaps all the simple ones, exert forces sufficiently strong on water molecules held in the first sphere of hydration, to make these distinguishable from other water molecules, which may also be affected. A general goal is to learn the limits for which such a distinction between "first sphere" water and remaining solvent is possible. A specific goal, of particular interest for the chemistry of the individual ions, is to learn the number of water molecules in the first hydration sphere, *i.e.*, to learn the "formulas" of the ion–water complexes. While in most cases, the formulas will probably be found to be those expected by considering ion sizes compared to the dimensions of the water molecules, important exceptions are to be expected. In any case, to make definite hydrate complex ions part of our vocabulary of thinking, it is necessary to raise the formulas from the level of conjecture, however probable, to proven conclusions. Specific effects of bonding will be largely absorbed in the first sphere of hydration, and a simple theory may suffice to describe the interaction of the hydrated ions with the solvent.

The most direct method of distinguishing water bound directly to the ions and water bound to water exploits the difference in the rate at which the two kinds mix with the solvent. The distinction can be made experimentally by enriching the solvent with H_2O^{18}, then applying some method of isotope sampling to follow the change in isotopic content of the solvent with time. This method has been used to help characterize some oxy-anions in solution[1,2] and in characterizing the oxy-cation UO_2^{++}.[3]

The sensitivity of the exchange method can readily be estimated. Consider a solution containing *a* moles of solute per mole of solvent and let it be mixed with water which has a different mole fraction of H_2O^{18}. Let *b* represent the ratio of the number of moles of water added compared to that in the original solution, and let *f* represent the enrichment ratio in the added solvent compared to the original solution. *Q* represents the ratio of the mole fraction H_2O^{18} in the mixed solution assuming that each mole of solute holds back one solvent molecule, compared to the mole fraction calculated for random mixing. *Q* is found to be given by the product

$$\left(\frac{1 - a + bf}{1 - bf}\right)\left(\frac{1 + b}{1 - a + b}\right)$$

The highest sensitivity (*Q* different most from unity) is obtained with an enrichment factor *f* so large that the first factor is unity, then choosing *b* sufficiently small to make *Q* practically equal to $1/1 - a$. At this highest sensitivity, to make a 1% change in *Q* for the hold-back of 1 mole solvent per mole of solute, a solution containing 0.01 mole solute per mole solvent is required. With an enrichment factor *f* of 8, the optimum range of *b* for dilute solutions is 0.3 to 0.5, and to cause a 1% change in *Q* with a hold-back of 1 mole solvent per mole of solute, a solution approximately 1 molal is needed. A precision of 1 or 2 parts per 1000 in sampling and isotopic ratio reading is attainable, so that an accuracy in the total hold-back of 0.1 mole solvent per

---

(1) G. A. Mills, *J. Am. Chem. Soc.*, **62**, 2833 (1940).

(2) N. F. Hall and O. R. Alexander, *ibid.*, **62**, 3455 (1940).

(3) H. W. Crandall, *J. Chem. Phys.*, **17**, 602 (1949).

mole solute can be achieved at this concentration level.

An experimental difficulty to overcome is that of mixing the added solvent and of sampling the mixed solution in periods of time short compared to the rate of exchange of bound water and solvent. Thus far only the simplest method has been used.[4] The enriched water is poured in while the solution is stirred, and the solvent is sampled by vacuum distillation. Not many aquo ions come within the scope of this method, the minimum sampling time for which is about 1 minute. Exchange is found to be complete by the time of the first sampling for hydrated forms of H^+, Al^{+++}, Fe^{+++}, Ga^{+++}, Th^{+4},[4] Co^{++}, Co^{+++} (with Co^{++} present),[5] Cr^{++}, Zn^{++}[6] (as well as for water bound to the anions NO_3^- and ClO_4^-). Two of the exchange systems mentioned have special features. There is apparently a slight hold-back of oxygen by Fe^{+++} when it has aged in solutions of low acidity. This hold-back has been interpreted as being caused by oxygen incorporated into polynuclear forms known to develop in such solutions. The observations on the exchange lability of $Co^{+++}_{aq.}$ are not unambiguous. $Co^{+++}_{aq.}$ may be rather substitution-inert and the observed exchange may be carried by electron exchange between $Co^{++}_{aq.}$ and $Co^{+++}_{aq.}$.[7]

Of the simple aquo ions tested, only Cr^{+++} holds back water for periods of time long compared to the minimum sampling time. The experiments with Cr^{+++} have shown that 6 ± 0.1 mole of water is held back for each mole of metal ion. In view of the size of water molecules compared to Cr^{+++}, the coördination sphere will be effectively completed by six of them, justifying the conclusion that the formula of the Cr^{+++}–H_2O complex in solution is $Cr(H_2O)_6^{+++}$. In any case, other water molecules which interact with the hydrated ion, do so without becoming equivalent to the six firmly bound molecules.

It does not seem likely that many other simple aquo ions will yield to the exchange method unless it is developed beyond the stage described. Using the correlation of exchange rates with electronic structure,[8] success can be expected even with a sampling time of one minute also with Rh^{+++}, Ir^{+++} and possibly V^{++}. Many aquo ions for which slow exchange rates would be expected, are difficult to obtain at sufficiently high concentration because formation of polynuclear forms, or of some solid phase intervenes. Numerous mixed aquo complex however can be expected to yield to the simplest exchange procedure. The method has already been applied to $Co(NH_3)_5H_2O^{+++}$[9] and $Co(NH_3)_4(H_2O)_2^{+++}$[10] in establishing the formulas as written for the ions in solution, and will undoubtedly yield conclusions for mixed complexes of Cr(III), Mo(III), Ru(II), Ru(III), etc., and for some complexes of Fe(II) and Fe(III). After the method has been applied to a few ions and, if as has proved to be the case in those studied thus far, the rate of exchange of bound water is found to be similar to other substitution rates for the ions, further exchange studies for learning formulas of substitution-inert cations may in fact seem to be redundant. The evidence thus far for such ions is that the formulas in solution can be inferred with some confidence from analyses made on compounds containing the ion when it is transferred to a new phase such as the solid.

Because the exchange method offers such a direct means of making a distinction between first sphere water, and other water, it is worthwhile to consider means of modifying it to bring the more substitution-labile cations within its scope. Measurements of rates of substitution on cations ordinarily considered labile with respect to such changes have recently been made[11] in CH_3OH as solvent at −75°. The results are useful in suggesting the order of magnitude of some of these specific rates for water exchange, and in planning the exchange experiments to meet the indicated requirements. The activation energies for substitution by CNS^- on the solvated ions were found to be 13 kcal. for Fe^{+++}, and 19 kcal. for Ni^{++}. Using these activation energies and a normal value for the frequency factor (10^{14} min.$^{-1}$) the half-time for exchange of water by water at 0° for Fe^{+++} is expected to be $\sim 10^{-4}$ min. and for Ni^{++}, ~ 0.1 min.

It may be possible to adapt a flow method to follow the water exchange reactions, using anodes spaced along a tube through which the mixed solution flows to sample the solvent as a function of time. A disadvantage of a method such as this is that it would require rather large quantities of enriched water. Preliminary research is required to test sampling by anodic oxidation. The oxygen liberated may not have the isotopic composition of the solvent at the electrode, but at some point downstream from it. This would be the case if the oxygen were formed from a water-exchangeable intermediate generated at the electrode and swept along with the solution. Another approach which is contemplated is to use a batch operation. One of the solutions contains an oxidizing agent, and the other a reducing agent. The properties of the oxidation–reduction system should be such that solvent oxygen is added to the reducing agent when it is oxidized, and the rate of oxidation, which can be controlled to some extent by adjusting the concentrations, should be such that this change is complete before much exchange of the hydrated cations has taken place. An oxidation–reduction reaction which may be adaptable to the use outlined is $SO_2 + Br_2$. The system is not ideal, however, because the rate of exchange of SO_2 with the solvent introduces a complication.

From the values of activation energy for substitution on a labile dipositive and tripositive ion which were quoted, it is evident that the exchange method in principle is capable of making a sharp distinction for them between directly bound and secondarily bound water. The activation energy for exchange of the latter should in all cases be

---

(4) J. P. Hunt and H. Taube, *J. Chem. Phys.*, **19**, 602 (1951).

(5) H. L. Friedman, J. P. Hunt and H. Taube, *ibid.*, **18**, 759 (1950).

(6) R. A. Plane and H. Taube, This Journal, **56**, 33 (1952).

(7) N. A. Bonner and J. P. Hunt, *J. Am. Chem. Soc.*, **74**, 1866 (1952).

(8) H. Taube, *Chem. Rev.*, **50**, 69 (1952).

(9) A. C. Rutenberg and H. Taube, *J. Chem. Phys.*, **20**, 825 (1952).

(10) F. A. Posey and H. Taube, unpublished observations.

(11) J. Bjerrum and K. G. Poulson, *Nature*, **169**, 463 (1952).

small, as it is for diffusion of water in water. It is by no means certain that such a sharp distinction is possible for all simple cations, even in principle. Thus water oriented in the first coördination sphere of Cs^+ for example may exchange as rapidly as solvent. Unfortunately it seems unlikely that a direct exchange procedure can be developed to investigate the interesting range of exchange lability in question.

The equilibrium fractionation of the oxygen isotopes in water exerted by salts is another phenomenon which can be exploited in learning about the interaction of ions and solvent.[12] In contrast to the exchange method, which leads to values of the first sphere hydration number without requiring the support of much additional observation or philosophy, the equilibrium method yields hydration number only indirectly, if at all. In spite of this limitation it appears to be a valuable tool for the problem at hand. Although a composite property is measured, it is informative to follow the variation of this property with ion charge, radius, geometry and electronic structure. Furthermore, observations can as readily be made for substitution-labile ions as for the substitution-inert ones, and if the value of the method is defined by work on ions which can be studied by independent means, there is hope of reward on applying it to very labile ions inaccessible to study by the exchange procedures for example.

The effect studied in the equilibrium fractionation method is the change in the ratio $(H_2O^{18}{}_l)/(H_2O^{16}{}_l)$ as a function of salt concentration (parentheses are used to denote activities). The activity ratio in question is conveniently measured using the equilibrium

$$CO_{2g} + H_2O^{18}{}_l = COO^{18}{}_g + H_2O_l$$

Assuming that the relative activities of CO_{2g} and $COO^{18}{}_g$ is given by their number ratio, the ratios of the quotients $(H_2O^{18}{}_l)/(H_2O^{16}{}_l)$ are directly measured by mass spectrometer readings on CO_2. The experiments demand high precision in mass spectrometer measurements, care in handling gas samples, and care in removing from the salts substances containing water-exchangeable oxygen.

The data can be analysed from the point of view that the ratio $(H_2O^{18}{}_l)/(H_2O^{18}{}_l)$ is altered by removal from the solution of one isotopic form of water in preference to the other, when the salts interact with solvent. The exchange of oxygen isotopes between hydrate water and solvent can be represented by the equation

$$H_2O^{16}{}_h + H_2O^{18}{}_l = H_2O^{18}{}_h + H_2O^{16}{}_l$$

so that

$$\frac{(H_2O^{18}{}_h)}{(H_2O^{16}{}_h)} \times \frac{(H_2O^{16}{}_l)}{(H_2O^{18}{}_l)} = K \qquad (3)$$

On the interpretation made, the activity ratios can be replaced by number ratios, and equation 3 becomes

$$\frac{W^{18}{}_h W^{16}{}_l}{W^{16}{}_h W^{18}{}_l} = K \qquad (4)$$

where W's represent number of water molecules. Consider a solution of molality m and let the number of molecules of water removed as hydrate water by each mole of salt be n. Then: $W^{18}{}_l + W^{18}{}_h + W^{16}{}_l + W^{16}{}_l = 55.51$ and $W^{18}{}_h + W^{16}{}_h = nm$. Let $W^{18}{}_l/W^{16}{}_l \equiv R$ (R_0 is the ratio with no salt present). From these, relation (5) follows

$$\alpha \equiv \left(\frac{R_0}{R} - 1\right) = \frac{nm(K-1)}{55.51} \qquad (5)$$

The equation is not exact (the approximation is made that the ratio of number ratios is the same as mole fraction ratios), but holds sufficiently well when R is small. The work is done with water of ordinary isotopic composition and the error due to the approximation is much less than other errors involved in the measurements.

Equation 5 requires a linear variation of α with molality of the salt. It shows, furthermore, that the composite property $n(K - 1)$ is measured in a study of the variation of α with m, and that additional philosophy is required to separate n and K.

Figure 1 shows typical results[13] for the variation of α with m. An important feature of the data is that whereas α/m is very sensitive to the nature of the anion, it is almost insensitive to change in the cation. This is illustrated by the large differences in α/m between $MgCl_2$ and NaCl on the one hand, and on the other, on the agreement of α/m for $MgCl_2$ with $Mg(ClO_4)_2$ as well as the mutual agreement of this ratio for NaCl, NaI and $NaClO_4$. The ratio α/m is therefore substantially a property of the cation only. The reason is presumably that cations but not anions orient water molecules making direct ion to oxygen bonds.

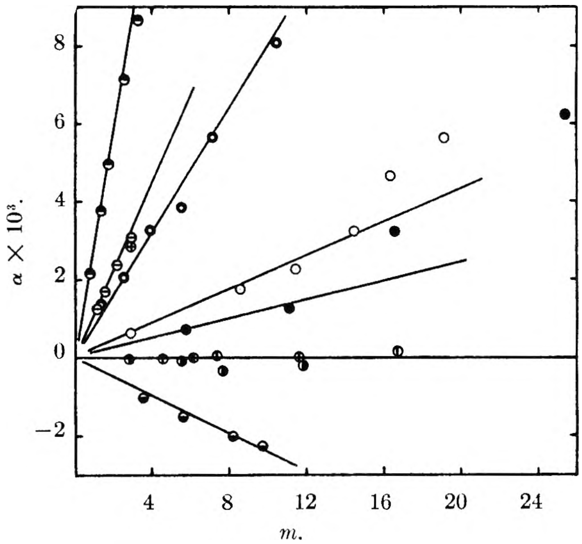

Fig. 1.—Effect of salts on fractionation of oxygen isotopes in water ($\alpha \equiv R_0/R - 1$; temp. 25° except for CsCl, data for which at 4°): ◓, $AlCl_3$; ⊖, $MgCl_2$; ⊕, $Mg(ClO_4)_2$; **O**, HCl; O, LiCl; ●, $AgClO_4$; ◑, NaI; ⦶, $NaClO_4$; ◐, NaCl; ◒, CsCl.

Another important question that arises in evaluating the data is the extent to which the isotope fractionation effect is accounted for by interactions in the first hydration sphere. The present indications are that at least with ions having relatively large values of charge/radius, the value of α/m depends largely on the effects in the primary hydra-

---

[12] H. M. Feder and H. Taube, *J. Chem. Phys.*, **20**, 1335 (1952).

[13] These data have been obtained by H. M. Feder, and will be incorporated in a Ph.D. Thesis to be submitted to the Department of Chemistry, University of Chicago.

tion sphere. Some direct evidence supporting this conclusion appeared as a by-product of the work on the exchange of hydrate water with solvent water.[4] The isotope ratio H_2O^{18}/H_2O^{16} in the distillate water from 1 M solutions of Al^{+++}, Ga^{+++}, Fe^{+++} or $Cr(H_2O)_6^{+++}$, each at exchange equilibrium, was observed to be in the range 7 ± 1 parts per 1000 below that expected for random distribution of isotopic forms, showing, as do the measurements presented in Fig. 1, that cations of high charge/radius tend to interact with H_2O^{18} in preference to H_2O^{16} in undergoing hydration. However, when the isotope composition of the distillate from a 1 M solution of $Cr(H_2O)_6^{+++}$ which has not undergone exchange with the solvent is examined, the ratio H_2O^{18}/H_2O^{16} is observed to be only 1 ± 1 parts per 1000 below that calculated for random distribution. The comparison of this result with those quoted previosuly shows that there is little selection between isotopic forms of water by forces outside the first sphere of hydration. A rationalization of the difference with respect to primary sphere and other water is this: whereas the oxygen of water makes new bonds when it enters the primary hydration sphere, when it interacts with the hydrated ion, it presumably does so by hydrogen bonding to the protons of the first hydration shell, and experiences much the same field as it does when it interacts with other solvent molecules. Thus the isotope discrimination exerted outside the first hydration sphere is not distinguishable from that exerted by the solvent.

The problem of the contribution to the fractionation effects by outer sphere interactions is also being approached making use of substitution-inert complex ions. The ion $Co\text{-}en_3^{+++}$ has the property that the en groups are not replaced by water under ordinary conditions. The value of α/m for $Co\text{-}en_3Cl_3$ is only $^1/_{13}$ of that found for $AlCl_3$. A more searching test is under way using the ion $Co(NH_3)_4(H_2O)_2^{+++}$. The over-all effect is measured, comparing the activity ratio $H_2O^{18}{}_l/H_2O^{16}{}_l$ after exchange equilibrium is reached with the value expected on the basis of the over-all composition of water in the system. The inner-sphere effect alone can be measured by removing the ion $Co(NH_3)_4(H_2O)_2^{+++}$ in the form of a solid (exchange equilibrium is attained slowly, and there is no isotope redistribution on precipitation) from which the hydiate water can be obtained, and comparing the isotopic composition of this water with the equilibrium $(H_2O^{18}{}_l/H_2O^{16}{}_l)$ ratio for the solution. The experimental procedures have been worked out, but the results are not yet complete.

The data of Fig. 1 show that at least for ions which have intense fields, α is a linear function of m. With HCl as solute, this has been proven for solutions up to 10 m. With both LiCl and $AgClO_4$, the linear relation fails at high concentrations of the salt. The deviations from the requirements of equation[5] may have the causes among others that coöperative effects involving also the anions, become important at high concentration or that the coördination numbers of the cations change. It seems possible that for ions such as H^+, which orient solvent strongly, the linear relation will be preserved to higher concentrations of electrolyte than is the case with LiCl and $AgClO_4$. An upper limit for the first-sphere hydration number can be calculated from the composition of the most concentrated solution, for which the linear relation is preserved. The general trend in the ratio α/m with properties of the cation is that it increases with the ratio charge/radius. Important deviations exist as illustrated by the comparison of the effects for Ag^+ and Na^+, and others are expected. As is evident from other data on affinities, the binding is not simply a function of the ionic potential, but bonding effects described as covalent become particularly important for ions with an exterior shell of 18 electrons.

It should be recognized that the isotope fractionation exerted by cations in constructing the hydration sphere is in competition with that exerted as a result of the mutual interaction of the molecules of the liquid. The oxygen isotope fractionation effects exerted on liquefaction are substantial, the equilibrium constant for the reaction

$$H_2O^{16}{}_l + H_2O^{18}{}_g = H_2O^{18}{}_l + H_2O^{16}{}_g$$

at 25° having a value of 1.0088.[14] One source of the fractionation effect for cations is the difference in vibration frequencies for the two isotopic forms of water along the new bond formed with water. When the force constants for this vibration are relatively great, the isotope discrimination in the hydration shell exceeds that exerted in the liquid, and positive values of α are observed, *i.e.*, H_2O^{18} is chosen in preference to H_2O^{16} in making the hydration shell. However, when the force constants for the vibration in question are low, the discrimination in the hydration shell may be less than that exerted in the liquid.[15] This is an explanation of the negative values of α observed for Cs^+ (as well as NH_4^+ and K^+, data for which are not reported), and suggests that these ions also make well defined hydration shells, but with relatively small values for the forces constant of the ion–water bonds. There is no paradox in requiring the force constants in the ion–water complex to be smaller than in water although the magnitude of the energy of interaction is known to be greater. The forces of attraction between water molecules falls off as the distance increases, more rapidly than between ions and water molecules. The value of $\alpha/m = 0$ for Na^+ can be regarded as resulting from the coincidence of the fractionation effects in the first hydration sphere and the liquid, rather than, as stated in an earlier communication,[12] as indicating that Na^+ does not hydrate. The alternative conclusion is suggested by the negative values of α/m for certain cations, as well as the observation that when the temperature changes, α/m for Na^+ changes.

An interesting subject for further study is the effect of increasing radius of the cations on the ratio α/m, using for example the series NH_4^+, $N(CH_3)_4^+$, etc. It seems likely that α/m cannot continue to

---

[14] M. H. Wahl and H. C. Urey, *J. Chem. Phys.*, **3**, 411 (1935).

[15] The fundamental frequency corresponding to the vibration of the water molecules as a unit in the liquid is *ca.* 175 cm.$^{-1}$. G. Bolla, *Nuovo. chim.*, **10**, 101 (1933); C. H. Cartwright, *Phys. Rev.*, **49**, 470 (1936); P. K. Narayanaswamy, *Proc. Ind. Acad. Sci.*, **27A**, 311 (1948)

become more negative, but that a minimum will be reached beyond which it will again approach zero. With cations of very large size, the effects presumably will not involve the orientation of water molecules to make a well defined hydration shell, but will involve largely distortions of the water–water interactions as the solvent adjusts to the form of the ion. The effect of a single substance of relatively low field has been tested. The solute CH_3CN gives a small negative value of α/m, about $^1/_8$ that for Cs^+.

Because the oxygen isotope discrimination appears to be largely a property of the first hydration shell for cations, it is of interest to investigate how this property can be used in arriving at hydration numbers. The approaches which are described below have not been tested, and must be regarded as speculative. They are offered, nevertheless, because there seems to be good likelihood of success with some of them, and because the experiments to test them will be undertaken.

1. One approach is to compare the measured values of $n(K - 1)$ with values calculated assuming a particular formula. A calculation which begins with fundamental properties of the particles interacting, cannot be carried through to a result which invites confidence. Rather, measured frequencies must be used, established in an environment in which the structure of the hydrated ion is known and in which the spectral analysis can be made. The complete vibration spectrum analysis for the ion in solution would of course obviate the necessity for the indirect approach to primary hydration numbers outlined here, but has not proven to be a practical procedure. 2. The comparison of the fractionation for the hydrated ion in an environment in which its formula can be proven with that in aqueous solution may lead to conclusions about the equivalence of the species in the different media. The hydrated ions can be characterized in the solid state, or in a non-aqueous solvent and the validity of the method can be tested using an ion such as $Cr(H_2O)_6^{+++}$ the formula for which is known in water as well as in a solid such as $Cr(H_2O)_6Cl_3$. 3. It may be possible to develop a relationship between K, the equilibrium constant for the isotope discrimination, and the acidity of the coördinated water. In general, factors which increase the force constants would be expected to increase the acidity of the water. A survey of some of the data on this basis, using plausible value of n is presented in Table I.

TABLE I

CORRELATION OF ISOTOPE DISCRIMINATION AND ACIDITY OF AQUO IONS

K_{diss} is the acidity per coördinated H_2O molecule; K' is the equilibrium constant for: $H_2O^{16}{}_h + H_2O^{18}{}_g = H_2O^{18}{}_h + HO^{16}{}_g$

Ion	K_{diss}	$n(K - 1)$	$(K' - 1)$
H_3O^+	37	0.040	0.048
$Al(H_2O)_6^{+++}$	2×10^{-6}	.149	.033
$Co(NH_3)_5H_2O^{+++}$	2×10^{-6}	.020	.028
$Mg(H_2O)_6^{++}$	10^{-12}	.059	.018
$Ag(H_2O)_2^+$	10^{-12}	.007	.012
$Li(H_2O)_4^+$	....	.011	.011

Substitution-inert ions will again be useful in testing the validity of the approach. The data shown in Table I, although they do not constitute an altogether dependable test, suggest that the relationship between K_{diss} and K' may be too indirect to survive large changes in coördination number, and will be of only limited usefulness. 4. A method which does seem promising for certain ions is to measure the effect on the observed fractionation of adding F^- to the cation. The fractionational change as a result of the substitution will depend at least in part on the fractional change in coördinated water. Even if the effect of the replacement is not merely statistical, as it would be for example if α/m decreased in the ratio $^5/_6$ for coördination of six water molecules, the contribution by additional effects can be determined, again exploiting a substitution-inert cation. The method depends for success among other things on the coördination number being unchanged when the complex ion is formed. For this reason the replacing group must be similar in size and polarizability to the water molecule.

It is evident that the indirect approach afforded by the equilibrium fractionation studies will not lead to conclusions which can be regarded as proven without making use of other methods. As the formulas of more ions are established, the validity of the method can be better defined. Even in its present form, it seems capable of supplying evidence, which together with that of another method of similar quality, can lead to dependable values of the first sphere hydration number. One such additional method, which does not appear to be appreciated generally but which indicates probable values of the first sphere hydration number for many colored ions is that of comparing the electronic absorption spectrum of the hydrated ion in solution with that of a known hydrated form in another medium. This method has been used with success by Friedman[16] in showing that the group $FeCl_4^-$ (in association with some cation) in ether does not interact with solvent or other molecules M $FeCl_4$ to increase the coördination number of Fe(III). The demonstration is particularly successful in this case because complexes with coördination numbers 4 and 6 can be separately characterized. Katzin and Gebert[17] have developed a strong case for the coördination number 6 for Co^{++} in water solution. Many tripositive aquo ions are known to have substantially the same spectrum in alums, where they are hexacoördinated as they have in solution.[18] However, in the absence of proof of the sensitivity of the spectrum of each particular ion to changes in coördination number the conclusions are not definite. In such cases, similarity of oxygen isotope fractionation in the two media would greatly raise the level of confidence in the conclusions.

Even if the fractionation studies fall short of the goal of establishing primary hydration numbers, they promise to be useful in solving a number of fundamental problems concerned with solvent ion interactions. Data of the kind shown in Fig. 1 will be of interest for series such as the dipositive ions

---

(16) H. Friedman, *J. Am. Chem. Soc.*, **74**, 5 (1952).

(17) L. I. Katzin and E. Gebert, *ibid.*, **72**, 5469 (1950).

(18) H. Hartmann and H. H. Schläfer, *Z. Naturforsch*, **6A**, 754, 760 (1951).

of the first transition series and the rare earth ions. The problem of whether in a labile complex ion system, the ligand replaces water, or interacts by outer-sphere association[19] can probably be answered by studying the change in the isotope fractionation exerted by the cation on mixing cation and ligand. Only if the ligand replaces water will the isotope fractionation be strongly affected. Also for a study such as this the method can be calibrated using a substitution-inert complex ion system.[19] It is likely that a number of irregularities in successive affinities as a ligand is added to a cation result from a change in coördination number along the series; thus in the system Cd^{++}–I^-, the aquo complex may well be $Cd(H_2O)_6^{++}$ and the terminal iodide complex $CdI_4^=$, may have no water in the first coördination sphere. Such an effect can probably be demonstrated by studying the oxygen isotope fractionation as a function of the concentration of the ligand species. Lastly is mentioned the possible usefulness of the measurements in learning the intensity of the interaction of square planar ions such at $Pt(NH_3)_4^{++}$ and water.

Fractionation studies of the type described for water promise to be particularly useful in a study of solvation in liquid ammonia. Complications due to solvent–solvent interaction are less severe than in water, and the lower temperatures which are accessible, as well as the generally stronger cation solvent interaction, combine to enhance the discrimination effect. The ammonia complexes of known formula in water can be exploited for comparison with the solvated cations in liquid ammonia.

Learning the coördination numbers of the principal forms of the solvated cations is only part of the problem when the chemical implications are considered. The principal form may exist in equilibrium with appreciable concentrations of a form of different coördination number. This equilibrium can exert a profound effect on equilibria involving the formation of complex ions such as $FeOH^{++}$ and $FeCl^{++}$. The addition of a large polarizable ion may favor the form of lower coördination number. Elucidation of the more complex problems implied is important not only in understanding equilibria, but also in interpreting rates of substitution on cations.

Acknowledgments.—I wish to acknowledge the contribution of the graduate students, whose experimental work forms the basis for this review, and many of whose ideas I have used without special acknowledgments. The experimental and theoretical work of H. M. Feder will be reported more fully in a separate paper. It is a pleasure also to acknowledge the financial support for the research by the Office of Naval Research (N6-ori-02026) and by the Atomic Energy Commission (Contract At(11-1)-92 for the purchase of a mass spectrometer).

---

[19] F. A. Posey and H. Taube, *J. Am. Chem. Soc.*, **75**, 1463 (1953).

THE ENTROPIES OF AQUEOUS IONS[1]

By R. E. Powell

Department of Chemistry and Chemical Engineering, University of California, Berkeley, California

Received April 12, 1954

Since the binding of a water molecule to an ion will occur with a decrease in entropy, the partial molal entropies of various ions can be correlated with their respective degrees of hydration. The literature on the entropies of individual ions is surveyed from this point of view. The entropies of monatomic ions, oxygenated ions and complex ions, of both positive and negative charges, can be systematized on the basis of their sizes and charges. The same treatment is applicable to ionic activated complexes, permitting the rationalization of the entropies of activation for reactions involving ions. Simple theoretical treatments, which regard the water as a continuous medium, or which regard water molecules as "frozen" to the ions, can be refined by taking into account the interaction of the ionic charge with the individual water dipoles.

It is natural to expect that the formation of a definite hydrate will be accompanied by the evolution of heat and a decrease in entropy, and, consequently, to accept these thermochemical changes as evidence of hydrate formation. A good example of the use of heat data in this fashion is found in the investigations by Katzin and coworkers,[2] who have found hydrates in solution for uranyl nitrate, cobaltous nitrate and cobaltous chloride in various organic solvents. In the following sections we shall examine the extent to which entropy data can indicate compound formation in solution, with particular reference to the problem of ion hydrate formation in aqueous solution. We must, however, be somewhat guarded in our acceptance of interpretations of thermochemical data, for it is now well known that heat and entropy effects can arise without the formation of definite compounds. One familiar example of this phenomenon is given by solutions of non-polar molecules whose sizes and solubility parameters are unequal.[3] Another is given by aqueous electrolyte solutions at finite concentrations, for which the now classic work of Debye and Hückel showed that the thermodynamic properties were explicable on the basis of long-range electrostatic interactions of the ions.

Entropies of Neutral Solutes.—As an illustration of the entropy behavior of non-electrolyte solutes in a non-polar solvent, the entropies of a number of solutes in benzene have been assembled from the

---

[1] Presented at the 123rd meeting of the American Chemical Society, Los Angeles, 1953.

[2] L. I. Katzin, D. M. Simon and J. R. Ferraro, *J. Am. Chem. Soc.*, **74**, 1191 (1952); L. I. Katzin and J. R. Ferraro, *ibid.*, **74**, 6040 (1952); **75**, 3821 (1953).

[3] J. H. Hildebrand and R. L. Scott, "The Solubility of Nonelectrolytes," *passim.*, 3rd ed., Reinhold Publ. Corp., New York, N. Y., 1950.

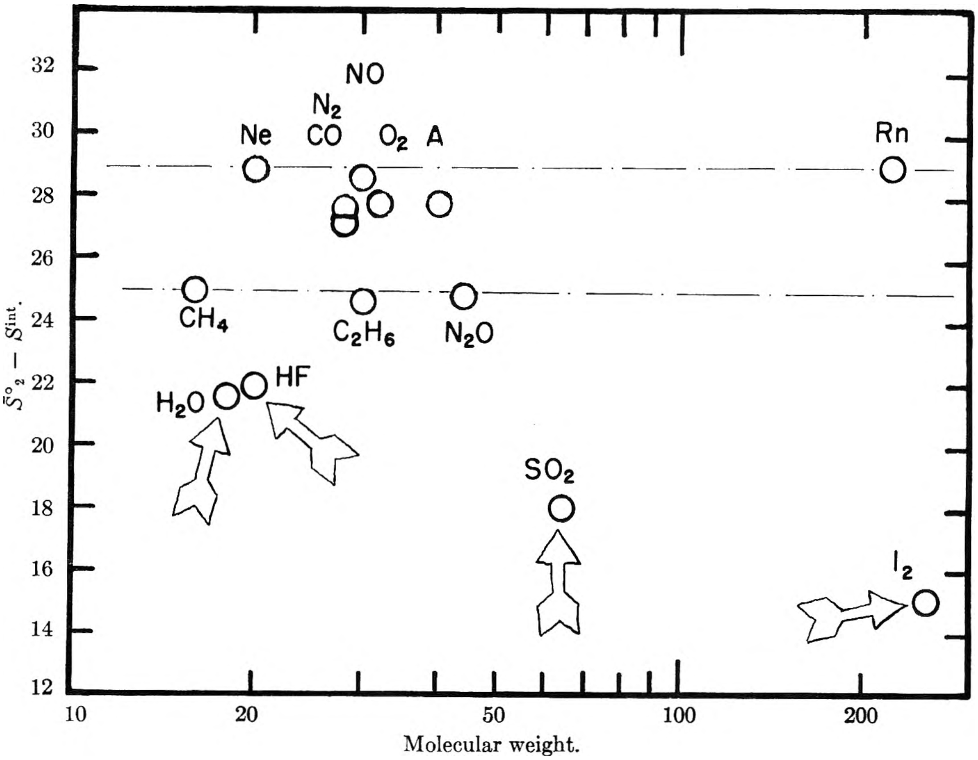

Fig. 1.—The entropies of some non-electrolytes in benzene solution.

literature and plotted in Fig. 1. Benzene was chosen as the solvent because a fairly large number of solubilities have been measured in it; other organic solvents, however, show about the same results. The plotted ordinate is the standard partial molal entropy of the solute (the standard state being the hypothetical 1 molal solution), diminished by the rotation and vibrational entropy of the molecule. The latter was evaluated by subtracting the Sackur–Tetrode entropy from the total entropy for the gaseous state; consequently, the entropy values displayed in Fig. 1 are to be regarded as the translational entropies in the condensed phase, on the assumption that the molecules are rotating and vibrating as freely as they do in the gas phase. Several features of Fig. 1 are worth pointing out.

(a) The entropies do not show any large dependence on molecular weight. Thus, the entropies of Ne and Rn are approximately the same.

(b) The entropies of the smaller polyatomic molecules are very nearly the same as the entropies of the monatomic gases, once the entropy of free rotation has been subtracted.

(c) A few solutes have abnormally low entropies: I_2, SO_2, HF and H_2O.

Observation (a), that the solute entropies do not show a great systematic increase with increasing molecular weight, turns out to be true also for other organic solvents and for water as a solvent. This is at first glance perplexing, for if the smoothed-potential partition function of the solute contains a factor $(2\pi mkT)^{3/2}V_f/h^3$, the corresponding entropy will surely contain a term ${}^3/{}_2R \ln M$. In an earlier paper,[4] this term was taken for granted, and ${}^3/{}_2R \ln M$ was therefore subtracted from each entropy value, with the result that a correlation was found between these modified entropies and the molar volumes. It now appears, of course, that the correlation was chiefly spurious, having been introduced by the intended correction. The theoretical explanation of the mass-independence of the entropy may take the following line. The smoothed-potential model of a liquid is, in its simplest form, not well suited to the description of a solute whose molecular weight is much greater than that of the solvent. The solute molecule is supposed to move like a particle in a rigid box, whose size and shape is determined by the average positions of the neighboring solvent molecules. But if the solute molecule is heavy, this is a poor description, because the solvent molecules will do most of the moving, while the solute molecule sits still. In this situation, there would be virtually no difference between a solute molecule 10 times as heavy as a solvent molecule, and a solute molecule 100 times as heavy. It would seem reasonable that the mass to be used in the description ought to be some sort of reduced mass of the respective molecules. The detailed statistical mechanics of such a system remains to be worked out.

Observation (b) leads one to conclude that the diatomic, triatomic and tetratomic molecules are very nearly freely rotating in solution. This observation is not entirely unexpected, for various investigators of pure liquids have concluded that there is, in general, a large degree of freedom of rotation in the condensed phase. As the solute molecules become larger and more unsymmetrical, it must be anticipated that they will rotate less and less freely in solution, so their entropies will be progressively lower. For the large group of solutes for which observations (a) and (b) are valid,

---

(4) R. E. Powell and W. M. Latimer, *J. Chem. Phys.*, **19**, 1139 (1951).

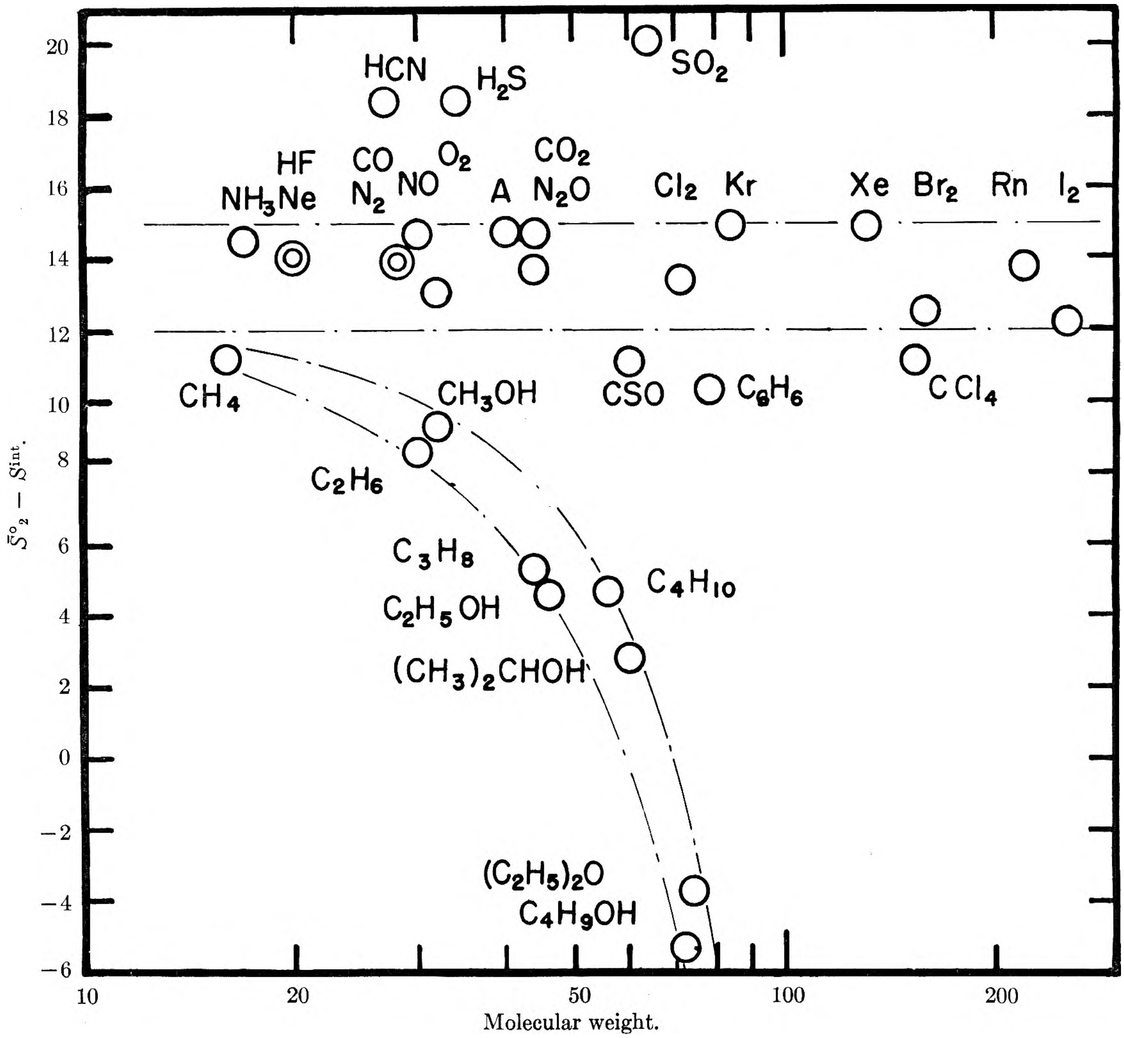

Fig. 2.—The entropies of some non-electrolytes in water solution.

we have several useful empirical rules for entropies in benzene (and, approximately, in other organic solvents). For monatomic gases, the partial molal entropy in solution is constant, approximately 28 e.u. For polyatomic gases, the entropy of free rotation and vibration must be added to this figure. The standard entropy change of vaporization of these solutes is then $\Delta S^\circ_{vap} = -2 + 3/2R \ln M$.

Observation (c) is the one of particular interest from the point of view of compound formation in solution. Iodine has an abnormally low entropy in benzene, and iodine has been shown to form an addition compound with benzene.[5] Sulfur dioxide has an abnormally low entropy, and it also has been shown to form a compound.[6] Hydrogen fluoride has an abnormally low entropy, and although there does not appear to be a direct experimental demonstration that it forms a compound with benzene, one is practically certain by analogy with the other halogen acids that it does so. The low entropy of water in benzene is suggestive of compound formation, although there is at present no evidence otherwise in support of this hypothesis. As to the numerical magnitudes of the entropy decreases which accompany compound formation in these cases, it is certainly an oversimplification to assign them to the loss of free rotation, for the situation must be more complicated; nevertheless, it is of interest to look at the figures. The entropy of rotation and vibration of I_2 is 19.8 e.u., and the entropy of I_2 in benzene is low by some 13 e.u.; the entropy of rotation and vibration of SO_2 is 20.8 e.u., and the entropy of SO_2 in benzene is low by some 10 e.u.

We turn now to the entropy of non-electrolyte solutes in water. The data from the literature have been plotted in Fig. 2. In a general way, the results are similar to those for benzene. The entropies of the rare gases are approximately constant at 14 e.u. With a few exceptions, the entropies of the smaller polyatomic molecules can be obtained by adding the entropy of free rotation and vibration to this figure. The corresponding entropy change of vaporization is $\Delta S^0_{vap} = 12 + 3/2R \ln M$. The comparatively low translational entropy of a solute in water (14 e.u.) compared with the same solute in benzene (28 e.u.) is consistent with the tightly-knit structure of liquid water and its high internal pressure, which would afford a comparatively small free volume to a solute molecule.

One class of exceptions to this simple entropy

---

(5) H. A. Benesi and J. H. Hildebrand, *J. Am. Chem. Soc.*, **71**, 2703 (1949).

(6) L. J. Andrews and R. M. Keefer, *ibid.*, **73**, 4169 (1951).

behavior is offered by the organic compounds of higher molecule weight—hydrocarbons, alcohols, ethers. For these compounds, $\bar{S}_2^0 - S^{\text{int}}$ is less than the usual +14 e.u., and the discrepancy becomes progressively greater for the larger molecules. This observation is easily explicable if we assume that the molecules of this sort are not entirely free to rotate; in fact, all of their entropies are brought into accord with the entropies of the smaller molecules if we assume them to retain only about 70% of their free rotational and vibrational entropy. It is not possible to be sure whether the diminution of entropy arises from the irrotational binding of the organic compound by the water molecules, or by some form of binding of water molecules by the organic compound (to give an "iceberg"), or by some combination of the two. However, the effect is so uniformly observed among organic solutes with different functional groups that one is unwilling to associate it with the formation of definite compounds; and, in this sense, it is unlikely that the organic compounds form definite hydrates in solution. On the other hand, it is entirely plausible that the water molecules arrange themselves in a "cage" about each solute molecule, while also remaining bound to the water molecules in the bulk of the solution, and such a cage may very well have a geometric structure like those which have been found for the crystalline gas hydrates.[7]

The other class of exceptions, for which $\bar{S}_2^0 - S^{\text{int}}$ is greater than +14 e.u., includes only SO_2, HCN and H_2S among those solutes we have examined. It seems fatuous to ascribe the discrepancy to a high polarity, inasmuch as the entropies of such substances as NH_3, HF, and the halogens appear to be quite normal. In the case of SO_2, the principal species present is probably H_2SO_3, and it is quite possible that the formation of this species, with its greater rotational entropy, has led to the actual increase in entropy. For HCN and H_2S this explanation cannot be offered, so at the moment they remain slightly anomalous. The experimental data, especially for HCN, are sufficiently uncertain that the entropy values may be somewhat in error.

Entropies of Ions in Water.—The utilization of ionic entropy data in the testing of various theories of the interaction of ions with water first became possible with the systematic experimental determination of these data. Thanks to the experimental work in a number of laboratories, particularly those of W. M. Latimer and of C. C. Stephenson, we now have at our disposal the entropy data for practically all of the common cations and anions. Moreover, now that the usefulness of entropy data has become widely recognized, measurements are being undertaken on a great many ions of special interest, such as the complex ions.

The ionic entropies cover a wide range of values, from about +60 e.u. for large ions of small charge to about −100 e.u. for small ions of large charge. The entropy effects arising from the interactions of ions and water are large ones, much larger, for example, than any of the effects noted for non-electrolytes in benzene or in water.

One of the simplest interpretations was that offered by Ulich.[8] He proposed that each ion is definitely hydrated, forming a little "iceberg," and that the entropy defect arising from this process could be computed by multiplying the hydration number by the entropy of crystallization of water, namely, −6 e.u. The hydration number he computed from conductivity data. In order to assess the validity of the model, we shall repeat some of his calculations, with the data currently available. The results are given in Table I for the ions Cs^+, Li^+, Ba^{++} and Mg^{++}. The entropy defect was calculated by subtracting 47 e.u. from the experimental entropy since any method of extrapolating to zero charge leads to a charge-independent entropy term of approximately this value. The hydration number was taken from a compilation by Tuck,[9] who obtained his results from equivalent conductances with the aid of a modified form of Stokes' law applicable to spheres of molecular dimensions. The ratio of these two quantities, as given in the last column of Table I, is supposed to represent the entropy of crystallization of water. As will be noted, this quantity is neither very constant nor very nearly −6 e.u., so the theory is not very satisfactory in a quantitative sense.

TABLE I

A TEST OF THE "ICEBERG" MODEL FOR IONIC ENTROPIES

Ion	Entropy defect	Hydration number	Entropy defect per mole of hydration
Cs^+	−15.2	3.93	−3.85
Li^+	−43.6	14.8	−2.95
Ba^{++}	−44	19.6	−2.25
Mg^{++}	−75.2	26.8	−2.80

An alternative theoretical approach which has received a great deal of attention is based on the famous Born model[10] in which the ion is regarded as a charged conducting sphere of radius r, and the water is regarded as a continuum of dielectric constant D. On this model, the electrostatic free energy of the ion in water is $Z^2/2Dr$ and the corresponding entropy is $(Z^2/2D^2r)\ (\mathrm{d}D/\mathrm{d}T)$. It will be observed that this model, in its simplest form, leads to an electrostatic entropy term which is proportional to the second power of Z. The comparison of this functional dependence with that found experimentally may be made by inspection of Fig. 3, in which the entropies of the monatomic ions are given, and of Fig. 4, in which the entropies of oxy-anions are given. In both cases, the entropy term is proportional to the first power of Z and not its second power. Figure 3 is taken, in a modified form, from reference 4; the modification consists in the omission of the $3/2R \ln M$ term, which has led to some changes in the numerical parameters. The empirical equation for the entropy of monatomic cations M^{+Z}, or anions A^{-Z}, becomes

$$\bar{S}_2^0 = 47 - 154Z/r_e^2$$

where the effective radius of the ion, r_e, is taken to be 1.3 Å. greater than the Pauling crystal radius for

---

(7) M. v. Stackelberg and H. R. Müller, *J. Chem. Phys.*, **19**, 1319 1951); W. F. Claussen, *ibid.*, **19**, 259, 1425 (1951).

(8) H. Ulich, *Z. Elektrochem.*, **36**, 497 (1930).

(9) L. D. Tuck, paper presented at the 118th meeting of the American Chemical Society, Chicago, 1950.

(10) M. Born, *Z. Physik*, **1**, 45 (1930).

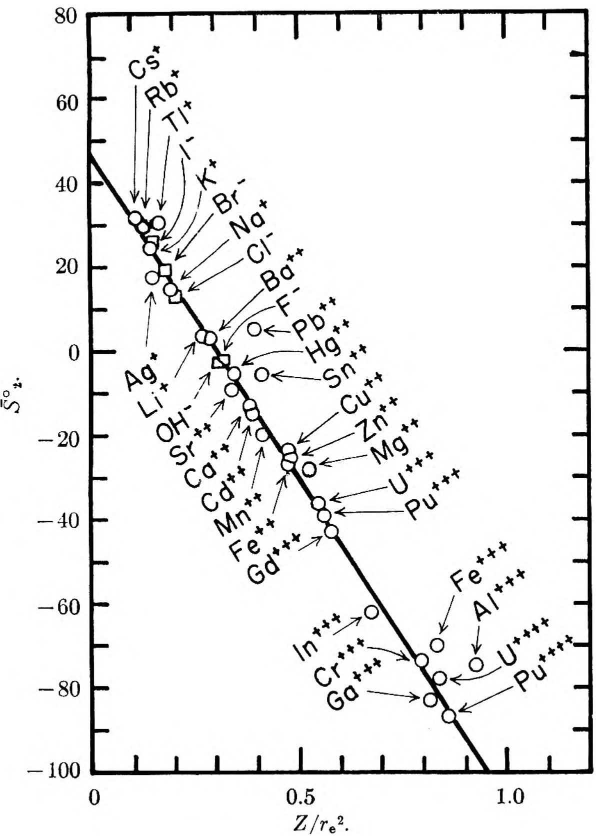

Fig. 3.—The entropies of some monatomic ions.

cations, and 0.4 Å. greater than the Pauling crystal radius for anions. The empirical equation for the entropy of an oxy-anion of the formula XO_n^{-Z} is, as illustrated in Fig. 4[11]

$$\bar{S}_2^0 = 43.5 - 46.5(Z - 0.28n)$$

While these empirical relations do not themselves provide a theory of the interaction of ions with water, they do serve as touchstones against which the existing theories may be tried. Clearly, the Born model cannot give ionic entropies satisfactorily without some modification. The empirical relation between the entropy and the first power of charge has been made use of by a number of authors.[12–14]

Several attempts have been made to calculate the entropy of interaction of ions with water on the basis of a more detailed molecular model of water.[4,15,16] Agreement between the theories and experiment can always be obtained, but, unfortunately, there are so many adjustable parameters in the theories that the agreement is not convincing.

In addition to the linear dependence upon ionic charge, there is one other respect in which ionic entropies require explanation, namely, in the magnitude of the charge-independent term. For monatomic ions this amounts to 47 e.u., and for oxy-

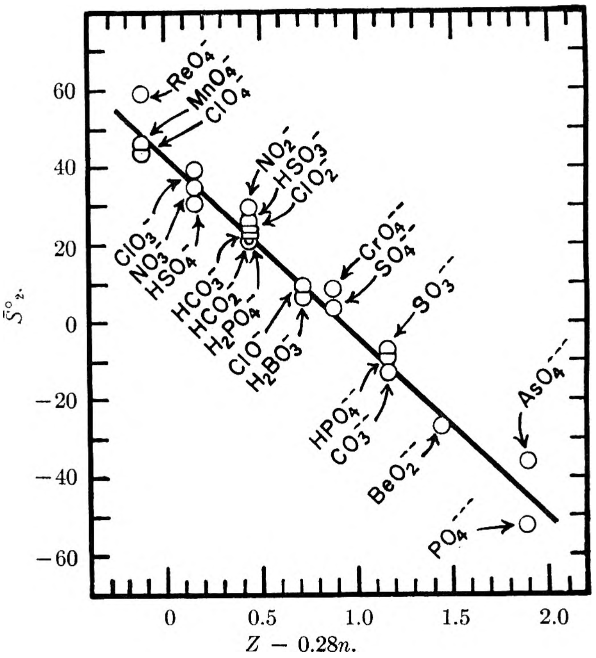

Fig. 4.—The entropies of some oxy-anions (from ref. 11, by permission of the *J. Chem. Phys.*).

anions to 43.5 e.u. or more. These figures are to be contrasted with the 14 e.u. for a typical non-electrolyte in water. What is the origin of this increase of thirty or more entropy units? One hypothesis, offered by Frank and Evans,[16] is that at some distance from each ion there is a disordered region, a "thawed belt," in which the bulk solvent has lost part of its usual quasi-crystalline structure. Another hypothesis which deserves some attention is that the additional entropy arises from rotation. One can easily calculate from their moments of inertia that the typical oxy-anions, if freely rotating, would have rotational entropy of 25–30 units. In addition they would have a somewhat smaller contribution from molecular vibrations. If this free-rotation hypothesis is to be applicable also to the monatomic ions, it becomes necessary to assume that the rotating unit is a definite ion hydrate.

Application to Reaction Kinetics.—When chemical reaction takes place between two ions, the entropy of activation depends strongly upon the charges on the respective ions. Those investigators who have concerned themselves with the theory of this effect[17] have made use of the Born model. As we have seen, the Born model is distinctly unsatisfactory for calculation of the entropies of stable ions, and there is no reason to expect it to be better for the ionic activated complexes. However, in default of a satisfactory theoretical treatment, the possibility remains that the entropies of activated complexes can be estimated fairly accurately on the basis of the same empirical rules applicable to ordinary species, and we shall examine this possibility.

We treat first the special case in which the two reactant ions have equal and opposite charges, so that the activated complex is a neutral molecule. Here the problem is to estimate the entropy of a neutral molecule, so we turn to the observations

(11) R. E. Connick and R. E. Powell, *J. Chem. Phys.*, **21**, 2206 (1953).

(12) L. V. Coulter and W. M. Latimer, *J. Am. Chem. Soc.*, **62**, 2557 (1940).

(13) A. F. Kapustinsky, *Acta Physicochem. U.R.S.S.*, **14**, 503 (1941).

(14) J. W. Cobble, *J. Chem. Phys.*, **21**, 1443, 1446 (1953).

(15) D. D. Eley and M. G. Evans, *Trans. Faraday Soc.*, **34**, 1093 (1938).

(16) H. S. Frank and M. W. Evans, *J. Chem. Phys.*, **13**, 507 (1945).

(17) For example, V. K. LaMer, *J. Franklin Inst.*, **225**, 709 (1938).

collected in Fig. 2. If two non-electrolyte molecules combine to form a single molecule, with no change other than the loss of translational entropy, the expected entropy change is -14 e.u. Consequently, if we can first evaluate the entropies of the pair of neutral molecules corresponding to the ions concerned, we need only add their entropies and subtract 14 units to have an estimate of the entropy of the activated complex. Let us consider, for example, the reaction

$$NH_4^+ + OCl^- = [NH_4OCl]^{\ddagger} = NH_2Cl + H_2O$$

which has been investigated kinetically by Weil and Morris.[18] We imagine the activated complex to be formed not from NH_4^+ and OCl^-, but from NH_3 (26 e.u.) and HOCl (31 e.u.). The estimated entropy of the activated complex is $26 + 31 - 14 = 43$ e.u. The experimental value for the entropy of the activated complex is 44 e.u.

For those reactions in which the activated complex is still ionic, we need to estimate the entropy of an ion which is not monatomic, or even relatively compact like the oxy-anions, but in which the charges are comparatively far separated. There are two methods of procedure here, which are, however, mathematically equivalent. The first, which was used successfully in ref. 11 to estimate the entropies of oxy-anions such as $Cr_2O_7^{--}$ and $S_2O_4^{--}$ is to estimate the entropy of each charged end of the molecule as though it were separate, and then to subtract a suitable amount of entropy (say 14 e.u.) for the loss on dimerization. The alternative procedure is to estimate the entropy as though the ion were a compact oxy-anion, and then to add some 30 e.u. to make allowance for the greater entropy of the extended ion (which presumably arises from the additional vibration and internal rotation, as well as the increased moment of inertia of the molecule as a whole).

As examples, let us take the reactions

$$OCl^- + OCl^- = [^-ClOClO^-]^{\ddagger} = Cl^- + ClO_2^-$$
$$OCl^- + ClO_2^- = [^-ClOClO_2^-]^{\ddagger} = Cl^- + ClO_3^-$$

which were studied by Foerster and Dolch.[19] For the first reaction, the activated complex is of the type XO_2^{--}, which if it were a compact oxy-anion would have an entropy of -23.5 e.u.; the estimated entropy of the complex is then $-23.5 + 30 = +6.5$ e.u., and the experimental value is found to be $+8$ e.u. For the second reaction, the activated complex is of the type XO_3^{--}, which if compact would have an entropy of -10.5 e.u.; the estimated entropy of the complex is then $-10.5 + 30 = +19.5$ e.u., which may be compared with the experimental value of $+21$ e.u. It must in all fairness be pointed out that this comparison of estimate with experiment is not as good as it appears, because the experiments are of relatively low precision and the experimental values cited, though carefully calculated from the original data, may be in error by as much as five to ten entropy units.

To take another example in which the charges are greater, there is the reaction

$$SO_3^{--} + S_2O_3^{--} = [^{--}O_3SSSO_3^{--}]^{\ddagger} = S_2O_3^{--} + SO_3^{--}$$

which was studied by Ames and Willard by means of radioactive exchange.[20] The estimated entropy of an ion of the type XO_6^{-4} is -64 e.u., so the estimated entropy of the complex is $-64 + 30 = -34$ e.u. From the average value of $\Delta S^{\ddagger}$ (-33 e.u.), and the entropy of SO_3^{--} (-7 e.u.) and $S_2O_3^{--}$ ($+15$ e.u.), the experimental value of the entropy of the activated complex is -25 e.u. Though the agreement is not very close, it must be pointed out that the experiments were carried out at ionic strength 2 rather than at zero ionic strength where the estimate is applicable.

---

[18] I. Weil and J. C. Morris, *J. Am. Chem. Soc.*, **71**, 1664 (1949).

[19] F. Foerster and P. Dolch, *Z. Elektrochem.*, **23**, 137 (1917).

[20] D. P. Ames and J. E. Willard, *J. Am. Chem. Soc.*, **73**, 164 (1951).

THE EFFECT OF PARAFFIN CHAIN SALTS ON THE CHARGE ON TEXTILE FIBERS

BY J. S. STANLEY

The University, Southampton, England

Received June 12, 1952

The electrokinetic potential of cotton, wool and nylon in solutions of paraffin chain salts has been determined, using streaming potential measurements and the charge density at the fiber surface calculated. On wool and nylon, paraffin chain anions are more strongly adsorbed from acid than from alkaline solutions; paraffin chain cations more strongly from alkaline than from acid solutions. The graph of the change of charge density, $\Delta\sigma$, with concentration of paraffin chain salt, resembles an adsorption isotherm, but it has not proved possible to identify $\Delta\sigma$ quantitatively with the amount of paraffin chain ion adsorbed.

Briggs,[1] Bull and Gortner,[2] Rabinov and Heymann,[3] Neale and Peters,[4] used streaming potentials to study the electrokinetic or zeta potential between textile fibers and aqueous solutions. Although in some cases the results are rather complicated, in general the potential tends to decrease as the salt concentration increases. The zeta potential is the difference in potential between the part of the double layer fixed so tightly that it does not move when the solution streams along the surface, and the interior of the solution; its value depends on the charge density at the surface and on the capacity of the double layer. The capacity increases as the thickness of the double layer decreases, and

---

[1] D. R. Briggs, THIS JOURNAL, **32**, 641 (1928).

[2] H. B. Bull and R. A. Gortner, *ibid.*, **35**, 309 (1931).

[3] G. Rabinov and E. Heymann, *ibid.*, **47**, 655 (1943).

[4] S. M. Neale and R. H. Peters, *Trans. Faraday Soc.*, **42**, 478 (1946).

since this thickness decreases with increasing concentration of electrolyte in the solution, the zeta potential should decrease, if the charge density remains constant, as the concentration of electrolyte increases. Assuming a Boltzmann distribution of ions in the diffuse double layer, the relation between the charge density σ and the potential ζ is, for a univalent electrolyte[5,6]

$$\sigma = \left(\frac{2NkT\epsilon}{\pi}\right)^{1/2} \sinh \frac{e\zeta}{2kT} \qquad (1)$$

ϵ is dielectric constant, e electronic charge, N number of anions or cations per cc. of solution. Neale and Peters[4] showed that the change in ζ with concentration of salt agreed fairly well with this equation, assuming σ constant.

Studies of the effect of surface-active solutes on ζ at fiber surfaces are few, but Neale and Peters[4] showed that a basic dyestuff caused the potential of cotton, initially negative, to become positive; and an acid dyestuff made ζ more negative.

Experimental

The apparatus (Fig. 1) was modified from that described by Lauffer and Gortner.[7] The fiber was packed in the cell C, 15 mm. long, 6 mm. diameter, internally, between two perforated platinum plates E_1, E_2, on which was deposited silver and silver chloride (or bromide), to render the plates (electrodes) reversible to chloride (or bromide) ions. The leads, L_1, L_2, from the electrodes were insulated from the water in the thermostat by enclosing in thick rubber tubing. The solutions were forced through the cell by applying a measured suction to one of the reservoirs, capacity about 150 cc., the other being at atmospheric pressure. The streaming potential was measured by an electrometer valve circuit, and the resistance of the cell by an audio-frequency bridge.

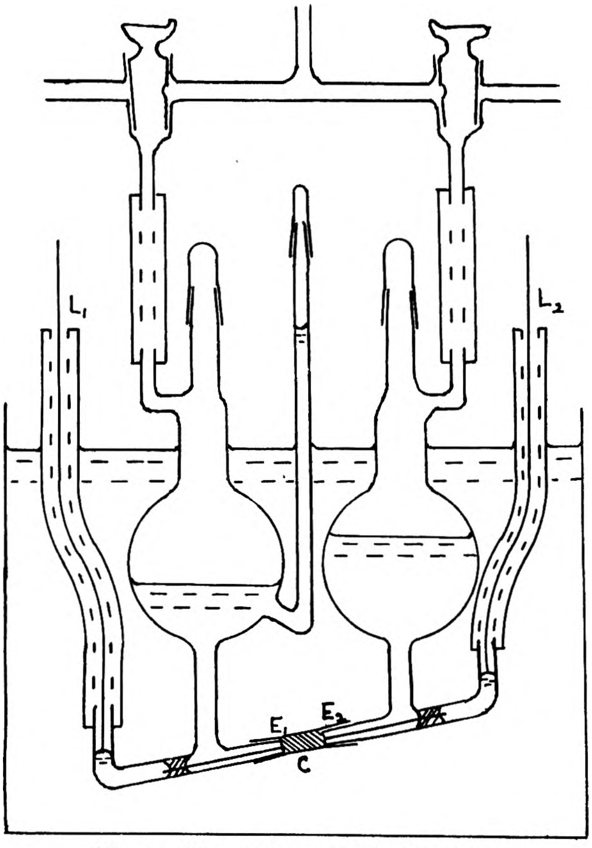

Fig. 1.—Streaming potential apparatus.

The zeta potential was calculated from the streaming potential H by the equation

$$\zeta = \frac{4\pi\eta\kappa_s H}{\epsilon P} \qquad (2)$$

P is the pressure driving the liquid through the cell, η the viscosity coefficient, ϵ the dielectric constant, taken as equal to that for water, κ_s the specific conductivity of the solution in presence of the fibre. κ_s was determined by measuring the resistance of the cell with the fiber plug in place, both with the solution and with KCl solution of known specific conductivity. The surface conductivity is thus included in κ_s.

Measurements were at first very erratic; this was traced to air bubbles forming on the surface of the fibers, and was cured by boiling the water used for the solution, and cooling under reduced pressure. The fiber plug was loosely packed; previous workers have found that ζ varies if the plug is too tightly packed, probably because some of the capillary channels are not much wider than the thickness of the double layer.

The streaming potential was accurately proportional to the pressure (*i.e.*, to the velocity of streaming) between 0 and 50 cm. of mercury pressure.

Cotton was first extracted with chloroform (Soxhlet, 6 hours), then with cold 2% acetic acid, and finally with water. Wool was extracted with light petroleum (40–60°), and with water, the temperature being kept always below 60°. Nylon was extracted with chloroform and water. All the fibers were given a final extraction with light petroleum after packing in the cell, to remove traces of grease which might have contaminated the surface when handling.

Cetylpyridinium chloride and cetylsodium sulfate were pure specimens provided by Professor Adam; dodecylsodium sulfate was prepared from carefully fractionated dodecyl alcohol (b.p. 102–103°, at about 0.03 mm.; m.p. 23.5–23.8°), by action of chlorosulfonic acid in ether[8]; Na, found 7.94%, theory 7.97%. Dodecylpyridinium bromide was prepared from dodecyl bromide by the method of Knight and Shaw.[9]

To ensure that the electrodes were reversible, small concentration of chlorides (or bromides) were added to all solutions. These decrease the critical concentrations for micelle formation (c.m.c.); and the c.m.c. in the presence of salts was determined approximately by measuring the surface tension (using Sugden's method[10]), and by taking as the c.m.c. the concentration at which the surface tension becomes practically constant. Table I shows the c.m.c.'s found.

TABLE I

Paraffin chain salt	C.m.c., M	Temp., °C.	Concn. of added salts
Cetylsodium sulfate	5×10^{-4}	55	0.004 M NaCl and NaOH at pH 11[a]
Dodecylsodium sulfate	5.8×10^{-3}	25	0.004 M NaCl and NaOH at pH 11[a]
Cetylpyridinium chloride	6.8×10^{-4}	25	0.001 M NaCl at pH 6[a]
Dodecylpyridinium bromide	9.3×10^{-3}	25	0.001 M KBr at pH 6[a]

[a] The pH was measured with a glass electrode (Marconi pH meter).

Results

ζ is negative for cotton, and is decreased continuously by increasing concentrations of NaCl (Fig. 2a); σ is negative and is increased by NaCl until a steady maximum is reached at about 0.002 M. This increase is probably due to preferential ad-

---

(5) H. A. Abramson, "Electrokinetic Phenomena," Chem. Catalog Co., New York, N. Y., 1934, p. 110.

(6) S. M. Neale, *Trans. Faraday Soc.*, **42**, 473 (1946).

(7) M. A. Lauffer and R. A. Gortner, THIS JOURNAL, **42**, 641 (1938).

(8) A. Grün and T. Wirth, *Ber.*, **55**, 2206 (1922).

(9) G. A. Knight and B. D. Shaw, *J. Chem. Soc.*, 682 (1938).

(10) S. Sugden, *ibid.*, 27 (1924).

sorption of chloride ions. Figure 2b closely resembles, quantitatively, the curve of σ against concentration found by Abramson[11] for graphite in NaCl solutions. The decrease in ζ at concentrations where σ is constant must be due to the thickness of the double layer decreasing, so that its capacity increases.

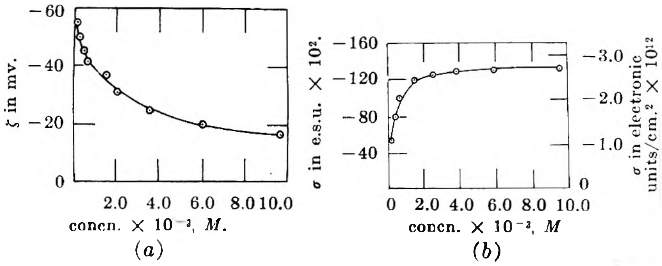

Fig. 2.—ζ and σ on cotton; NaCl solutions, pH 6.4, 25°.

Figures 3a and 3b show the effect of pH and of dodecylpyridinium bromide on wool. All concentrations were well below the c.m.c. (0.0093 M for this concentration of added salt). In the absence of paraffin chain salt, ζ is constant between pH 7 and 11.5, indicating that the number of dissociated basic groups on the wool surface becomes negligible at pH 7. Between pH 6 and 3, ζ falls almost linearly with decreasing pH, the iso-electric point being 3.4.

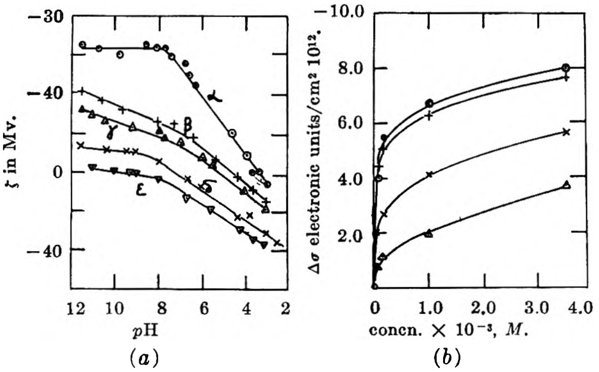

Fig. 3.—Wool, dodecylpyridinium bromide solutions, 25°: (a) variation of ζ with pH; concentration of dodecylpyridinium: (α) 0; (β) 6 × 10^{-5}; (γ) 2 × 10^{-4}; (δ) 10^{-3}; (ε) 3.6 × 10^{-3} M; (b) variation of $\Delta\sigma$ with c: ⊙, pH 9; +, pH 7; ×, pH 5; △, pH 3.

The dodecylpyridinium ion renders the surface more positive and, although there is a definite change in the slope about pH 7, when dodecylpyridinium ions are present, ζ is not constant but slowly rises as the alkalinity increases. It seems possible that ion-pairs are formed between dodecylpyridinium and carboxyl ions on the wool surface, and that these tend to be dissociated in the presence of large hydroxyl ion concentrations. The iso-electric point is displaced to more alkaline pH by the dodecylpyridinium ions, no doubt because these ions neutralize many of the COO^- ions on the surface. The increase in $\Delta\sigma$ as the acidity decreases (Fig. 3b) may be due to the number of dissociated COO^- groups increasing between pH 3 and 7 so that the adsorptive capacity of the surface for dodecylpyridinium ions increases in this range of pH. The curves in Fig. 3b resemble adsorption isotherms.

Figures 4a and 4b show that, at pH 11, wool adsorbs many more dodecyl sulfate ions than does cotton; the maximum adsorption on cotton appears to be reached about 0.001 M, while on wool the adsorption is still increasing at 0.0025 M. Figure 4c shows that ζ becomes constant at concentrations slightly below the c.m.c., with cetylsodium sulfate; with both fibers ζ changes by nearly the same amount, 7 mv. Figure 4d shows that cetylpyridinium, below the c.m.c., requires a very much smaller concentration to produce a given change in ζ than does dodecylpyridinium; the ratio of concentrations required to reduce ζ, −44 mv. initially, to zero, is about 80. This agrees with Traube's rule, since there are four additional CH_2 groups in the cetylpyridinium ion, so that the ratio of concentrations should be $3^4 = 81$. ζ again becomes nearly constant for some distance above the c.m.c.; at still higher concentrations ζ diminishes slightly, perhaps because the salt concentration is increasing and the thickness of the double layer is decreasing. $\Delta\sigma$ was not calculated for the cetyl salts, since above the c.m.c. the concentration of ions, N, required for equation 1, is unknown.

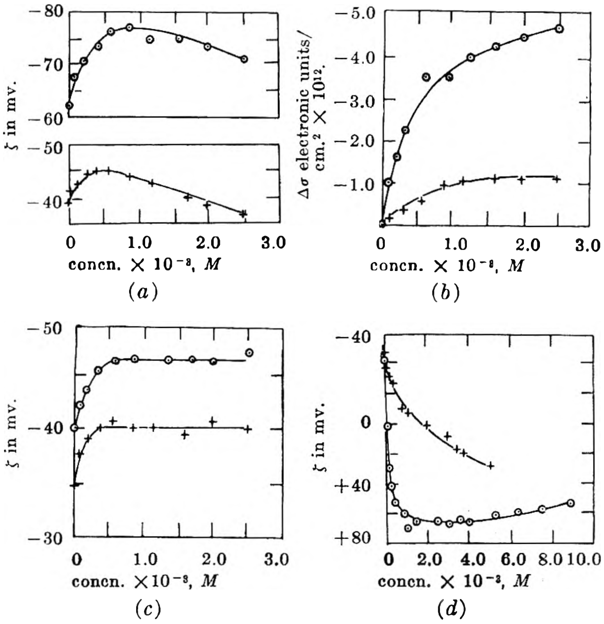

Fig. 4.—(a) and (b), effect of dodecylsodium sulfate solutions, pH 11, 25°, on ζ and $\Delta\sigma$ for wool (⊙) and cotton (+); (c) effect of cetylsodium sulfate solutions on ζ for wool (⊙) and cotton (+), pH 11, 55°; (d) effect of dodecylpyridinium bromide (+) and cetylpyridinium chloride (⊙) solutions on cotton, pH 6.4, 25°.

ζ for nylon was found to vary with pH in much the same way as found by Neale and Peters, except that the isoelectric point was found at pH 2.6 instead of 3.1 and the negative ζ-potentials were larger than found by Neale and Peters, in alkaline solutions. Figures 5a to 5d show that the adsorption of dodecyl sulfate ion is greater at pH 3 than at pH 11; while adsorption of dodecylpyridinium is greater at pH 11 than at pH 3. This difference is no doubt due to the sign and magnitude of the charge on the fiber. Adsorption does not reach saturation even at 0.005 M.

---

(11) H. A. Abramson, *Trans. Faraday Soc.*, **36**, 15 (1940).

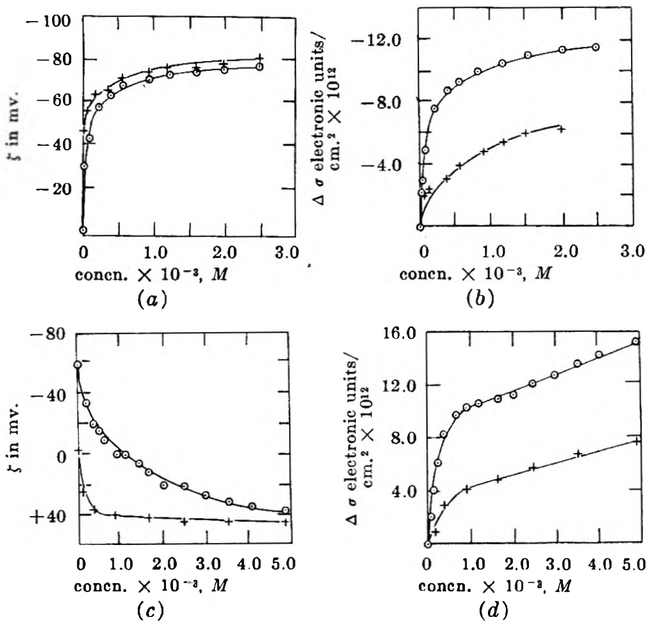

Fig. 5.—Effect of (a) and (b), dodecylsodium sulfate solutions at *p*H 11 (+) and *p*H 3 (⊙); (c) and (d), dodecylpyridinium bromide solutions on ζ and Δσ for nylon, 25°, at *p*H 11 (⊙) and at *p*H 3 (+).

An attempt was made to estimate whether the change in charge density, Δσ, caused by the paraffin chain salts, was quantitatively equal to the number of ions adsorbed. It is not possible to determine the number of ions adsorbed on a fiber surface with any accuracy; but it was hoped that, by comparing the values of Δσ on paraffin wax, and of Γ, the surface excess at the interface between paraffin oil and the aqueous solutions, some information on this point could be obtained. The paraffin wax was cut into lumps 1 to 2 mm. across before packing in the streaming potential cell. Γ was calculated from measurements of interfacial tension, made by the drop-volume method with a micrometer syringe, using Gibbs' adsorption equation

$$\Gamma = -\frac{1}{2RT}\frac{\partial \gamma}{\partial \ln c} \qquad (3)$$

2 being introduced in the denominator because the salt has two ions. Figures 6a and 6b show that the curves of Γ and Δσ against concentration are of similar shape, but that Γ, measured in ions per sq. cm., is about twenty times larger than Δσ in electronic units, except at very low concentrations. This difference may be due in part to the paraffin chain ions displacing some of the ions which imparted the charge to the fiber surface before paraffin chain ions were present; perhaps also to adsorption of gegenions on top of the adsorbed paraffin chain ions, and to differences between the structure of the interfacial films between water, and liquid and solid paraffin.

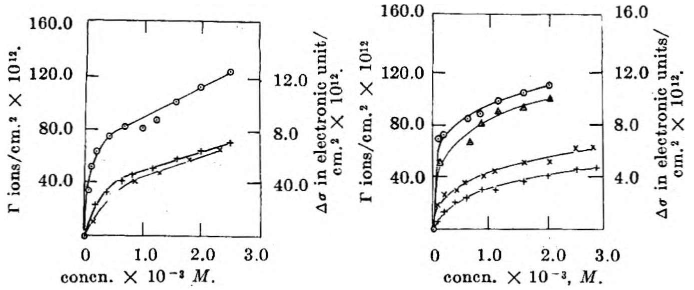

Fig. 6.—Comparison of Γ on paraffin oil with Δσ on paraffin wax: (a) dodecylpyridinium bromide ⊙, *p*H 3 and 11, Γ on oil; +, *p*H 11, Δσ on wax; ×, *p*H 3, Δσ on wax. (b) dodecylsodium sulfate solutions (⊙) *p*H 3, Δ, *p*H 11, Γ on oil (both); ×, *p*H 3, Δσ on wax; +, *p*H 11, Δσ on wax.

A few experiments were made on solutions of the commercial non-ionic detergent Lissapol N, which is a condensation product of polyethylene oxide with an alkylated phenol. At *p*H 11, ζ is decreased on wool from −70 mv. to −23 mv., at quite low concentrations of Lissapol N, about half that (c.m.c. in Fig. 7) at which the surface tension of solutions of this detergent become constant. At *p*H 3 Lissapol N has almost no effect on ζ. A specimen of nearly pure *p*-octylphenyloctaglycol ether, supplied by I.C.I. (Dyestuffs) Ltd. gave very similar results at *p*H 11, the minimum value of ζ being reached at about 0.0006 *M*.

My thanks are due to the Council of the British Launderers' Research Association for a maintenance grant, and to Mr. E. W. Balson and Professor N. K. Adam for valuable suggestions.

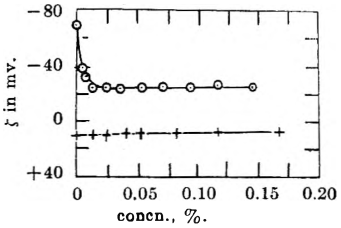

Fig. 7.—Effect of Lissapol N solution on ζ for wool, 25°: ⊙, *p*H 11; +, *p*H 3.

NOTE by Professor N. K. Adam.—The value 3.4 found here for the isoelectric *p*H of wool is equal to the lowest reported previously; Neale and Peters[4] found 3.4 on wool *fibers* in salt solutions with little buffering power, as used in this work. Harris[12] obtained 3.4 on *ground* wool in buffer solutions containing phthalate ions, but later Sookne and Harris[13] found 4.2 to 4.5 on ground wool or wool cortical cells in acetate buffers, ascribing the lower value to adsorption of phthalate ions on the ground wool particles. Adsorbed ions would displace the isoelectric point to a lower *p*H. Neale and Peters cleaned their wool with an anionic detergent; but in this work there seems no obvious source of adsorbed anions since the wool was cleaned with light petroleum. All these determinations were made by streaming potential or electrophoretic measurements, and refer to the surface, either of the intact fiber or of the ground wool particles. Determinations of the *internal* isoelectric point by combination with acids, bases, or other ions give results usually at least 4.5 and sometimes considerably higher.[14]

Whether the low value obtained here and by Neale and Peters[4] is the correct value for the surface of the intact wool fiber, or is due to some adsorbed substance which lowers isoelectric *p*H, is difficult to decide with certainty; but it seems not unlikely that the keratin molecules are oriented at the surface of the wool fiber so that the surface isoelectric *p*H is very different from that in the interior.

---

(12) M. Harris, *Am. Dyestuffs Reporter*, **21**, 399 (1932).

(13) A. M. Sookne and M. Harris, *ibid.*, **28**, 593 (1939).

(14) J. B. Speakman and E. Scott, *Trans. Faraday Soc.*, **30**, 539 (1934).

A DIELECTRIC STUDY OF THE AUTOXIDATION OF ETHYL SORBATE

By STERLING E. VOLTZ[1] AND M. WESLEY RIGG[2]

Chemistry Department of Temple University, Philadelphia, Pa.

Received December 17, 1953

The autoxidation of ethyl sorbate has been studied between 30 and 90° by measuring the change in dielectric constant. The energy of activation of the steady state is 15.7 kcal. per mole. The initial stages of the autoxidation are first order with an activation energy of 22.5 kcal. per mole. These values are in agreement with those obtained by independent methods. The catalytic effect of benzoyl peroxide and the inhibiting action of 2,5-di-*t*-butylhydroquinone have been studied. The autoxidation of ethyl sorbate has also been studied in benzene and glacial acetic acid. Sorbic acid has also been studied in the latter solvent. There is a maximum peroxide concentration observed during the early stages of the autoxidation of ethyl sorbate and a second one occurs during the maximum change in viscosity and color change (white to yellow). Acids are formed in the early stages of the autoxidation and their concentrations increase as the reaction proceeds.

Introduction

In many autoxidations and polymerizations the products have different electrical polarizations than the reactants, and the determination of the change in dielectric constant is a convenient means of studying the kinetics of the reaction. This method has been used to study the autoxidations and polymerizations of various hydrocarbons and oils.[3-9] In many cases the change in dielectric constant has been shown to be an accurate measure of oxidation; the slope of the curve was generally dependent on the experimental conditions. In most of the autoxidations studied, the dielectric constant increased along with the viscosity, refractive index, specific gravity, acid number and molecular weight; the iodine number may increase or decrease depending on the particular substances involved in the reaction. In most thermal polymerizations the dielectric constant does not change, but the power factor increases during oxidation or polymerization. The d.c. resistivity decreases during autoxidation, but in most cases it is very high.[10] Balsbaugh and co-workers[6] found that the a.c. conductivity usually increased during autoxidation, but peculiar conductivity curves were obtained in some instances due to the different types of products formed in the various stages of reaction. The calculation of an apparent dipole moment per oxygen molecule absorbed gave information relative to the type of oxygen compound formed.

In the autoxidation of conjugated olefins the oxygen generally adds 1,4 to the diene system.[11-13] The stable peroxides formed are polymeric and have often been reduced and hydrogenated to 1,4-diols; the corresponding 1,4-ketols have never been isolated. The polymeric peroxides contained as high as 20% of oxidation scission products. Carbon-to-carbon linked polymers are formed in the early stages of the autoxidation and are responsible for the decrease in refractive index and increase in viscosity and molecular weight. Non-peroxidic oxygen linked polymers have been observed in the later stages of oxidation.

Heinanen[14] found that the primary product in the autoxidation of methyl sorbate in benzene was a 1,4-cyclic peroxide and the other products included acetic acid and $CH_3OCOCH{=}CHCHO$. The first is from 1,4-addition of oxygen and that latter results from 3,4-addition.

Sorbic acid and its esters polymerize to dimers and trimers; the principal reactions are Diels–Alder additions.[15]

Experimental

Ethyl sorbate was prepared from sorbic acid by a modification of the method of Steffens[16] in which an acid catalyst was employed.[15] The yellow color was removed from the ethyl sorbate by steam distillation in the presence of sodium oleate or commercial soap powders. The distillate was then dried over anhydrous magnesium sulfate, redistilled and stored under nitrogen at −10°. Absorption studies indicated the color probably resulted from traces of unreacted sorbic acid or oxidation products of ethyl sorbate.

Benzene was purified by the method of Daniels[17] and reagent grade glacial acetic acid was used without further purification. Benzoyl peroxide and 2,5-di-*t*-butylhydroquinone were purified by recrystallization.[18,19]

Preliminary dielectric measurements were made with an apparatus similar to that described by Alexander[20] and Bender.[21] The changes in capacitance during the autoxidations were determined at 3.5 megacycles with a resonance apparatus similar to an amateur radio transmitter.[22] Modifications included voltage regulator circuits, milliammeters in the plate circuits of the oscillator and amplifier and efficient shielding. A model 722-D General Radio calibrated condenser was used; a polystyrene rod was mounted on the handle to eliminate capacitive effects.

The dielectric constant cell consisted of three concentric, gold-plated brass cylinders. The inner and outer ones (electrically connected) served as one plate of a condenser and the middle one, which was insulated from the other two,

---

[1] Houdry Process Corp., Marcus Hook, Pa.

[2] C. F. Braun and Co., Alhambra, Calif.

[3] T. G. Kovalov, *Izvest. Tsentral' Nauch. Issledovatel' Inst. Pishchevoĭ i Vkussyoi Prom. Narkomsnaba S.S.S.R.*, 3 (1931).

[4] E. M. Yakimetz, *J. Tech. Phys. (U.S.S.R.)*, **4**, 499 (1934).

[5] E. A. Arnold, *J. Inst. Fuel*, **10**, 418 (1937).

[6] J. C. Balsbaugh and co-workers, *Ind. Eng. Chem.*, **30**, 287 (1938); **31**, 318 (1939); **32**, 1497 (1940); **33**, 1321 (1941); **34**, 92 (1942) .

[7] E. Hazlehurst, *Paint Manuf.*, **13**, 302 (1942).

[8] G. A. O'Hare, P. S. Hess and A. F. Kopacki, *J. Am. Oil Chemists' Soc.*, **26**, 484 (1949).

[9] G. A. O'Hare and W. J. Winthrow, *Ind. Eng. Chem.*, **30**, 101 (1947).

[10] T. E. Reamer and R. G. Larsen, *ASTM. Bull.*, **149**, 58 (1947).

[11] R. W. Bauer and L. T. Steadman, *J. Am. Chem. Soc.*, **66**, 563 (1944).

[12] E. H. Farmer, *Discs. Faraday Soc.*, 230 279 (1945); *Trans. Faraday Soc.*, **42**, 228 (1946); *Trans. Inst. Rubber Ind.*, **21**, 122 (1945).

[13] R. T. Holman and co-workers, *J. Am. Chem. Soc.*, **67**, 1386, 1390, 1669 (1945); **68**, 562 (1946); *Arch. Biochem.*, **7**, 47 (1945); **10**, 519 (1946).

[14] P. Heinanen, *Acta Chem. Fennica*, **8B**, 5 (1935).

[15] M. W. Rigg and R. Rosenthal, *J. Am. Chem. Soc.*, **71**, 2865 (1949). This reference cites earlier references.

[16] J. A. Steffens, U. S. Patent 1,421,604 (1922).

[17] F. Daniels, J. H. Mathews and J. W. Williams, "Experimental Physical Chemistry," McGraw–Hill Book Co., Inc., New York, N. Y., 1941, p. 445.

[18] P. F. Oesper and C. P. Smyth, *J. Am. Chem. Soc.*, **64**, 768 (1942).

[19] P. F. Oesper, C. P. Smyth and M. S. Kharasch, *ibid.*, **64**, 937 (1942).

[20] F. Alexander, *Electronics*, **18**, No. 4, 116 (1945).

[21] P. Bender, *J. Chem. Educ.*, **23**, 179 (1946).

[22] "Radio Amateurs Handbook," A.R.R.L., 1948, p. 170.

was the second plate. The condenser was sealed in a glass reactor directly above a sintered glass disk. The reactor was then placed in a thermostated oil-bath.

Tank oxygen was used without purification except for drying. A reflux condenser was mounted at the outlet of the reactor and the exit gases were passed through a cold trap at −78°.

Peroxide values were determined by the method described by Lundberg and Chipault.[23] The acid concentrations were determined by titrating samples of the oxidized products with standard sodium hydroxide with phenolphthalein as the indicator.

In a typical run, one-half mole of ethyl sorbate was placed in the reactor and oxygen was passed through. In all the runs reported in this paper, the oxygen was bubbled through the reactor sufficiently fast that the rate of oxidation was independent of the oxygen flow rate.

Results

The autoxidation of ethyl sorbate has been studied between 30–90° and typical curves of the changes in capacitance are shown in Fig. 1. These curves are similar to the oxygen absorption curves obtained by Smith.[24] The average rate constants for the steady state have been calculated from the results of a number of experiments (not only those shown in Fig. 1) and are tabulated in Table I. The corresponding rate constants from Smith's data are summarized in Table II. The average energies of activation of the steady state from these data are 15.7 and 14.8 kcal. per mole, respectively. Clearfield[25] has reported a value of 17.5 kcal. per mole.

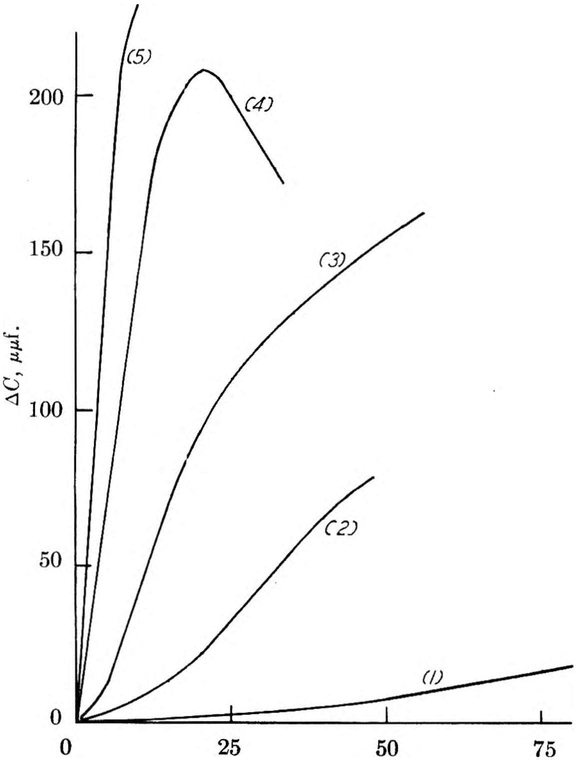

Fig. 1.—Capacitance changes during the autoxidation of ethyl sorbate: curve (1), 30°; (2), 45°; (3), 60°; (4), 75°; (5), 90°.

TABLE I

STEADY STATE REACTION CONSTANTS FROM DIELECTRIC DATA

k, $\mu\mu f$./hr.	0.392	2.13	6.65	15.4	28.0
Temp., °C.	30	45	60	75	90

TABLE II

STEADY STATE REACTION CONSTANTS FROM OXYGEN ABSORPTION DATA

E.S. = ethyl sorbate

k, mole O_2/mole E.S./hr.	0.0183	0.0652	0.250
Temp., °C.	45	60	75

During the initial stages of the autoxidation the changes in capacitance are first order and can be represented by the equation

$$\log(\Delta C_f - \Delta C_t) = -kt + \log \Delta C_f$$

where

ΔC_f = capacitance of the oxidized products − initial capacitance

ΔC_t = capacitance at time t − initial capacitance

The average first-order rate constants are given in Table III. The corresponding energy of activation is 22.5 kcal. per mole.

TABLE III

FIRST-ORDER REACTION RATE CONSTANTS

k, hr.$^{-1}$	0.00026	0.0012	0.0039	0.0302
Temp., °C.	30	45	60	75

The average first-order rate constants from the oxygen absorption curves of Smith[24] are 0.0078 hr.$^{-1}$ at 45° and 0.046 hr.$^{-1}$ at 60°. The energy of activation corresponding to these rate constants is 25.5 kcal. per mole.

Smith[24] applied a first-order rate equation throughout the complete oxidation. Careful analysis of his results show that his calculations are in error, and that a first-order equation is not applicable throughout the entire reaction. The rate constants presented in this paper have been independently calculated by the authors from the original data of Smith.

Plots of capacitance changes against oxygen absorption are linear over the range for which absorption data are available. Similar results have been reported by Balsbaugh and co-workers for several other substances.[6] These workers generally employed a kinetic equation with two constants, which was applicable throughout most of the reaction. This type of equation can be applied to the data for ethyl sorbate, but the authors feel that separate treatments of the initiation and propagation steps are fully justified.

The decrease in capacitance observed in the final stage of the reaction at 75° (Fig. 1) is probably due to the decomposition of an unstable intermediate product. This effect was observed in all the runs at 75° and undoubtedly would have occurred at 90°, if the reactions could have been continued longer. In most cases the reactions were discontinued, when the oxidation products became too viscous for the passage of oxygen through them.

The peroxide concentrations during the autoxidations of ethyl sorbate were determined at various time intervals and the results are shown in Fig. 2.

---

(23) W. O. Lundberg and J. R. Chipault, *J. Am. Chem. Soc.*, **69**, 833 (1947).

(24) R. Smith, Thesis, Temple University, 1949.

(25) A. Clearfield, Thesis, Temple University, 1950.

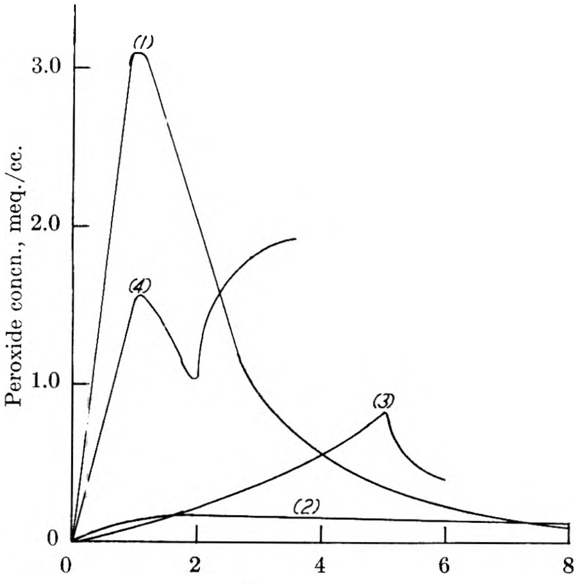

Fig. 2.—Peroxide concentrations during the autoxidation of ethyl sorbate: curve (1), 45°; (2), 60°; (3), 75°; (4), 90°.

Large maxima were observed at 45 and 90° after one hour. At 60° the peroxide concentrations are much lower, but a slight maximum occurred in the initial stages of the reaction. At 75 and 90° there were high peroxide concentrations at times corresponding to the maximum changes in viscosity and color (white to yellow). The large peroxide values at 45° probably result from the increased stability of the intermediate peroxide at that temperature. At 60° and higher the peroxide concentrations increased with increasing temperature.

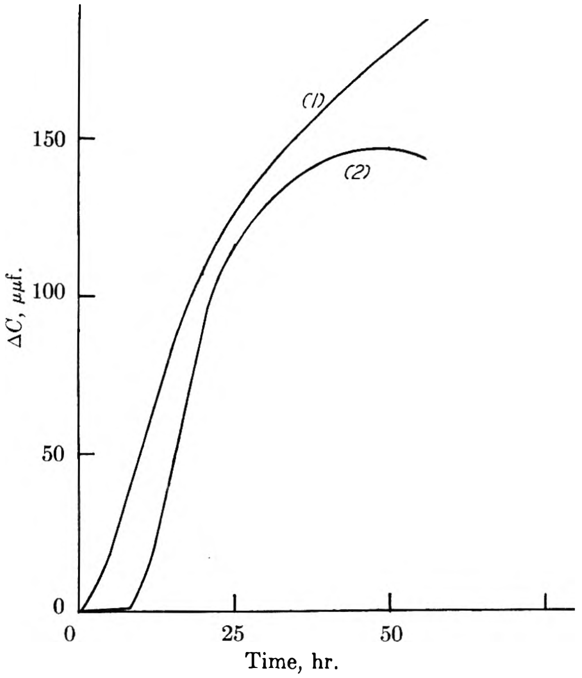

Fig. 3.—Effects of benzoyl peroxide (curve 1) and 2,5-di-*t*-butylhydroquinone (curve 2) on the autoxidation of ethyl sorbate at 60°.

Most autoxidations are considered to take place by free radical mechanisms. Benzoyl peroxide is used as a catalyst in many commercial processes that involve free radical reactions such as polymerizations. The effect of this catalyst on the autoxidation of ethyl sorbate at 60° is shown in Fig. 3 (curve 1). In this experiment 0.01 g. of benzoyl peroxide was added to one-half mole of ethyl sorbate. Curve (2) shows the effect of the same amount of a free radical inhibitor, 2,5-di-*t*-butylhydroquinone. Runs were made at higher concentrations of these substances, but the effects were only slightly greater than those shown in Fig. 3. The catalytic action of benzoyl peroxide and the inhibiting effect of the hydroquinone suggest that the autoxidation of ethyl sorbate involves a free radical mechanism. At the end of the inhibition periods, the rates of reaction were very fast; a slight decrease in capacitance was observed near the end of these runs.

The autoxidation of ethyl sorbate in benzene was studied at 45 and 60°. In these experiments the oxygen was saturated with benzene at the temperature of the reaction, before it entered the oxidation

TABLE IV

AUTOXIDATION OF ETHYL SORBATE IN BENZENE (45°)

Time, hr.	Capacitance changes, μμf.	Peroxide concn., meq./cc.	Acid concn., meq./cc.
	8.26% Ethyl Sorbate		
0.5	0.05	0.47	....
1	.13	.50	0.0054
2	.25	.24	.0062
3	.42	.12	.0066
4	.37	.16	.0077
6	1.48	.09	.0091
8	2.59	.02	.0122
	16.42% Ethyl Sorbate		
0.5	0.24	0.39	....
1	0.58	.44	0.0110
2	1.21	.78	.0120
3	1.68	.26	.0165
4	1.98	.23	.0140
6	2.97	.33	.0340
8	4.77	.12	.0321

TABLE V

AUTOXIDATION OF ETHYL SORBATE IN BENZENE (60°)

Time, hr.	Capacitance changes, μμf.	Peroxide concn., meq./cc.	Acid concn. meq./cc.
	8.22% Ethyl Sorbate		
0.5	0.08	0.50	....
1	0.16	1.17	0.0067
2	0.36	1.06	.0077
3	0.86	0.60	.0079
4	1.72	.45	.0085
6	2.25	.12	.0102
8	3.45	.02	.0118
	15.79% Ethyl Sorbate		
0.5	0.42	0.77	....
1	0.81	.29	0.0117
2	2.04	.16	.0124
3	2.99	.11	.0155
4	4.04	.15	.0196
6	5.93	.31	.0241
8	6.82	.16	.0342

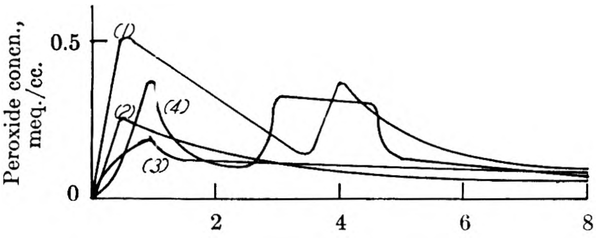

Fig. 4.—Autoxidation of ethyl sorbate (10%) in glacial acetic acid: curve (1), 45°; (2), 60°; (3), 75°; (4), 90°.

cell. This technique reduced the loss of benzene from the oxidation mixture. The changes in capacitance, peroxide concentrations and acid concentrations are given in Tables IV and V. Maximum peroxide concentrations occurred during the first few hours of the autoxidations. Appreciable amounts of acids were formed in the initial stages of the reaction, and there were steady increases in the acid concentrations as the reaction proceeded. The high peroxide values at 60° are difficult to understand.

Ten per cent. solutions of ethyl sorbate and sorbic acid in glacial acetic acid were oxidized from 45 to 90°. The peroxide concentrations are shown in Figs. 4 and 5. Maximum peroxide values were observed during the first hour at the autoxidations of the ethyl sorbate solutions. The maximum at 45° is greater than the one at 90°, both of which are larger than those at 60 and 75°. These results are similar to those obtained for pure ethyl sorbate (Fig. 2). Secondary maxima were also observed at 45 and 90°.

The autoxidation of sorbic acid was only studied in glacial acetic acid as this compound is a solid at all the temperatures studied, and its solubility in benzene was found to be much lower than that reported by earlier workers. Solutions of sorbic acid in glacial acetic acid are light yellow, but during the autoxidation they turn red; at 90° the most pronounced color change occurred after two hours and at 75° after 3.5 hours. There were maxima in the peroxide curves during the first hour of the oxidations (Fig. 5). The solutions at 75 and 90° had low peroxide concentrations (0.06–0.08 meq. per cc.) at 2.5 hours. These values are much lower than the smooth curves (3 and 4 of Fig. 5) obtained from all the other values at these temperatures. The inclusion of these values would require sharp minima in curves (3) and (4) of Fig. 5 at 2.5 hours, which seems unreasonable upon consideration of all the other values. It may be, however, that these low values are related to the observed color changes.

All attempts to isolate urea complexes of the autoxidation products of ethyl sorbate and sorbic acid were unsuccessful. When ethyl sorbate was added to methyl alcohol saturated with urea, a white precipitate (unreacted urea) was obtained,

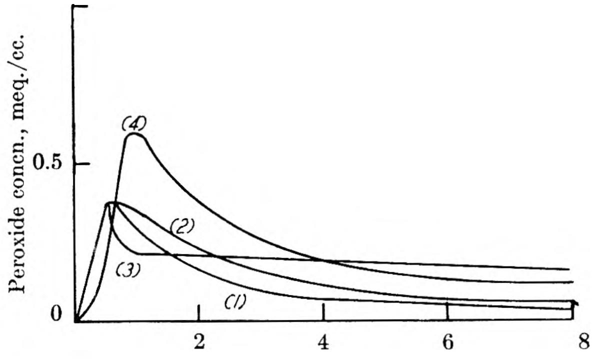

Fig. 5.—Autoxidation of sorbic acid (10%) in glacial acetic acid: curve (1), 45°; (2), 60°; (3), 75°; (4), 90°.

probably due to a decrease in the solubility of urea in the presence of ethyl sorbate.

Samples of ethyl sorbate were oxidized for one hour at 45° (a maximum peroxide value was obtained under these conditions) and then the reaction mixture was reduced by the method used for peroxide determinations. The reduced forms of any peroxide or hydroperoxide present should conceivably be alcohols. Analyses of the reduced materials indicated the probable presence of an unsaturated diol.

Discussion

There are three possible mechanisms by which the initial oxygen attack can take place, which can be identified as 1,2-, 1,4-, and 3,4-addition. The probable sequences of reactions initiated by each one are outlined below

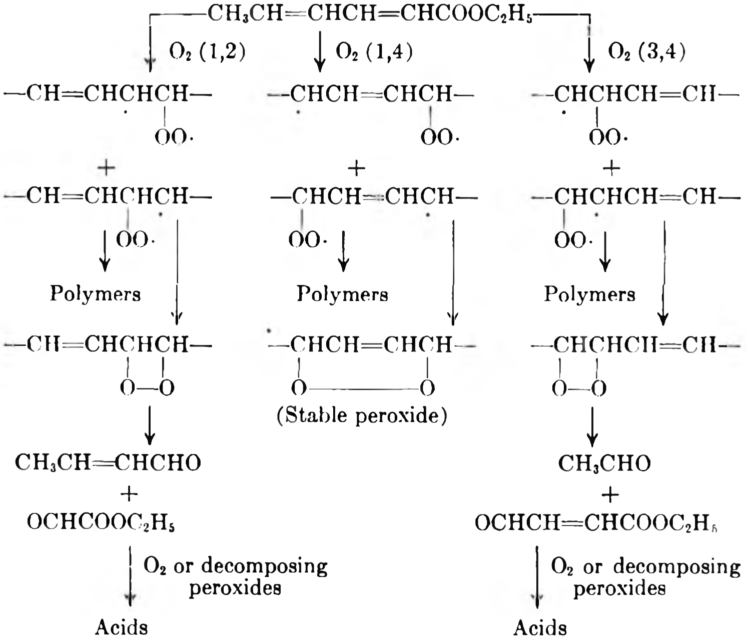

The primary product obtained in the cold trap was acetaldehyde, and appreciable quantities were only obtained at the higher temperatures used. No aldehydes or ketones could be detected in the liquid phase at the lower temperatures studied. Since the final oxidation products of 1,2- and 3,4-additions are aldehydes (or acids), it seems reasonable to conclude that the initial attack by the oxygen is primarily 1,4-addition. The concentrations of acids present can be assumed to be a measure of the amounts of 1,2- and 3,4-additions that take place. At 45° the acid concentrations are very small compared to the peroxide values, which is further evidence that the initial reaction must be primarily 1,4-addition. The extent of 3,4-addition appears to increase with increasing temperatures as evidenced by the amounts of acetaldehyde obtained at higher temperatures. There is no experimental evidence to show that 1,2-addition takes place. These results are similar to those obtained by Farmer[12] and Heinanen.[1]

The six-membered cyclic peroxide is undoubtedly much more stable against decomposition than either of the possible four-membered cyclic peroxides. This type of behavior has been observed in many organic compounds.

The initial first-order portion of the autoxidation of ethyl sorbate decreases with increasing temperature and actually disappears at 75°. This behavior may result from the decreased 1,4-addition that takes place at higher temperatures. This would infer that the initiation step of 1,4-addition is first order and that of 3,4-addition is zero order. Of course, the disappearance of the first order initiation step may only be a temperature effect. The peroxide values at 45 and 90° are much larger than those at 60 and 75°, which indicates that the peroxide concentrations go through a minimum between 45–90°. This strongly suggests that different mechanisms are operative at 45 and 90°.

The presence of such large numbers of unsaturated compounds in the reaction mixture probably leads to numerous side reactions, such as the formation of low molecular weight polymers, through Diels–Alder type reactions.[15] Farmer has indicated that the polymers, which are formed from the peroxide radicals, can undergo decomposition to aldehydes.[12]

One of the outstanding results of this study is the close correspondence between the dielectric curves and the oxygen absorption curves. This is especially significant in view of the complexity of the reaction mixture. The dielectric method should prove exceedingly valuable in studies of the autoxidations of compounds, which form stable peroxides and do not lead to so many side reactions.

Acknowledgment.—The authors wish to express their appreciation to the Research Council of Temple University for the research grant that made this work possible and to the members of the Chemistry Department for their coöperation.

THE CRITICAL MICELLE CONCENTRATION OF SOAP MIXTURES (TWO-COMPONENT MIXTURE)

BY KŌZŌ SHINODA

Department of Physical Chemistry, Faculty of Engineering, Yokohama National University, Minamiku Yokohama, Japan

Received January 25, 1954

The critical micelle concentration of soap mixtures has been determined for the combination of seven potassium soaps: hexanoate, heptanoate, octanoate, decanoate, undecanoate, dodecanoate and tetradecanoate. A theoretical equation $C_{m_1}^{1+K}x + C_{m_2}^{1+K}(1-x) = C_{mix}^{1+K}$ and/or $C_{m_1}^{1+K}\dfrac{x'}{x' + (1-x')\exp(m_2 - m_1)\omega/kT} + C_{m_2}^{1+K}\dfrac{(1-x')\exp(m_2 - m_1)\omega/kT}{x' + (1-x')\exp(m_2 - m_1)\omega/kT} = C_{mix}^{1+K}$ for the critical micelle concentration (c.m.c.) of soap mixture was derived. Experimental results were in good agreement with theory. The curves for the c.m.c. of soap mixtures *versus* mole fraction were quite similar, when the difference in the number of carbon atoms between two soaps was equal. Some difference between the calculated values and the experimental results was observed, when there existed a large difference in the number of carbon atoms between two soaps. This discrepancy was attributed to the incompleteness of the penetration of longer soap molecules into the palisade layer of shorter soap micelle.

Introduction

The c.m.c. of several soap mixtures were investigated by Klevens.[1,2] However, the theoretical explanation of the c.m.c. of aqueous soap mixture has not yet been done.

The present investigation was undertaken to obtain more extensive data on the c.m.c. of two component soap mixtures, and on the other hand to derive an equation for the c.m.c. of soap mixture from the equation for the c.m.c. of pure soap presented in the previous paper.[3] In comparing the experimental results with the calculated values, the mechanism for the formation of micelle has come more clearly and the theory was confirmed more extensively.

Experimental Details

Hexanoic and heptanoic acids were saponified and then the unsaponified portion was extracted with ethyl ether. After the addition of sulfuric acid, separated fatty acids were purified by fractional distillation through a 3-ft. column, whose boiling points were given as 109.5° (20 mm.) and 121° (16 mm.). Octanoic acid was purified also by fractional distillation through a 3-ft. column, whose boiling point was 120.5° (9 mm.). Decanoic acid (m.p. 31.5°), undecanoic acid (m.p. 26°), dodecanoic acid (m.p. 44.1°) and tetradecanoic acid (m.p. 54.1°) used were "purest" grade materials.

The soap solutions were prepared by neutralizing a known quantity of carbonate-free potassium hydroxide solution with the proper quantity of fatty acids. The c.m.c. of soap mixtures was determined by the change in color of pinacyanole chloride.[4,5] Measured volumes of soap solutions of

---

(1) H. B. Klevens, *J. Chem. Phys.*, **14**, 742 (1946).

(2) H. B. Klevens, THIS JOURNAL, **52**, 130 (1948).

(3) K. Shinoda, *Bull. Chem. Soc. Japan*, **26**, 101 (1953).

(4) M. L. Corrin and W. D. Harkins, *J. Am. Chem. Soc.*, **69**, 679 (1947).

(5) M. L. Corrin, H. B. Klevens and W. D. Harkins, *J. Chem. Phys.*, **14**, 480 (1946).

known normalities were mixed in varying ratios. These soap solutions were diluted to the proper concentration with proper quantity of dye solution and distilled water. Each mixture was brought by dilution at constant concentration of dye (same concentration, 5×10^{-5} mole/liter, as in soap solution) to the critical concentration. Then various amounts of dye solution near this end-point were added to a series of vessels which contained a definite quantity of aqueous soap mixture. In the course of time, the end-point shifts gradually to the higher concentration, and in about 2 hours the color change stops. The final end-point, which is always a somewhat more concentrated point than that of the preliminary test, was determined after 2–4 hours from the boundary concentration between the blue solution and the reddish-violet solution. Critical micelle concentration was calculated from the titration end-point and was subjected to titration error and to ambiguity of color change. The temperature in all instances was kept at 25°.

Results

The c.m.c. of soap mixtures (sum of the concentration of the two soaps) has been determined for the combination of various potassium soaps: hexanoate, heptanoate, octanoate, decanoate, undecanoate, dodecanoate and tetradecanoate. The results are plotted in Figs. 1, 2, 3 and 4.

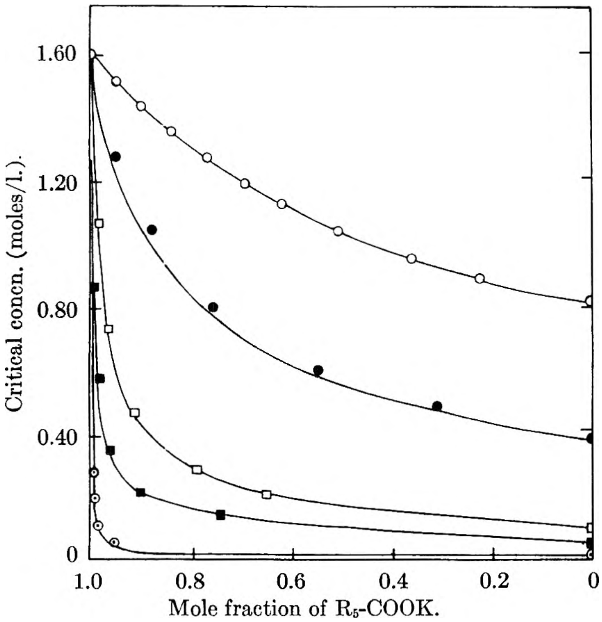

Fig. 1.—Plot illustrates the c.m.c. of soap mixtures at 25°: O, potassium hexanoate + potassium heptanoate; ●, potassium hexanoate + potassium octanoate; □, potassium hexanoate + potassium decanoate; ■, potassium hexanoate + potassium undecanoate; ⊙, potassium hexanoate + potassium tetradecanoate.

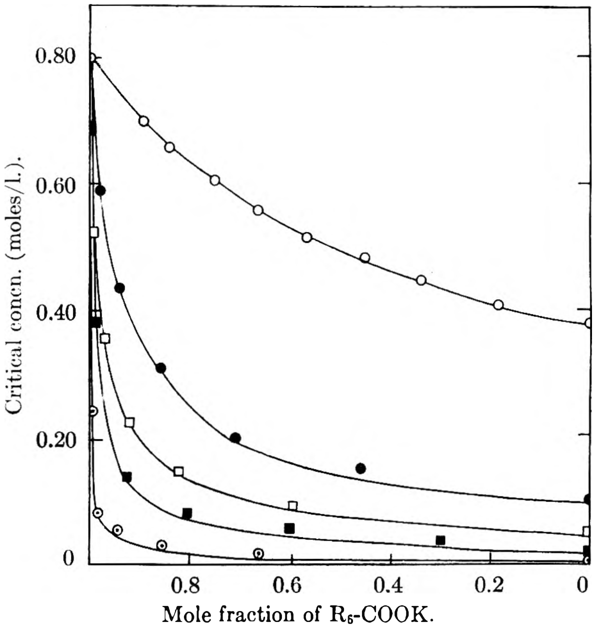

Fig. 2.—Plot illustrates the c.m.c. of soap mixtures at 25°: O, potassium heptanoate + potassium octanoate; ●, potassium heptanoate + potassium decanoate; □, potassium heptanoate + potassium undecanoate; ■, potassium heptanoate + potassium dodecanoate; ⊙, potassium heptanoate + potassium tetradecanoate.

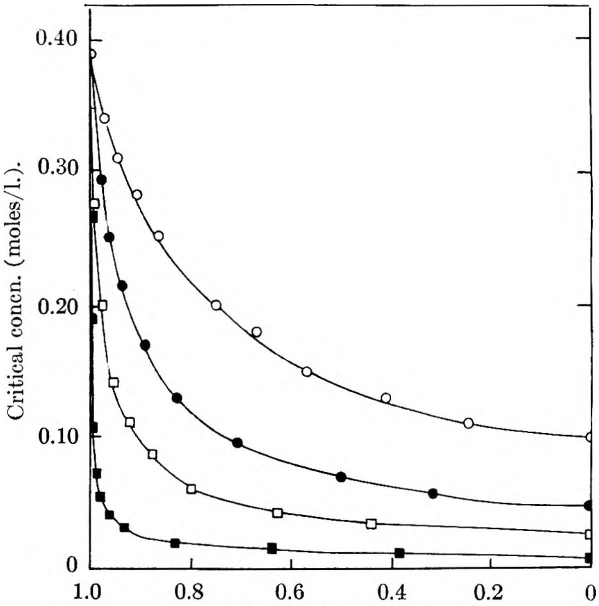

Fig. 3.—Plot illustrates the c.m.c. of soap mixtures at 25°: O, potassium octanoate + potassium decanoate; ●, potassium octanoate + potassium undecanoate; □, potassium octanoate + potassium dodecanoate; ■, potassium octanoate + potassium tetradecanoate.

In every case it is evident that there are no c.m.c. values which do not fall within the range of the pure soaps. It can also be seen from the curves in Figs. 1–4 that the greater change in c.m.c. of soap mixtures is observed when there is a larger difference in the number of carbon atoms between component soaps. The curves of the c.m.c. of soap mixtures *versus* mole fraction are quite similar when the difference in the number of carbon atoms between component soaps is the same. Though mixed micelle of homologous soap mixture is thought to be almost in a state of ideal mixing, the curves provisionally seem to show a great departure from an ideal mixing. However, the correspondence between the theoretical values, in which ideal mixing has been assumed, and the experimental results are, as was shown in Figs. 1–4, exceedingly well. Some difference between the theoretical values and the experimental results was observed when there exists a large difference in the number of carbon atoms between two soaps. This discrepancy was explained as being due to the incompleteness of the penetration of longer soap molecules into the palisade layer of shorter soap micelle.

Theory and Discussions

The c.m.c. of soap mixture has been discussed only qualitatively over certain mole fraction ranges,[1,2] but the theoretical explanation has not been done yet. In the present paper, all phenomena on the c.m.c. of two-component soap mixtures has been explained inclusively by the theory presented here over all mole fraction ranges.

Relation for the c.m.c. of long-chain salts was observed[6,7] and derived[3,8] as a function of the number of carbon atoms in soap chain, m, and of the concentration of counter ions in gram equivalents per liter, C_s

$$\log C_m = -\frac{m\omega}{kT} - K \log C_s + \text{Const.} \qquad (1)$$

where C_m is the c.m.c. of long-chain salt (m-carbon chain) in moles per liter; K is the constant in each homologous series of long-chain salts[2,9]; ω is the surface energy change per methylene radical passing from the aqueous environment into the interior of the micelle. The value of K for fatty acid soaps was given as 0.56,[6,7] and the energy change per methylene radical, ω, was given as $1.08kT$.[3,10,11]

If no salt is added, C_s is equal to C_m, and we obtain

$$(1 + K) \log C_m = -\frac{m\omega}{kT} + \text{Const.} \qquad (2)$$

Consider a mixed micelle of two soaps. If we denote the number of carbon atoms in respective soaps m_1 and m_2, and the mole fractions of the soaps with x and $(1 - x)$, respectively, the concentration of these soaps in the bulk of the solution in equilibrium with the mixed micelle are given from (1), assuming an ideal mixing of the homologous soaps in the micelle (where the term ideal mixing impresses the athermal mixing of two kinds of molecules sufficiently similar in size and shape).

$$\log C_{m_1,x,c_{mix}} = -\frac{m_1\omega}{kT} - K \log C_{mix} + \log x + \text{Const.} \qquad (3)$$

and

$$\log C_{m_2,1-x,c_{mix}} = -\frac{m_2\omega}{kT} - K \log C_{mix} + \log (1 - x) + \text{Const.} \qquad (4)$$

From (2) and (3), we obtain

$$\log C_{m_1,x,c_{mix}} = (1 + K) \log C_{m_1} - K \log C_{mix} + \log x \qquad (5)$$

Similarly from (2) and (4), we obtain

$$\log C_{m_2,1-x,c_{mix}} = (1 + K) \log C_{m_2} - K \log C_{mix} + \log (1 - x) \qquad (6)$$

Evidently the c.m.c. of soap mixture is given by the summation of the concentration of respective soaps

$$C_{m_1,x,c_{mix}} + C_{m_2,1-x,c_{mix}} = C_{mix} \qquad (7)$$

Introducing (5) and (6) into (7), we obtain

$$C_{m_1}^{1+K}\, x + C_{m_2}^{1+K}(1 - x) = C_{mix}^{1+K} \qquad (8)$$

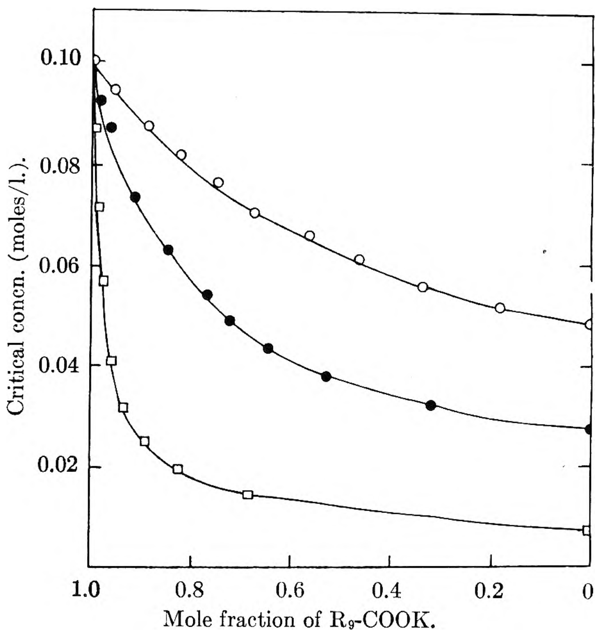

Fig. 4.—Plot illustrates the c.m.c. of soap mixtures at 25°: ○, potassium decanoate + potassium undecanoate; ●, potassium decanoate + potassium dodecanoate; □, potassium decanoate + potassium tetradecanoate.

This equation expresses the c.m.c. of two-component soap mixture. From this equation 8, it is evident that there are no c.m.c. values which do not fall within the range of the pure soaps.

From (3) and (4), the ratio of the concentration of soaps in a state of molecular dispersion is

$$\frac{C_{m_1,x,c_{mix}}}{C_{m_2,1-x,c_{mix}}} = \frac{x}{1 - x} \exp(m_2 - m_1)\omega/kT \qquad (9)$$

If we assume the mole fractions of composite soaps in molecular dispersion are x' and $(1 - x')$, we obtain

$$\frac{x'}{1 - x'} = \frac{x}{1 - x} \exp(m_2 - m_1)\omega/kT \qquad (10)$$

Introducing the relation (10) into (8), we derive

$$C_{m_1}^{1+K} \frac{x'}{x' + (1 - x')\exp(m_2 - m_1)\omega/kT} + C_{m_2}^{1+K} \frac{(1 - x)\exp(m_2 - m_1)\omega/kT}{x' + (1 - x')\exp(m_2 - m_1)\omega/kT} = C_{mix}^{1+K} \qquad (11)$$

This equation 11 expresses the c.m.c. of two-component soap mixture in the mole fractions of soaps in a state of molecular dispersion. As the majority of soap molecules are in a state of molecular dispersion and there are few micelles at the c.m.c., equation 11 also expresses the c.m.c. of soap mixture in the mole fraction of mixed soaps (sum of the concentration of soap in micellar state and in molecularly dispersed state).

Introducing $K = 0.56$, $\omega = 1.08kT$ and the values of the c.m.c. of component soaps, the c.m.c. of two-component soap mixtures was calculated. Comparison between the observed values and the calculated lines were plotted in Figs. 1–4. Experimental results are in good agreement with the calculated values.

The author wishes to express his sincere thanks

---

(6) M. L. Corrin and W. D. Harkins, *J. Am. Chem. Soc.*, **69**, 683 (1947).

(7) S. H. Herzfeld, THIS JOURNAL, **56**, 959 (1952).

(8) M. E. Hobbs, *ibid.*, **55**, 675 (1951).

(9) H. B. Klevens, *J. Am. Oil Chemist's Soc.*, **30**, 74 (1953).

(10) J. T. Davis, *Trans. Faraday Soc.*, **48**, 1052 (1952).

(11) K. Shinoda, THIS JOURNAL, in press.

to Prof. K. Kinoshita for his kind advice and encouragement throughout this research. The expense of this research has been partly defrayed by aid from the Scientific Research Expenditure of the Ministry of Education to which his thanks are due.

THE SHAPES OF PARTICLES FROM DIELECTRIC CONSTANT STUDIES OF SUSPENSIONS

BY AUBREY P. ALTSHULLER

Lewis Flight Propulsion Laboratory of the National Advisory Committee for Aeronautics, Cleveland, Ohio

Received February 1, 1954

The variation of the theoretical linear coefficients, $\beta = (\epsilon - \epsilon_D)/\epsilon_D V$, of spherical non-metallic particles in dilute suspensions is considered. The linear coefficients and shape factors, f, for dilute suspensions of randomly oriented spheroidal particles are discussed and the linear coefficients are tabulated as a function of particle shape and dielectric constant. The treatment by Polder and Van Santen of the dielectric constants of heterogeneous mixtures containing randomly distributed ellipsoidal particles or holes is expanded to include the case of dilute suspensions of ellipsoidal particles oriented with respect to the electric field. The variations of linear coefficients with particle shape and dielectric constant are tabulated for the case of complete orientation with respect to the electric field.

Recently considerable interest has been shown in the dielectric properties of suspensions and mixtures of solids.[1-5] Voet in particular[3,4] has investigated experimentally the dielectric constants of a number of systems consisting of solid particles dispersed in liquids.

The relationships between the dielectric constants of the suspensions and the shapes of the dispersed particles are of considerable interest and importance. Although theoretical formulas have been derived relating the dielectric constants of suspensions to the properties of their components for spherical[1,6] and ellipsoidal particles,[2] no theoretical formulas exist which are satisfactory for arbitrary shapes of particles.

Voet[3] has employed the semi-empirical equation $\epsilon = \epsilon_D(1 + 3fV)$ for conducting particles ($\epsilon_p \to \infty$), where ϵ_D is the dielectric constant of the particles; V is the volume fraction of the particles, and f is the shape factor. The shape factors were derived from experimental data using the empirical equation $\epsilon = \epsilon_D(1 + bV)$ for volume fractions around 10 and below. For metallic particles b equals $3f$. The shape factors, although related to the actual shapes of the particles, were not employed by Voet to find the actual shapes of the particles but merely to represent a numerical deviation from spherical shape ($f = 1$ for spheres).

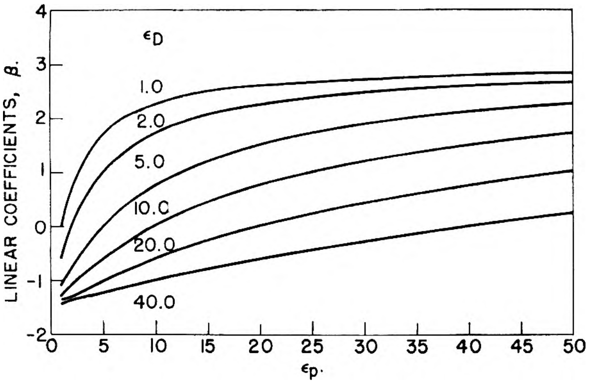

Fig. 1.—Linear coefficients as a function of ϵ_p at various ϵ_D for spheres.

In the present investigation the mathematical relationships connecting the dielectric constants of dilute suspensions with the dielectric constants and volume fractions of the components and with the shapes of the suspended particles will be considered in detail for particles distributed at random and oriented with respect to the electric field. The linear coefficients, β, of the equations relating the dielectric constant of the suspension to the volume fraction of suspended particles, V, will be shown to be calculable from the ratio of ϵ_p/ϵ_D and from the assumed axial ratios of the particles. Such calculated values may then be compared with the corresponding experimentally derived values and the shapes (axial ratios) of the particles may be determined.

When the spherical particles are non-metallic, the linear coefficient is not equal to three as it is for spherical metallic particles. From the theoretical equations, β, the linear coefficient for spheres, equals $3(\epsilon_p - \epsilon_D)/(\epsilon_p + 2\epsilon_D)$ at low concentrations of particles in suspensions. The value of the coefficient of the linear term for spheres actually depends only on the ratio of ϵ_p to ϵ_D and this ratio must be known also before f can be calculated for non-spherical particles of the same material. The theoretical curves for β at various values of ϵ_D and ϵ_p are shown in Fig. 1. It may be seen that even for a particle with a dielectric constant of around 50 in a medium such as mineral oil ($\epsilon_D \sim 2$), $\beta = 2.7$ not 3.

A linear relationship between the dielectric constant of a suspension and the volume concentration may be expected to be valid at volume concentrations of a few volume % and below. The theoretical equations[1,2,6] also may only be justified rigorously to the linear term in volume concentration.[2]

The validity of the theoretical equations at low concentrations is sufficient to make possible com-

---

(1) C. J. Bottcher. *Rec. trav. chim.*, **64**, 47 (1945).

(2) D. Polder and J. H. Van Santen, *Physica*, **12**, 257 (1946).

(3) A. Voet, THIS JOURNAL, **51**, 1037 (1947).

(4) A. Voet and L. R. Suriani, *J. Colloid Sci.*, **7**, 1 (1952).

(5) A. Bondi and C. J. Penther, THIS JOURNAL, **57**, 72 (1953).

(6) D. A. G. Bruggeman, *Ann. Physik*, **24**, 636 (1935).

TABLE I

VALUES OF LINEAR COEFFICIENTS β FOR METALLIC AND NON-METALLIC SPHEROIDS IN MEDIA ASSUMING RANDOM DISTRIBUTION

				Linear coefficients										
p	A_1	A_2	$\epsilon_p/\epsilon_D = \infty$	25	10	5	4	2.5	2	0.5	0.4	0.25	0.2	0.1
0.1	0.861	0.070	9.97	6.36	4.03	2.39	1.93	1.12	0.802	−0.638	−0.831	−1.23	−1.42	−1.97
.2	.751	.125	5.79	4.43	3.21	2.11	1.76	1.08	.783	− .622	− .796	−1.12	−1.26	−1.60
.3	.661	.169	4.44	3.36	2.81	1.96	1.66	1.05	.771	− .613	− .777	−1.07	−1.18	−1.45
.4	.588	.206	3.81	3.22	2.58	1.86	1.60	1.03	.763	− .608	− .765	−1.04	−1.14	−1.37
.5	.527	.236	3.45	2.98	2.44	1.80	1.56	1.02	.757	− .604	− .759	−1.02	−1.12	−1.33
.6	.476	.262	3.25	2.84	2.35	1.76	1.53	1.01	.754	− .602	− .755	−1.01	−1.105	−1.31
.7	.433	.284	3.12	2.75	2.30	1.74	1.515	1.005	.752	− .601	− .752	−1.005	−1.10	−1.30
.8	.396	.302	3.05	2.70	2.27	1.72	1.505	1.00	.751	− .600	− .751	−1.00	−1.095	−1.29
.9	.362	.319	3.01	2.675	2.255	1.715	1.50	1.00	.750	− .600	− .750	−1.00	−1.09	−1.285
1.0	.333	.333	3.00	2.665	2.25	1.715	1.500	1.000	.750	− .600	− .750	−1.00	−1.09	−1.285
1.2	.286	.357	3.03	2.69	2.26	1.72	1.505	1.00	.751	− .600	− .751	−1.00	−1.09	−1.29
1.4	.248	.376	3.12	2.75	2.30	1.735	1.51	1.005	.752	− .601	− .751	−1.005	−1.095	−1.295
1.6	.219	.391	3.23	2.82	2.34	1.75	1.52	1.01	.753	− .601	− .753	−1.005	−1.10	−1.30
1.8	.194	.403	3.37	2.91	2.39	1.77	1.54	1.01	.754	− .602	− .754	−1.01	−1.10	−1.305
2.0	.174	.413	3.53	3.01	2.44	1.79	1.55	1.015	.756	− .603	− .755	−1.01	−1.105	−1.31
2.5	.135	.432	4.01	3.29	2.58	1.84	1.58	1.02	.759	− .604	− .758	−1.015	−1.115	−1.325
3.0	.109	.446	4.56	3.59	2.71	1.89	1.61	1.03	.762	− .605	− .760	−1.025	−1.12	−1.335
3.5	.090	.455	5.18	3.88	2.84	1.93	1.63	1.035	.764	− .606	− .762	−1.025	−1.125	−1.34
4.0	.075	.462	5.86	4.17	2.95	1.96	1.65	1.04	.766	− .607	− .763	−1.03	−1.13	−1.35
5.0	.056	.472	7.38	4.72	3.14	2.01	1.68	1.045	.769	− .608	− .765	−1.035	−1.135	−1.36
10.0	.020	.490	17.79	6.63	3.65	2.13	1.75	1.06	.774	− .610	− .769	−1.045	−1.15	−1.38

parisons between the values of the theoretically calculated coefficients of the linear term, β, and the experimentally determined linear coefficients. Since the theoretical value, β, is calculated on the assumption of a particle shape, information as to the experimental linear coefficient for the suspension allows conclusions to be made as to at least the regular shape (ellipsoidal) corresponding to the actual shapes of the particles in suspension.

Rather than apply f as has been done by Voet,[3,4] it will be seen whether it is possible to derive particle shapes from dielectric constant measurements by considering the equations that may be derived for ellipsoidal particles or cavities.

Polder and Van Santen[2] have derived the equation

$$\epsilon = \epsilon_e\left[1 - \frac{1}{3}\sum_j V_j(\epsilon_j - \epsilon_e)\sum_{i=1}^{3}\frac{1}{\epsilon + (\epsilon_j - \epsilon)A_i}\right]^{-1} \tag{1}$$

where the A_i are depolarization factors and there are j kinds of particles or holes in the medium e. If only two substances are present then let $\epsilon_e = \epsilon_D$ and $\epsilon_j = \epsilon_p$. At sufficiently low concentrations all terms in a series expansion of equation 1 beyond the linear term become negligible and equation 1 may be written as follows (remembering that $\epsilon \rightarrow \epsilon_D$).

$$\epsilon = \epsilon_D\left[1 + \frac{1}{3}V(\epsilon_p - \epsilon_D)\sum_{i=1}^{3}\frac{1}{\epsilon_D + (\epsilon_p - \epsilon_D)A_i}\right] \tag{2}$$

It should be emphasized that equations 1 and 2 hold only for the situation where all orientations of the ellipsoidal particles with respect to the electric field are equally probable. For the general case where the individual ellipsoids are oriented at angles θ and φ to E, the electric field, the following equation results

$$\epsilon = \epsilon_D\left[1 - \frac{1}{3}V(\epsilon_p - \epsilon_D)\sum_{k=1}^{N}\frac{\cos^2\theta_k}{\epsilon_D + (\epsilon_p - \epsilon_D)A_1} + \frac{\sin^2\theta_k\cos^2\varphi_k}{\epsilon_D + (\epsilon_p - \epsilon_D)A_2} + \frac{\sin^2\theta_k\sin^2\varphi_k}{\epsilon_D + (\epsilon_p - \epsilon_D)A_3}\right] \tag{3}$$

where there are N particles contributing to the volume fraction V.

For particles dispersed homogeneously in a liquid medium or for holes scattered throughout a solid, equation 2 should be satisfactory at low concentrations of particles in the absence of external orienting forces.

For metallic ellipsoidal particles equation 2 reduces to the expression

$$\epsilon = \epsilon_D\left[1 - \frac{1}{3}V\sum_{i=1}^{3}\frac{1}{A_i}\right] \tag{4}$$

If the discussion is now limited to the cases of prolate and oblate spheroids with axes $a \gtrless b = c$, the A_i's, the depolarization factors, reduce to integrals of the form[7,8]

$$A_1 = \frac{ab^2}{2}\int_0^\infty \frac{ds}{(s + a^2)^{3/2}(s + b^2)} \tag{5}$$

For prolate spheroids with axes a, b, c with $p = a/b$ and $a > b = c$

$$A_1 = \frac{-1}{p^2 - 1} + \frac{p}{(p^2 - 1)^{3/2}}\ln\left[p + (p^2 - 1)^{1/2}\right] \tag{6}$$

and for oblate spheroids with $a < b = c$

$$A_1 = \frac{1}{1 - p^2} - \left[\frac{p}{(1 - p^2)^{3/2}}\right]\cos^{-1} p \tag{7}$$

In both cases $A_2 = A_3 = \frac{1}{2}(1 - A_1)$. The linear coefficients, β, calculated from equation 2 are tabulated for metallic and non-metallic spheroids in Table I for a range of values of A, ϵ_p and ϵ_D. The shape factors relative to spheres may be calculated simply by dividing the β for a spheroid by the β for the sphere at $A_1 = 0.333$ and with the same values of ϵ_p/ϵ_D. The shape factors for metallic spheroids relative to spheres are given by

$$f = \frac{1}{9}\sum_{i=1}^{3}\frac{1}{A_i} = \frac{1}{9}\left[\frac{1}{A_1} + \frac{4}{1 - A_1}\right] \tag{8}$$

---

(7) Th. G. Scholte, *Physica*, **15**, 437 (1949).

(8) J. A. Stratton, "Electromagnetic Theory," McGraw-Hill Co., Inc., New York, N. Y., 1941, p. 214.

TABLE II

VALUES OF LINEAR COEFFICIENTS β FOR METALLIC AND NON-METALLIC SPHEROIDS IN VARIOUS MEDIA ASSUMING COMPLETE ORIENTATION

			Linear coefficients												
p	A_1	$\epsilon_p/\epsilon_D = \infty$	25	10	5	4	2.5	2	0.5	0.4	0.25	0.2	0.1	0.04	0.00
0.1	0.861	1.17	1.11	1.03	0.90	0.84	0.65	0.54	−0.88	−1.24	−2.12	−2.57	−4.01	−5.53	−7.18
.2	.751	1.33	1.26	1.16	1.00	0.92	.71	.57	− .80	−1.09	−1.72	−2.00	−2.77	−3.44	−4.01
.3	.661	1.51	1.42	1.29	1.10	1.00	.75	.60	− .75	−1.00	−1.49	−1.70	−2.22	−2.63	−2.95
.4	.588	1.70	1.59	1.43	1.19	1.08	.80	.63	− .71	−0.93	−1.34	−1.51	−1.91	−2.21	−2.43
.5	.527	1.90	1.76	1.57	1.29	1.16	.84	.65	− .68	− .88	−1.24	−1.38	−1.71	−1.94	−2.12
.6	.476	2.10	1.93	1.70	1.38	1.23	.88	.68	− .66	− .84	−1.17	−1.29	−1.58	−1.77	−1.91
.7	.433	2.31	2.11	1.84	1.46	1.31	.91	.70	− .64	− .81	−1.11	−1.22	−1.47	−1.64	−1.76
.8	.396	2.56	2.38	1.97	1.55	1.37	.94	.71	− .62	− .79	−1.07	−1.17	−1.40	−1.55	−1.66
.9	.362	2.76	2.48	2.11	1.63	1.44	.97	.73	− .61	− .77	−1.03	−1.12	−1.34	−1.47	−1.57
1.0	.333	3.00	2.67	2.25	1.71	1.50	1.00	.75	− .60	− .75	−1.00	−1.09	−1.28	−1.41	−1.50
1.2	.286	3.49	3.05	2.51	1.86	1.61	1.05	.77	− .58	− .72	−0.95	−1.04	−1.21	−1.32	−1.40
1.4	.248	4.03	3.45	2.78	2.00	1.72	1.09	.80	− .57	− .71	− .92	−1.00	−1.16	−1.26	−1.33
1.6	.219	4.57	3.84	3.03	2.13	1.81	1.13	.82	− .56	− .69	− .90	−0.97	−1.12	−1.22	−1.28
1.8	.194	5.15	4.24	3.28	2.25	1.90	1.16	.84	− .55	− .68	− .88	− .95	−1.09	−1.18	−1.24
2.0	.174	5.76	4.65	3.51	2.36	1.97	1.19	.85	− .55	− .67	− .86	− .93	−1.07	−1.15	−1.21
2.5	.135	7.40	5.66	4.06	2.60	2.13	1.25	.88	− .54	− .65	− .84	− .90	−1.02	−1.10	−1.16
3.0	.109	9.20	6.65	4.55	2.79	2.26	1.29	.90	− .53	− .64	− .82	− .88	−1.00	−1.07	−1.12
3.5	.090	11.2	7.62	4.98	2.94	2.36	1.32	.92	− .52	− .63	− .80	− .86	−0.98	−1.05	−1.10
4.0	.075	13.3	8.54	5.36	3.07	2.45	1.35	.93	− .52	− .63	− .79	− .85	− .97	−1.03	−1.08
5.0	.056	17.9	10.26	5.99	3.27	2.57	1.38	.95	− .51	− .62	− .78	− .84	− .85	−1.01	−1.06
10.0	.020	49.3	16.1	7.61	3.70	2.83	1.46	.98	− .51	− .61	− .76	− .81	− .92	−0.98	−1.02

and for non-metals by the expression

$$= \frac{1}{9}\sum_{i=1}^{3} \frac{(\epsilon_p/\epsilon_D) + 2}{1 + (\epsilon_p/\epsilon_D - 1)A_i}$$

$$= \frac{1}{9}\left[\frac{(\epsilon_p/\epsilon_D) + 2}{1 + (\epsilon_p/\epsilon_D - 1)A_1} + \frac{4\,(\epsilon_p/\epsilon_D) + 8}{1 + (\epsilon_p/\epsilon_D - 1)(1 - A_1)}\right] \tag{9}$$

It should be noted again that β and f for non-metals depend on the ratio of ϵ_p/ϵ_D and A_i and not on the individual values of ϵ_D and ϵ_p.

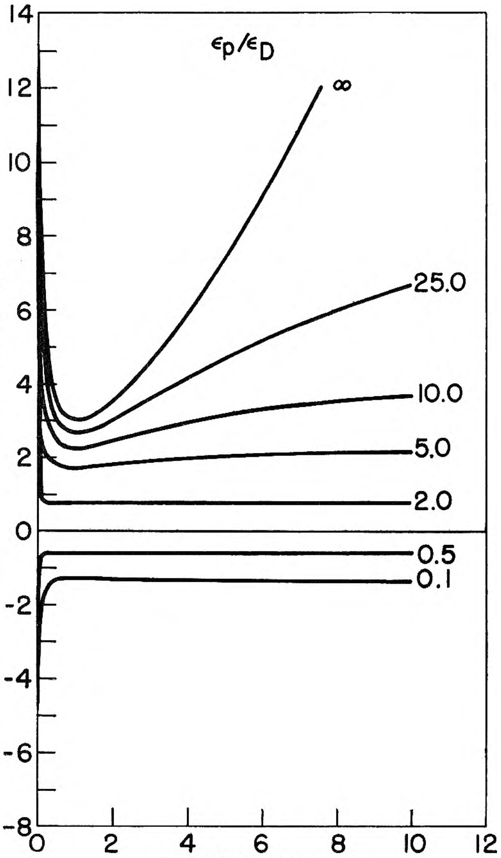

Fig. 2.—Linear coefficients as functions of ratio of axes at various values of ϵ_p/ϵ_D for randomly oriented particles.

The linear coefficients β are plotted against p for various values of ϵ_p/ϵ_D in Fig. 2. It is evident that only when $\epsilon_p/\epsilon_D < 0.1$ or $\epsilon_p/\epsilon_D < 10$ are the minima narrow enough to make it possible to distinguish between p's in the vicinity of one. Table I and Fig. 2 also make it evident that p is a double valued function of β or f. Unfortunately, therefore, unless qualitative information is available from another method such as microscopy, the corresponding prolate and oblate shapes cannot be distinguished. If it is known that the particles are plate-like or needle-like then the dielectric constant measurements will allow a quantitative value of p to be determined. This would be particularly useful in distinguishing among several different shapes of particles all plate-like or all needle-like in form.

If the previous treatment[2] is extended to cover the situation in which the particles are completely oriented parallel to (or perpendicular to) the electric field, the equations assume a somewhat different form. If a is the axis parallel to the electric field and A_1 is the corresponding depolarization factor, then the terms involving A_2 and A_3 equal zero, since the other field components would be equal to zero. If this is the case, then β and f prove to be single valued functions of p. The equations corresponding to 2, 4, 8 and 9 are as follows

$$\epsilon = \epsilon_D\left[1 + V\frac{(\epsilon_p/\epsilon_D) - 1}{1 + (\epsilon_p/\epsilon_D - 1)A_1}\right] \tag{10}$$

$$\epsilon = \epsilon_D[1 - V/A_1] \tag{11}$$

$$f = 1/3A_1 \tag{12}$$

$$f = \frac{1}{3}\,\frac{(\epsilon_p/\epsilon_D) + 2}{1 + (\epsilon_p/\epsilon_D - 1)A_1} \tag{13}$$

Table II and Fig. 3 give the values and shapes of the curves relating β to p at various ratios of ϵ_p/ϵ_D for complete orientation of the particles.

Comparing the linear coefficients in Tables I and II, it may be seen that the dielectric constant of the suspension for $\epsilon_p > \epsilon_D$ is predicted to have a maximum value for particles oriented with their major axes parallel to the electric field, an intermediate value for random orientation, and a minimum value for particles oriented with their major axes perpendicular to the electric field. For $\epsilon_p < \epsilon_D$ the reverse is true. These conclusions are in qualitative agreement with the results obtained by Bruggeman.[6]

The case in which $\epsilon_p/\epsilon_D = 1$ is also of interest. Equation 2 may be written as

$$\epsilon = \epsilon_D + (\epsilon_p - \epsilon_D)F(\epsilon_p, \epsilon_D, V, S) \qquad (14)$$

where S is some complex shape function. Thus for particles of any shape the dielectric constant of the particles may be obtained when $\epsilon = \epsilon_D$. When this relation holds, $\epsilon_p = \epsilon_D$ and ϵ is independent of the volume fraction and shape of the particles. The dielectric constant of the dispersing medium may be varied by using different liquids, varying the proportions of a liquid mixture which forms the dispersing medium, or by varying the temperature of the dispersing medium until $\epsilon_D = \epsilon_p$.

Actually suspensions contain particles which vary somewhat in shape even if the particles are regular in shape. The result will be that the axial ratios found will be average values. Furthermore, many particles which are useful and available are rather irregular in shape. It would be extremely difficult if not entirely impossible to derive theoretical equations to represent such shapes.[2] The regular shapes which can be analyzed theoretically may be considered equivalent (shapes) to the irregularly shaped particles whose axes would be in about the same ratio. If the irregularities of the particles are not too extreme, the correspondence might well be a fairly satisfactory one.

The influence of agglomeration in liquid suspensions has not been considered in the previous discussion. This additional problem may be avoided by employing very dilute suspensions, by adding surface active agents to aid in deagglomerating the particles, or by employing high rates of shear to deagglomerate when orientation of the particles is also desired. Probably a combination of these methods would be most satisfactory.

The treatment given here is particularly applicable to particles suspended in non-polar or low conductivity liquids. One or both components may be insulators. The derivation applies to static dielectric constants and is not applicable in dispersion regions. Fricke[9,10] has recently derived equations for components which are pure conductors and has considered the behavior of suspensions of conducting ellipsoids in dispersion regions. Such a treatment is useful for biological cellular materials, *i.e.*, red blood cells in plasma, at ultra-high frequencies. The equations derived in the present investigation are not applicable to such systems.

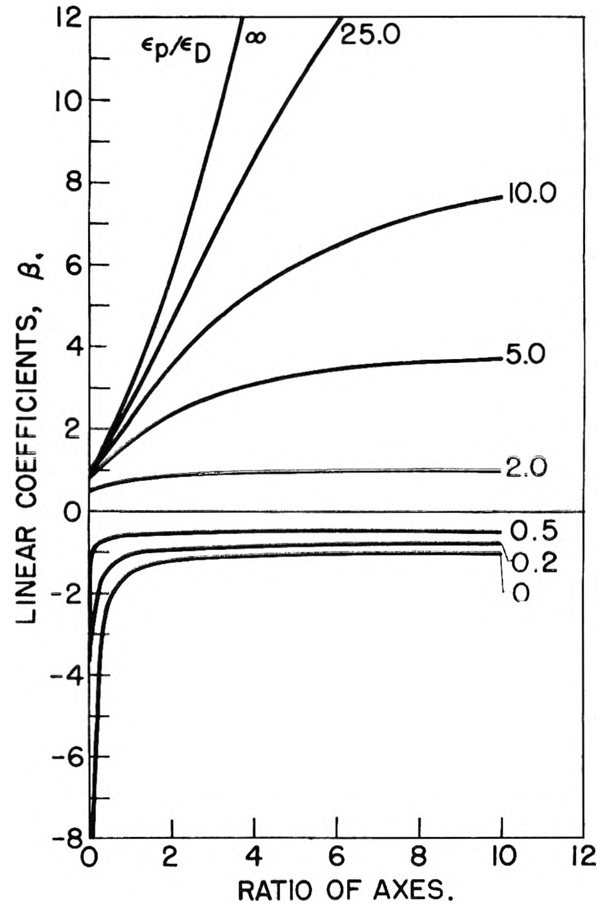

Fig. 3.—Linear coefficients as functions of ratio of axes at various ϵ_p/ϵ_D for oriented particles.

Conclusion.—The mathematical results of the present investigation indicate that measurements of the dielectric constants of dilute suspensions may be employed in obtaining the average shapes of the suspended particles. Dielectric constant measurements on suspensions consisting of particles completely oriented with respect to the electric field by some external force should be particularly useful.

---

(9) H. Fricke, *Experientia*, **8**, 376 (1952).

(10) H. Fricke, THIS JOURNAL, **57**, 934 (1953).

ULTRAVIOLET ABSORPTION SPECTRA AND DISSOCIATION CONSTANTS OF PICOLINIC, ISONICOTINIC ACIDS AND THEIR AMIDES

BY H. H. G. JELLINEK AND J. R. URWIN

The Johnson Laboratories, University of Adelaide, Adelaide, Australia

Received February 20, 1954

Ultraviolet absorption spectra of nicotinic acid and its amide as a function of *p*H values were presented in two previous communications.[1,2] Dissociation constants were derived from the experimental data. This paper brings an extension of the work to picolinic, isonicotinic acid and their amides. When the work comprising this paper was actually completed, a paper by Evans, Herington and Kynaston[3] was published dealing with the absorption spectra and dissociation constants of the pyridine monocarboxylic acids.

Experimental

Materials.—Isonicotinic acid, picolinic acid, isonicotinamide and picolinamide were the same samples as described in a previous paper.[4] All other chemicals were of Analar grade.

Apparatus.—Measurements were made with a Hilger Uvispek spectrophotometer. *p*H values were determined by means of a glass electrode.

Solutions.—Solutions were prepared by adding requisite amounts of hydrochloric acid solutions and solutions of the amide or acid to 0.05 *M* sodium acetate and making up the volume to a total of 50 ml. The concentrations of the respective acid or amide ranged from 1×10^{-4} to 5×10^{-4} *M*. The ionic strength of the solutions down to about *p*H 3.5 had a constant value of 0.01. The measurements were carried out at room temperature, 20 ± 2°.

Experimental Results and Discussion

The absorption spectra as a function of *p*H values for picolinamide and isonicotinamide are shown in Figs. 1 and 2. The spectra of the respective acids will not be presented, as they have been given by Herington and co-workers[3] and we have found no essential differences. The spectra of picolinic acid show maxima at about 2650 Å. and a shoulder, which shift with the *p*H values in the region of about 2700 Å. At very low *p*H values the maximum absorption shifts to longer wave lengths. There are indications of two pairs of isosbestic points in the region of 2350 and 2750 Å.

Picolinamide shows absorption maxima at 2655 Å. and a definite isosbestic point at 2400 Å., the absorption curves for *p*H values 0 and lower do not pass through this isosbestic point.

Isonicotinic acid presents a picture of greater complexity. The absorption maxima shift appreciably with *p*H values. The absorption spectra of isonicotinamide, on the other hand, are again simpler. The absorption maxima shift moderately with *p*H values from about 2680 to 2630 Å. There are indications of two isosbestic points at about 2800 and 2340 Å.

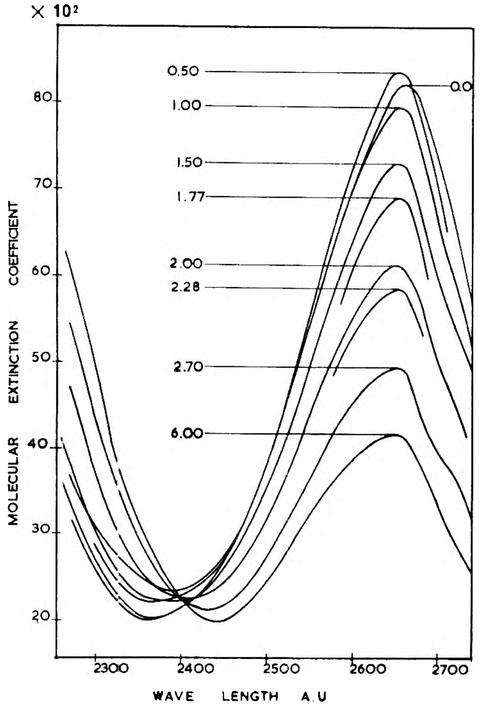

Fig. 1.—Absorption spectra of picolinamide at various *p*H values.

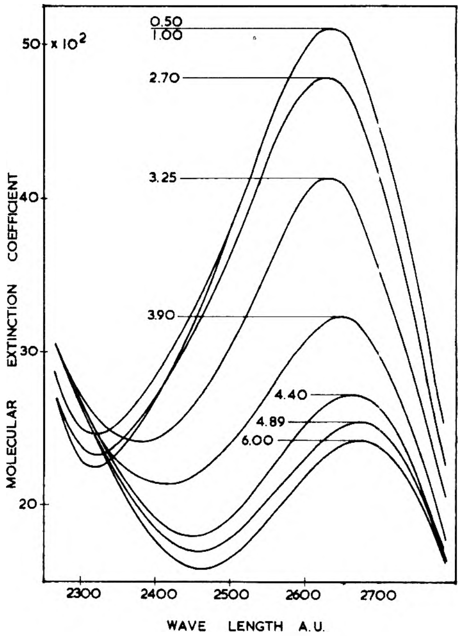

Fig. 2.—Absorption spectra of isonicotinamide at various *p*H values.

It was ascertained that Beer's law was obeyed at constant *p*H values for the ranges of concentrations of acid and amide used in this work.

Molecular extinction coefficients for these compounds as function of *p*H values for constant wave

---

[1] E. B. Hughes, H. H. G. Jellinek and B. A. Ambrose, THIS JOURNAL, **53**, 414 (1949).

[2] H. H. G. Jellinek and M. G. Wayne, *ibid.*, **55**, 173 (1951).

[3] R. F. Evans, E. F. G. Herington and W. Kynaston, *Trans. Faraday Soc.*, **49**, 1284 (1953).

[4] H. H. G. Jellinek and J. R. Urwin, THIS JOURNAL, Vol. **58**, 168 (1954).

lengths are shown in Figs. 3 and 4. The theoretical curves are drawn through the experimental points and will be discussed below.

Picolinic acid shows two distinct sections and the points appear to pass through a maximum at low *p*H values. The points for picolinamide also pass through a maximum at low *p*H values.

Isonicotinic acid shows a very distinct maximum at intermediate *p*H values, whereas isonicotinamide passes through a maximum at low *p*H values.

The acids have an acid group and a basic group each, whereas the amides have two basic groups. The respective equilibria can be written as follows

$$^{+}HNRCOOH + H_2O \rightleftharpoons NRCOOH + H_3O^{+}$$
$$NRCOOH + H_2O \rightleftharpoons NRCOO^{-} + H_3O^{+}$$

and

$$^{+}HNRCONH_3{}^{+} + H_2O \rightleftharpoons H^{+}NRCONH_2 + H_3O^{+}$$
$$^{+}HNRCONH_3 + H_2O \rightleftharpoons NRCONH_2 + H_3O^{+}$$

Calculations were carried out to fit the experimental points in Figs. 3 and 4 by choosing suitable pK_a values and *p*H values for the isoelectric points. The calculations were carried out either according to the first method described in the previous paper on nicotinic acid[1] or that given in the paper on nicotinamide,[2] respectively. The curves drawn through the experimental points in Figs. 3 and 4 were obtained in this way.

Picolinic acid could be fitted by two constants, picolinamide by one constant; the decrease in extinctions at low *p*H values may be an indication of the equilibrium pertaining to the amido group. Isonicotinic acid could be fitted very well by two dissociation constants. The extinction values for the species $^{+}HNRCOOH$ are here smaller than those for NRCOOH for this particular wave length in contrast to nicotinic acid where the reverse was the case.[1] Isonicotinamide could be fitted by one pK_a value and there is an indication of an equilibrium pertaining to the amido group at low *p*H values.

TABLE I

ISOELECTRIC POINTS AND pK_a VALUES

Substance	Iso-electric point	Carboxyl group	Nitrogen ring	Amido group	Ref.
Picolinic acid	3.48	5.40*	1.60	...	This work
	3.21	5.40*	1.08*	...	3
Isonicotinic acid	3.45	4.95*	1.70	...	This work
	3.31	4.84*	1.77*	...	3
Nicotinic	4.24	4.95*	3.55*	...	1
acid	3.42	4.83*	2.08*	...	3
Picolinamide	...	...	2.10	<−1.0	This work
Isonicotinamide	...	...	3.61*	<−1.0	This work
Nicotinamide	...	...	3.35*	0.5	2
Pyridine	...	...	5.12*	...	5
			5.16*	...	7
Benzoic acid	...	4.20	...	...	6
Acetamide	...	...	...	−0.5	6

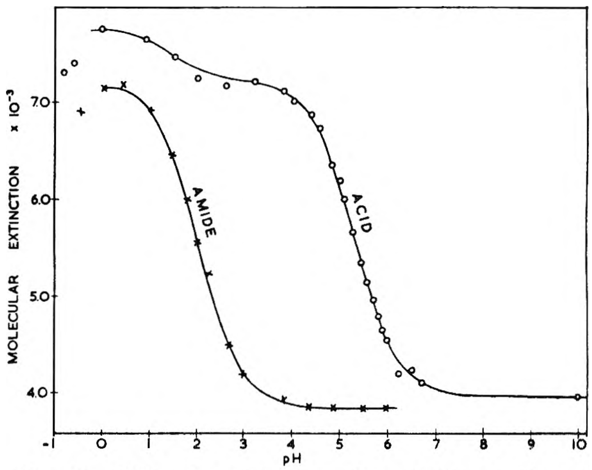

Fig. 3.—Molecular extinctions for picolinic acid and picolinamide as a function of *p*H values. Curves are calculated, points are experimental (λ ~2650 and 2600 Å., respectively).

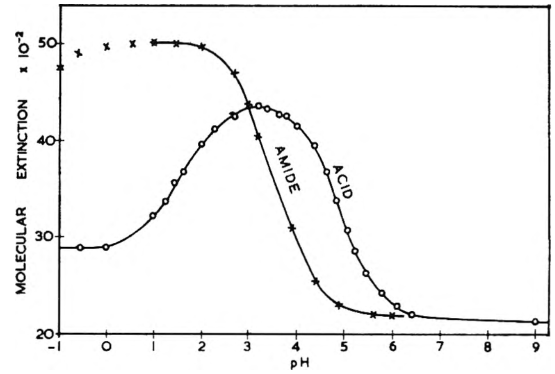

Fig. 4.—Molecular extinctions for isonicotinic acid and isonicotinamide as a function of *p*H values. Curves are calculated, points are experimental (λ ~2600 Å.).

All pK_a values are comprised in Table I. The values marked by asterisks are thermodynamic dissociation constants, where the ionic strength has been taken into account according to the Debye–Hückel theory. Table I contains also values obtained by Herington and co-workers[3] and values for benzoic acid, pyridine and acetamide.

It can be seen that the K_a values belonging to the carboxyl groups are very similar, though somewhat smaller than that for benzoic acid. However, there are some discrepancies in the values for the nitrogen in the ring. The difference between our value and that of Herington, *et al.*,[3] is due to the fact that our solutions contained hydrochloric acid for small *p*H values, whereas Herington, *et al.*, used sulfuric acid. These authors pointed out that the extinctions decreased in HCl solutions with decreasing *p*H, whereas the reverse is true for sulfuric acid solutions. They ascribe this different behavior to the formation of a hydrochloride. The discrepancies found for the nitrogen of nicotinic acid probably are due to the less accurate photographic method used by Hughes, Jellinek and Ambrose, as pointed out by Herington and co-workers.[3]

---

(5) E. B. Hughes, H. H. G. Jellinek and B. A. Ambrose, THIS JOURNAL, 53, 410 (1949).

(6) "Handbook of Physics and Chemistry," Chemical Rubber Publishing Company, Cleveland, Ohio.

(7) E. F. G. Herington, *Disc. Faraday Soc.*, No. 9, 26 (1950).

It is possible that the decrease in extinctions for the amides at low pH values is due also to hydrochloride formation, though in the present work it has been taken as an indication for the dissociation of the amido group.

The weakest acid is picolinic, where the carboxyl group is in *ortho* position to the nitrogen in the ring. The nitrogen in the ring is a weaker base in the case of isonicotinamide than for isonicotinic acid. It also may be noted that the nitrogen in the ring for the acid shows a similar trend as that for the corresponding picolines.[6] Whereas the methyl groups, being electron-donating, increase the basic strength of the nitrogen, the carboxyl groups act in the opposite way. β-Picoline is the weakest base, whereas nicotinic acid is the strongest. (Thermodynamic dissociation constants for α, β and γ picoline are as follows: 8.77×10^{-9}, 4.54×10^{-9} and 10.62×10^{-9}, respectively.[7])

The basic strength of the amido groups is smaller than that for acetamide with the exception of nicotinamide, which is appreciably stronger.

THE CATALYTIC DECOMPOSITION OF CARBON MONOXIDE ON LARGE METALLIC SINGLE CRYSTALS[1]

BY VICTOR J. KEHRER, JR. AND HENRY LEIDHEISER, JR.

Virginia Institute for Scientific Research, Richmond, Virginia

Received February 27, 1954

The catalytic decomposition of carbon monoxide was studied on electrolytically polished single crystals of cobalt, copper nickel, silver, iron, chromium and molybdenum in the form of spheres with a small shaft, and on electrodeposits of palladium and rhodium on copper single crystals. Carbon was identified as one of the products of the reaction on iron, nickel and cubic cobalt crystals at 550° and on hexagonal cobalt at 410°. None of the other metals exhibited appreciable catalytic activity. In the case of the three active cubic metals, the minor faces such as (321), (432) and (431) were most active catalytically and in the case of hexagonal cobalt the minor faces such as the (0113) and (1124) were most active. The (100) major face was the least active face of the cubic metals and the (0001) major face was the least active for hexagonal cobalt. The reaction patterns which formed during decomposition on cobalt and nickel single crystals, which have a face-centered cubic structure and similar interatomic spacings, were similar.

Introduction

Previous studies have shown that the catalytic activity of metals is a function of the crystal face exposed at the surface. Pronounced differences in the catalytic activity of the various faces of large single crystals have been determined in the case of the reaction of hydrogen and oxygen on copper,[2] the decomposition of carbon monoxide on nickel,[3] and the catalytic deposition of cobalt from solutions of potassium formate on copper.[4] It was next of interest to study a single reaction on a number of different metal crystals in order to note if any generalizations could be drawn concerning the relationship between the structure of the crystal faces and their activity.

The reaction chosen for study was the decomposition of carbon monoxide since the product, carbon, is a solid and hence would be deposited on the surface where the decomposition took place. Thus large spherical single crystals exposing all crystal faces could be used.[5] The rate of formation of the product could then be determined simultaneously on all crystal faces in one experiment. The use of the solid catalyst in the form of a sphere had the added advantage that X-ray analysis of the products could be made very conveniently at grazing incidence.

The results reported herein emphasize that the crystal face exposed at the surface of a catalyst is an important factor in catalytic activity.

Method of Experiment.—Single crystals of cobalt, copper, nickel and silver were prepared in the form of rods, $^{3}/_{8}''$–$^{5}/_{8}''$ in diameter, by slowly lowering the molten metal in a pointed mold through a temperature gradient.[6] Single crystals of Armco iron, $^{3}/_{8}''$ in diameter and 1″ to 3″ long, were prepared by the anneal-strain-anneal method.[7] Single crystals of electrolytic chromium were obtained in the form of irregular chunks from the Metals and Thermite Corp., New York, and a single crystal of molybdenum in the form of a wire, $^{1}/_{8}''$ in diameter and 1″ long, was kindly furnished to us by Professor Robert Maddin of the Johns Hopkins University. Palladium and rhodium were electrodeposited on electrolytically polished single crystals of copper following the directions furnished by the supplier, Baker and Co., Newark, New Jersey. The single crystals were machined (or filed in the case of chromium) in the form of spheres with a small shaft. The strained layer resulting from the machining operation was removed by deep etching.

A smooth and strain-free surface was obtained by electrolytic polishing. Copper was polished in 42.5% orthophosphoric acid by the method of Jacquet[8]; nickel was polished in 70 wt. % sulfuric acid by the method of Hothersall and Hammond[9]; cobalt was polished in 42.5% orthophosphoric acid by the method of Elmore[10]; iron was polished in the perchloric acid–acetic anhydride bath described by Jacquet and Rocquet[11]; silver was polished by the method of Powell[12] in a 5% potassium cyanide bath to which

---

[1] This research was sponsored by The Texas Company.

[2] H. Leidheiser, Jr., and A. T. Gwathmey, *J. Am. Chem. Soc.*, **70**, 1200 (1948). See also papers by R. Cunningham and A. T. Gwathmey, *ibid.*, **76**, 391 (1954); J. B. Wagner and A. T. Gwathmey, *ibid.*, **76**, 390 (1954).

[3] H. Leidheiser, Jr., and A. T. Gwathmey, *ibid.*, **70**, 1206 (1948).

[4] H. Leidheiser Jr., and R. Meelheim, *ibid.*, **71**, 1122 (1949).

[5] See H. Leidheiser, Jr., and A. T. Gwathmey, *Trans. Electrochem. Soc.*, **91**, 97 (1947), for a description of the single crystal method of study.

[6] The furnace described by A. T. Gwathmey and A. F. Benton, THIS JOURNAL, **44**, 35 (1940), was modified by using a copper furnace jacket instead of quartz and by lowering the crucible by means of a supporting rod passing through a vacuum seal.

[7] The basic facts upon which the anneal-strain-anneal method is based were first outlined by C. A. Edwards and L. B. Pfeil, *J. Iron Steel Inst.*, **59**, 129 (1924).

[8] P. Jacquet, *Compt. rend.*, **202**, 402 (1936).

[9] A. W. Hothersall and R. A. F. Hammond, *J. Electrodepositors' Tech. Soc.*, **16**, 83 (1940).

[10] W. C. Elmore, *Phys. Rev.*, **53**, 757 (1938).

[11] P. Jacquet and P. Rocquet, *Compt. rend.*, **208**, 1012 (1939).

[12] A. S. Powell, Dissertation, University of Virginia (1943).

was added 2 ml. of a 10% sodium chloride solution just prior to polishing; molybdenum was polished in 20% sulfuric acid by the method of Coons.[13] Chromium was electrolytically polished in a solution consisting of 85% orthophosphoric acid and 15% distilled water. The most lustrous surfaces were obtained with chromium when the bath was operated under the following conditions: a temperature of 50°, an aluminum sheet cathode, a current density of 3 amp./sq. dm., 3 volts, 20 minutes, and with constant agitation.

After being electrolytically polished and thoroughly washed in water, the metal crystal was placed shaft downward in a glass tube sealed to the movable section of a ground glass joint. This tube projected up into the reaction chamber so that the crystal was immediately opposite a small window in the furnace. The window permitted the crystal to be viewed frequently during the course of an experiment and the method of support permitted rotation of the crystal about its axis while it was in the reaction chamber. In order to reduce oxide films and to remove residual strain, the crystals were heated in hydrogen at 550° in most of the experiments for 2–16 hours before being exposed to carbon monoxide. In some of the experiments the residual strain was removed by heating the crystals to the reaction temperature *in vacuo*. Both procedures yielded identical results.

Carbon monoxide was prepared by the dehydration of formic acid with sulfuric acid and it was stored over water in 5-gallon bottles. The gas was purified before admission to the reaction vessel by passage over copper wire heated to 500°, and then over tubes containing sodium hydroxide on asbestos (Ascarite) and anhydrous calcium sulfate. Tank hydrogen was purified in the same manner but through a separate train. Unless otherwise noted the gas remained in contact with the crystal in a closed system.

Powder X-ray analysis was made by collecting a small amount of the product on the surface of a small fiber coated with rubber cement. Iron or copper radiation was used. Analysis of the product before removal from the surface was made by placing the spherical crystal in the X-ray beam such that it intersected one-half of the beam.

The minor faces were located on the surface of the sphere by an application of the orthographic projection. An orthographic projection normal to a major plane was drawn and a photographic negative was prepared. After reaction, the crystal was photographed and a print was made. The orthographic projection was then projected on the photograph of the reaction pattern by means of a photographic enlarger. The major planes on the orthographic projection and the photograph were superimposed by rotation, and the minor faces were located on the pattern. In order to achieve even moderate accuracy with this technique, it was necessary to be certain that the photograph was taken exactly normal to the plane which formed the center of the orthographic projection.

Results

Approximately 100 experiments with nickel single crystals have been performed since the original publication.[3] In the original note the large area surrounding the (111) pole was identified as the most active region. Careful examination during the course of the reaction indicated that the regions surrounding the (111) faces were slightly more active than the (111) faces themselves. These regions are associated with the minor crystal faces of high index surrounding the (111) face. The order of appearance of carbon, and hence the order of activity of the faces, is given in Table I.

TABLE I

THE RELATIVE ACTIVITY IN DECREASING ORDER OF THE CRYSTAL FACES OF NICKEL DURING THE DECOMPOSITION OF CARBON MONOXIDE AT 550°

Crystal face: minor faces about (111), (111), (110), (100)

It is of interest that exactly the same pattern of carbon deposition was formed in microscopic pits when the decomposition of carbon monoxide was carried out on flat nickel single crystals.[14] These pits, of approximately hemispherical shape, were formed occasionally during electrolytic polishing.

X-Ray analysis of the products of the reaction on the (111) faces at grazing incidence indicated the presence of only graphitic carbon. However, chemical analysis had previously indicated the presence of nickel in the black product formed on the surface.[3] Further evidence for the presence of nickel in the material was obtained by noting that the product was attracted by a strong magnet. Electron microscopic examination of the carbon product indicated that it was very porous and consisted of tangled thread-like segments.

A series of experiments with nickel crystals was carried out in order to assess the importance of roughness of the surface in controlling the relative rates of reaction. Roughening procedures were used in which selected areas on the surface were preferentially roughened. These results are reported in Table II. It will be noted that in all nine procedures the large area surrounding the (111) pole was the most active. Although the absolute rate of reaction varied greatly in the experiments, the relative rates of reaction of the areas surrounding the three major faces remained the same as the relative rates noted in Table I.[15]

Cobalt.—Cobalt single crystals were of special interest because of the fact that the metal is hexagonal close-packed below 420° and face-centered cubic above 420°. Previous results[16] had indicated that the crystal could be heated and cooled through the transition temperature and would continue to exhibit the properties of a hexagonal close-packed crystal below 420° and of a face-centered cubic crystal above 420°. It was found that cobalt crystals were active in the carbon monoxide reaction above and below 420°.

The results of a typical experiment carried out at 550° were as follows: Carbon began to deposit in large areas surrounding the (111) poles within several hours after the admission of carbon monoxide. These areas include many of the minor faces with unequal indices such as (321), (432), (431), etc. Narrow bands radiating from the (111) poles toward the neighboring (100) faces were next in activity, followed by the small area immediately adjacent to the (111) face. The (110) faces showed low activity and the (100) faces were relatively inert as shown by the fact that these faces remained free of carbon for 16 hours, at which point the experiments were stopped. Results similar to those at 550° were ob-

---

[13] W. C. Coons, *Trans. Am. Soc. Metals*, **41**, 1415 (1949).

[14] At the editor's request ten photographs describing the results have been deleted from the paper. Printed sheets containing these photographs will be furnished by the authors to interested readers. Address request to the authors at 326 N. Boulevard, Richmond 20, Virginia.

[15] J. B. Wagner in a study of the decomposition of carbon monoxide on nickel at the University of Virginia also concluded that the relative rates of reaction on the various crystal faces were independent of the roughness of the surface. Similar conclusions within limits had been reached earlier by H. L. in a study of the oxidation of copper crystals and by L. B. Johnson in a study of the electrode potential of plane faces of copper crystals.

[16] H. Leidheiser, Jr., and V. J. Kehrer, *J. Chem. Phys.*, **21**, 570 (1953).

TABLE II

A SUMMARY OF THE RESULTS OBTAINED DURING THE CATALYTIC DECOMPOSITION OF CARBON MONOXIDE ON NICKEL SINGLE CRYSTALS SUBJECTED TO VARIOUS PRE-TREATMENTS

Pre-treatment of surface	Active area	Remarks
(1) Electrolytically polished	(111)	Use procedure as ref. (100) and (110) areas inactive
(2) Electrolytically polished and etched in hot 6 N HCl	(111)	(100) and (110) inactive. Etching developed good etch pattern. C deposition did not follow each pattern
(3) Electrolytically polished and etched in hot 3 N acetic acid	(111)	Etching caused the development of smooth (111) and rough (100). However, reaction took place fastest on (111)
(4) Electrolytically polished, electroplated with nickel, and electrolytically polished	(111)	Reaction pattern same as electrolytically polished specimens even though (111) areas were polycrystalline and (100) areas were monocrystalline[a]
(5) Electrolytically polished, oxidized in O_2 at 550°, reduced with H_2, CO admitted	(111)	(100) areas rougher than (111) yet (111) areas were most active
(6) Electrolytically polished and etched electrolytically in H_2SO_4	(111)	(100) and (110) inactive
(7) Electrolytically polished and alternately oxidized in O_2 and reduced in H_2 ten times	(111)	Sphere was uniformly rough after alternate oxidation and reduction. (100) and (110) inactive
(8) Electrolytically polished, CO decomposition reaction, C burned off with O_2, CO admitted again	(111)	(111) areas were most active even after continued cyclic operations involving C deposition and then burning off with O_2
(9) Copper single crystals, electrolytically polished, electropolated with nickel, nickel deposit polished electrolytically	(111)	Same results as observed with nickel single crystals. (100) and (110) inactive

[a] See H. Leidheiser, Jr., and A. T. Gwathmey, *J. Electrochem. Soc.*, **98**, 225 (1951) for a description of the electrodeposition of nickel on copper and nickel single crystals.

tained at 500 and 600°. The results are summarized in Table III.

TABLE III

THE RELATIVE ACTIVITY IN DECREASING ORDER OF THE CRYSTAL FACES OF COBALT DURING THE DECOMPOSITION OF CARBON MONOXIDE

Cubic cobalt at 450–600°	Hexagonal cobalt at 410°
Minor faces with unequal indices	(0113) and (1124)
(211), (311), (411)	(0110)
(111)	(0111)
(110)	(0001)
(100)	

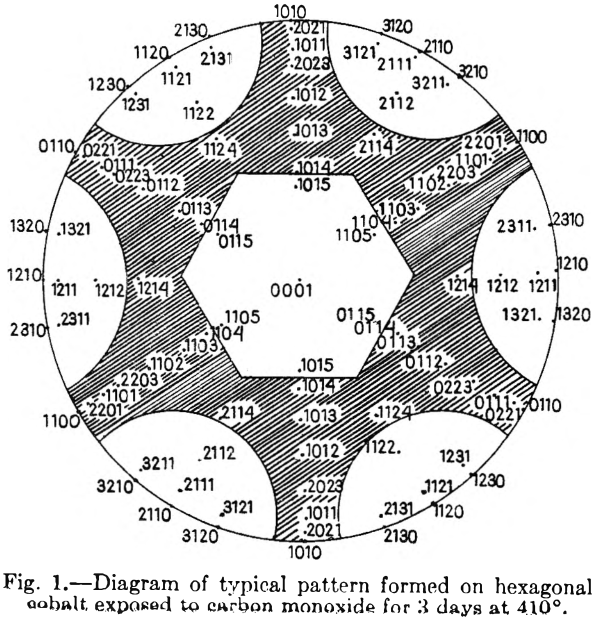

Fig. 1.—Diagram of typical pattern formed on hexagonal cobalt exposed to carbon monoxide for 3 days at 410°.

X-Ray analysis at grazing incidence of the deposit in the areas surrounding the (111) face indicated the presence of only graphitic carbon. X-Ray analysis of the (100) areas at grazing incidence yielded no diffraction lines. The X-ray measurements confirmed the visual observation that no product was formed on the (100) faces even after exposure to carbon monoxide at 550° for 16 hours.

Cobalt single crystals were relatively inactive in the hexagonal phase below 420°. No change in the appearance of the crystal occurred after exposure for 12 days at 350°. At 410° a symmetrical pattern showing the sixfold symmetry about the (0001) faces was observed in 3 days. A schematic diagram of this pattern is given in Fig. 1. The most active regions of the surface were in the areas surrounding the (0113) and (1124) faces. Faces such as the (0110) and (0111) showed slight activity, whereas the (0001) faces showed no activity. X-Ray diffraction analysis of the deposit on the (0113) faces indicated the presence of only graphitic carbon.

A few experiments were carried out with cobalt crystals in which the crystal was electrolytically etched in hydrochloric acid or in the phosphoric acid polishing bath. The etch pattern which was thus formed at room temperature had the symmetry of the hexagonal close-packed structure. However, when the reaction was carried out at 600°, the minor faces surrounding the (111) poles had the highest activity and the (100) face and surrounding area had the lowest activity. There appeared to be no difference in the behavior of the two (111) faces which became the (0001) faces in the hexagonal structure from the behavior of the other six (111) faces. The resulting reaction pattern showed some evidences of the hexagonal etch pattern, indicating that the roughening of specific planes of the hexagonal structure increased the reactivity of these positions on the surface at 600° in the face-centered cubic structure.

Iron.—Experiments with iron crystals were carried out at 550, 450, 350 and 250°. The following sequence of events was noted at 550°. Approximately 15 minutes after admission of the carbon monoxide, the first darkening of the sphere was noted in regions neighboring the three major faces. These most active regions corresponded to crystal faces whose three indices are all different and unequal to zero. Faces such as (321) and (432) represent members of this class. Narrow bands lying between the (100) and (111) faces next became darkened in 20–30 minutes. The faces occupying these positions on the surface have indices of the class (211), (311), (411), etc. After approximately 40 minutes, carbon was observed on the regions between the (110) and (111) faces and between the (110) and (100) faces. The faces occupying these positions on the surface have indices of the class (221), (331), (441), etc., and (210), (310), (410), etc. The (111) and (110) major faces became dark after approximately 60 minutes, and finally after approximately 90 minutes, the (100) faces began to turn dark. These results are summarized in Table IV.

TABLE IV

THE RELATIVE ACTIVITY IN DECREASING ORDER OF THE CRYSTAL FACES OF IRON DURING THE DECOMPOSITION OF CARBON MONOXIDE AT 450 AND 550°

Minor faces with unequal indices
Minor faces of type (211), (311), (411), etc.
Minor faces of type (221), (331), (441), etc.
Minor faces of type (210), (310), (410), etc.
(111) and (110)
(100)

Microscopic examination of an iron sphere which had been exposed to carbon monoxide indicated the presence of needle-like growths on the surface. A series of observations were thus made in order to study the surface deposit as a function of time. An iron sphere was heated for increasing periods of time in carbon monoxide at 550° and the microscopic appearance of the areas on the surface was studied. After being exposed for 8 minutes the sphere exhibited no discoloration and no carbon was visible to the naked eye or under the microscope on any part of the surface. The inactive (100) area remained completely unchanged in appearance whereas fine needles were observed on the active faces. With increased exposure to the carbon monoxide the needles grew in size until they practically covered the surface. After being exposed for 45 minutes to the carbon monoxide at 550°, large masses of carbon began to form on the active areas whereas only the first signs of carbon were visible on the inactive (100) areas. All crystal faces passed through the same sequence of events, but the rate of formation of the needles and of the carbon followed the order shown in Table IV.

X-Ray powder photographs of the loose black powder which formed on an iron crystal exposed to carbon monoxide for several hours at 550° indicated the presence of both graphitic carbon and cementite. The product was attracted to a strong magnet, confirming the presence of iron or a ferromagnetic iron compound. Electron micrographs of the product indicated that the deposit formed as long coiled threads. Some of the images on the fluorescent screen of the microscope gave the observer the impression that these coils were formed by an extrusion process. Electron diffraction examination of the powder yielded only rings characteristic of graphite.

X-Ray studies at grazing incidence were made in order to identify these surface crystals and to follow the reaction taking place on the surface. Cementite, Fe_3C, was detected on the surface in all of the catalytic experiments carried out at 550°. It was detected before the active areas of the surface turned black (presumably because of carbon) as well as after the reaction had proceeded sufficiently far to cover the entire sphere with carbon. The major diffraction lines of cementite were always found in the diffraction patterns, but carbon appeared only when a relatively heavy black deposit was examined. The correlation between the visual observance of the needle-like crystals and the appearance of the major lines of cementite in the diffraction patterns suggests that these surface crystals were cementite. Barrett[17] reports the existence of several solid solutions of α-iron and cementite. The forms differ according to the temperature of formation. The high temperature form is pearlite. If the solid solution is cooled too rapidly for pearlite to be formed, martensite is the product. The low temperature form is bainite which is produced between 200 and 550°. Vilella, Guellich and Bain[18] have published photomicrographs of bainite which appear identical to the crystals seen in the present study. A striated structure surrounding the acicular crystals strongly resembled the published photographs of pearlite.

An attempt was made to alter the acicular crystals by heating in hydrogen, since the data of Emmett[19] indicated that the direct reduction of Fe_3C by hydrogen was thermodynamically favorable at 550°. An iron sphere was exposed to carbon monoxide for an hour at 550° and the reaction was halted after carbon had formed only on the minor faces, but the acicular crystals had formed on all faces, being more concentrated on the minor faces. X-Ray diffraction analysis showed the presence of cementite and carbon on the (321) face but only cementite on the (100) face. After being heated in hydrogen at 550° for 20 hours the sphere showed no change as judged either by its microscopic appearance or by its X-ray diffraction pattern. The sphere had assumed a grayish cast. The change in appearance suggested that hydrogen had a reducing effect on some constituent, but this constituent was not identified by X-ray analysis. The sphere was again heated to 550° in hydrogen and exposed to carbon monoxide. The decompo-

(17) C. S. Barrett, "Structure of Metals," McGraw-Hill Book Co., Inc., New York, N. Y., 1943, p. 475.

(18) J. R. Vilella, G. E. Guellich and E. C. Bain, *Trans. Am. Soc. Metals*, **24**, 225 (1936).

(19) L. C. Browning, T. W. DeWitt and P. H. Emmett, *J. Am. Chem. Soc.*, **72**, 4211 (1950).

sition of the monoxide proceeded rapidly and the deposit soon covered the entire sphere. The (321) areas still retained the heaviest deposit. X-Ray analysis again showed Fe_3C and carbon on the (321) face and only Fe_3C on the (100) face.

The results obtained during the decomposition of carbon monoxide at 450° were essentially the same as those at 550°. The minor faces were most active and the (100) face was by far the least active. X-Ray analysis at grazing incidence of the surface products formed during the reaction revealed the presence of carbon and cementite. The acicular crystals were again noted and the relative rates of formation on the various crystal faces were similar to the relative rates found at 550°.

The results obtained at 250° were very similar to those obtained at 350°. At both temperatures an interference color pattern formed. The pattern consisted of large areas of uniform appearance surrounding the (111) faces and large areas of uniform appearance surrounding the (100) faces. X-Ray analysis at grazing incidence of the products formed at 350° indicated the presence of $Fe_{20}C_9$ and Fe_3O_4. When a sphere, which had been previously exposed to carbon monoxide at 250 or 350°, was heated at 600° *in vacuo*, carbon was formed which was concentrated around the (111) and (110) faces with smaller amounts along the bands forming the planes connecting these two major faces. At 250° the major product formed after exposure to carbon monoxide for 4–10 days was Fe_3O_4 as indicated by X-ray diffraction. The oxide exhibited a strong preferred orientation. Similar results were obtained when carbon monoxide was continuously flowed through the system.

Copper, Silver, Chromium, Molybdenum and Electrodeposited Rhodium and Palladium on Copper Single Crystals.—The results obtained with these metals are summarized in Table V. Only in the case of chromium were reproducible differences in the behavior of the crystal faces observed. The composition of the film on the surface was not determined.

TABLE V

A SUMMARY OF THE RESULTS OBTAINED WITH COPPER, SILVER, CHROMIUM AND MOLYBDENUM CRYSTALS AND WITH ELECTRODEPOSITS OF RHODIUM AND PALLADIUM ON COPPER CRYSTALS

Metal single crystal	Temp., °C.	Results
Copper	550–800	Completely inactive
Silver	550	Completely inactive
Chromium	400–550	Interference color films which formed more rapidly on (111) than (100) areas
Molybdenum	550–700	Showed activity in only 1 of 12 experiments; small size limited useful life
Rhodium electrodeposited on copper crystal	550	Completely inactive
Palladium electrodeposited on copper crystal	550	Completely inactive

Discussion

The major objective of this research was to relate the arrangement of the atoms in the surface with catalytic activity using a single reaction and single crystals of a number of different metals. Of the nine metals investigated in this study, only three were found to have appreciable activity in the decomposition of carbon monoxide, namely, nickel, iron and cobalt (in both the hexagonal and cubic phases). In the case of iron, nickel and cubic cobalt at 550° and hexagonal cobalt at 410°, graphitic carbon was identified as one of the products of the reaction. On all three metals the reaction, $2CO = CO_2 + C$ occurred. On the iron crystals other reactions occurred also as shown by the fact that products such as $Fe_{20}C_9$, Fe_3O_4 and Fe_3C were identified. No evidence was found for side reactions on cobalt or nickel.

Of greatest interest to the relationship between the arrangement of atoms and catalytic activity is the fact that the regions of high activity were the same and the regions of low activity were the same on the three cubic metals iron, nickel and cobalt. The minor faces lying on the surface between the areas surrounding the major faces were the most active in all cases. Even in the case of hexagonal cobalt the minor faces such as (0113) and (1124) were the most active. The appearance of the pattern formed on iron crystals was very much more complicated than that formed on nickel or cubic cobalt, in that the large areas of high activity were further divided into areas of slightly different activity. Furthermore, iron, nickel and cubic cobalt were similar in that at 550° the (100) face was by far the most inactive area on the surface. Both visual observation and X-ray diffraction analysis of the surface led to the same conclusion. In fact, compared to minor faces, the (100) faces were almost inert. In some cases it appeared that the (100) face became covered with carbon by lateral growth of the carbon from neighboring minor faces rather than by virtue of its own activity.

One of the strongest pieces of evidence concerning the relationship between the arrangement of atoms and the catalytic activity was found in the studies with nickel and cubic cobalt. The carbon patterns which were observed at 550° on both of these metals were the same. This similarity is to be expected since both metals possess identical crystal structures[20] at 550° and the lattice constants are very similar. In both cases the order of activity in decreasing order was: minor faces, (111), (110) and (100).

In the case of nickel as shown in Table II the relative rates at which carbon formed on the crystal faces of the spherical crystal were independent of the roughness of the surface. Similar relative rates of reaction were obtained on electrolytically polished specimens as were obtained on crystals which had been roughened by treatments such as etching, electroplating, and alternate oxidation and reduction. In some cases the area surrounding the

---

[20] Throughout this paper the terms cubic cobalt and hexagonal cobalt have been used although it is generally known that below 420° the crystal consists of a mixture of the hexagonal and cubic phases (O. S. Edwards, *J. Inst. Metals*, **69**, 177 (1943)). However, as previously described in reference (16) and further observed in the study reported herein, chemically cobalt single crystals behave as a face-centered cubic metal above 420°, and as a hexagonal close-packed metal below 420°.

(100) face was roughest, whereas in other cases the area surrounding the (111) face was roughest. Nevertheless in all cases the minor faces were the most active and the (100) face was the least active. It should be emphasized that, although the relative rates of reaction were independent of the roughness of the surface, the absolute rate of reaction on any face was greatly dependent upon the pre-treatment of the surface. In the case of cubic cobalt the minor faces surrounding the (111) planes exhibited the highest activity and the (100) face and surrounding area exhibited the lowest activity on crystals which had been electropolished as well as on crystals which had been electrolytically etched at room temperature to give a hexagonal close-packed etch pattern.

One of the most interesting features of the catalytic reaction on cobalt single crystals was the fact that the (111) areas of the face-centered cubic structure were the most active whereas in the hexagonal close-packed structure the (0001) areas were the least active. In order to appreciate fully the significance of this difference in activity, it is necessary to understand the relation between the face-centered cubic and hexagonal close-packed structures. Both structures may be considered as a stacking of planes of atoms arranged in densest packing: that is, within each plane each atom has 6 neighbors at an equal distance. The two structures differ only in the method of stacking these planes of densest packing. In the hexagonal close-packed structure alternate planes are identical in spatial arrangement, whereas in the face-centered cubic structure every plane is identical in arrangement to the fourth plane above or below it. The stacking in the hexagonal close-packed structure may thus be represented by the sequence *abababab*, etc., and the stacking of the planes in the face-centered cubic structure may be represented by the sequence *abcabcabc*, etc. From the foregoing it is apparent that the (111) and (0001) planes, which are the planes of the densest packing, are identical in atomic configuration two-dimensionally but differ in that the positions of the atoms in planes beneath the surface are different in the two structures.

The detection of discrete compounds each as Fe_3C, $Fe_{20}C_9$ and Fe_3O_4 on iron, the presence of cobalt and nickel in the carbon deposit, and the formation of polycrystalline nickel on the areas surrounding the (111) faces during the passage of a 2:1 mixture of hydrogen and carbon monoxide over nickel single crystals at 550°,[21] all point to the view that atoms below the surface are also involved in some way in the catalytic reaction.

The filamentary shape of the carbon formed during the decomposition of carbon monoxide on iron has been observed independently by two other groups of workers.[22,23] Under certain conditions filaments of the same general appearance are formed during the photographic development of single crystals of silver bromide[24] and silver chloride.[25] Very fine whiskers are also formed under certain conditions on a metal such as tin.[26] Studies are needed to understand the origin of this filamentary structure, which appears to occur more often than is generally realized.

Acknowledgment.—We wish to express our deep appreciation to Dr. Allan T. Gwathmey for his ideas which formed the basis of this work and for his continued encouragement and suggestions. We are grateful to the Texas Company, and especially to Dr. W. E. Kuhn, for permission to publish this work. Discussions with Dr. Frank J. Moore and other members of the Research Laboratories, Texas Company, were most helpful. We are indebted to Mr. Fred B. Hayes for the preparation and machining of the crystals and to Mr. Felix von Gemmingen for carrying out the electron microscope studies.

[21] Unpublished results.

[22] W. R. Davis, R. J. Slawson and G. R. Rigby, *Nature*, **171**, 756 (1953).

[23] L. V. Radushkevich and V. M. Luk'yanovich, *Zhur. Fiz. Khim.*, **26**, 88 (1952); known through *C. A.*, **47**, 6210 (1953).

[24] H. D. Keith and J. W. Mitchell, *Phil. Mag.*, **44**, 877 (1953).

[25] F. H. Cook and H. Leidheiser, Jr., *J. Am. Chem. Soc.*, **76**, 617 (1954).

[26] S. E. Koonce and S. M. Arnold, *J. Applied Phys.*, **24**, 365 (1953).

ION EXCHANGE IN MIXED SOLVENTS

By O. D. Bonner and Jane C. Moorefield[1]

Department of Chemistry of the University of South Carolina, Columbia, S. C.

Received March 1, 1954

Equilibrium studies of the silver–hydrogen system on Dowex 50 have been made in ethanol–water and dioxane–water media. The characteristic solvent uptake of the pure silver and hydrogen resinates and the composition of the imbibed solvent have been determined. The over-all selectivity of the resin is increased by the addition of an organic solvent. The swollen volume of the hydrogen resinate remains relatively constant if water is present in the solvent phase. The presence of organic solvent, however, appears to shrink the silver resinate. Theoretical considerations are difficult, due to a lack of knowledge of the behavior of electrolytes in non-aqueous or mixed media.

Introduction

Although many results of ion-exchange experiments in aqueous media have been published, there are very few literature references to ion exchange in non-aqueous media or in mixed solvents. Chance, Boyd and Garber[2] have recently completed a study of the kinetics of ion exchange in non-aque-

---

[1] From a thesis submitted by Jane C. Moorefield to the University of South Carolina in partial fulfillment of the requirements for the degree of Master of Science.

[2] F. S. Chance, Jr., G. E. Boyd and H. J. Garber, *Ind. Eng. Chem.*, **45**, 1671 (1953).

ous media and of the feasibility of industrial use of certain resins in which they report that organic solvents which allow the water wet resin to retain its aqueous volume are suitable as exchange media. These results seemed to indicate that a similar study of ion exchange equilibria should be of interest.

This research was thus of an exploratory nature, the purpose of which was to compare ion-exchange equilibria of one pair of ions in certain mixed solvents with those in aqueous media and to attempt to ascertain whether there was a relationship between these equilibria and the solvent uptake of the resin.

Experimental

Exchange Experiments.—Silver and hydrogen ions were chosen as the pair to be studied since quantitative analysis for these ions is very simple. Approximately 8% DVB Dowex 50 was chosen as the cation-exchange resin.[3] The experimental procedures for the equilibrium studies were identical with those used for similar studies in aqueous media.[4] In each exchange experiment both the resin and the solvent phase were subjected to analysis for both ions when equilibrium was attained. When radioactive methods of analysis were to be used, a trace of Ag^{110} isotope was added to the influent silver solution.

Solvent Uptake.—The uptake of each solvent mixture by both pure hydrogen resinate and pure silver resinate was determined experimentally. A one-gram sample (approximate) of the resin was placed in a column and eluted with 25 ml. of the appropriate solvent. After elution the samples were immersed in the solvent for five minutes, removed by filtration, dried superficially by blotting until no excess moisture was apparent, and weighed. The samples were then dried to constant weight at 115° and the maximum solvent uptake computed from the loss in weight.

Solvent Composition.—The composition of each solvent mixture imbibed by the resin was determined by equilibrating a resin sample with the appropriate solvent, separating by filtration, superficially drying and distilling to dryness at 115°. The composition of the ethanol–water distillates was determined from specific gravity measurements. In the case of dioxane–water distillates, the composition was determined from dielectric constant measurements.

Discussion and Results

From the solvent uptake data, presented in Tables I–IV, it is apparent that whenever water is present in the solvent mixture, the hydrogen resinate imbibes a volume of solvent which is at least as large as when it is equilibrated with pure water. The presence of more than 25 weight per cent. organic solvent substantially decreases the uptake of solvent by the silver resin, however, and thus decreases the swollen volume. The composition of the solvent imbibed by the hydrogen resinate is close to that of the influent solution, except that the resinate phase is relatively richer in organic solvent when the solution is predominantly aqueous. Ethanol is always taken up to a greater extent from aqueous ethanol solutions than is dioxane from aqueous dioxane solutions containing an equal weight fraction of organic solvent. The silver resinate, on the contrary, imbibes considerably less ethanol from ethanol–water solutions and almost no dioxane from dioxane–water solutions. This behavior appears to be analogous to the "salting in" properties of the hydrogen ion in certain solutions. For example, isoamyl alcohol and concentrated hydrochloric acid form a one-phase system, but such is not the case when concentrated silver nitrate solutions and isoamyl alcohol are used. The greater affinity of the resinates for ethanol than for dioxane is probably due to the "polar character" of the former substance.

Table I

Solvation of Hydrogen Resinate in Ethanol–Water Solutions

Influent solvent (wt. % ethanol)	0	25	50	75	100
Solvent uptake by resinate compn. (wt. % ethanol)	0	47	52	79	100
G. solv./eq. resin	205	215	202	178	94
Moles solv./eq. resin	11.4	8.5	7.7	5.1	2.0
Ml. solv./eq. resin	205	234	223	211	117

Table II

Solvation of Hydrogen Resinate in Dioxane–Water Solutions

Influent solvent (wt. % dioxane)	0	25	50	75	100
Solvent uptake by resinate compn. (wt. % dioxane)	0	29	42	68	100
G. solv./eq. resin	205	224	229	202	83
Moles solv./eq. resin	11.4	9.6	8.4	5.1	0.9
Ml. solv./eq. resin	205	220	222	195	80

Table III

Solvation of Silver Resinate in Ethanol–Water Solutions

Influent solution (wt. % ethanol)	0	25	50	75	100
Solvent uptake by resinate compn. (wt. % ethanol)	0	29	36	39	100
G. solv./eq. resin	118	95	66	43	23
Moles solv./eq. resin	6.6	4.3	2.9	1.8	0.5
Ml. solv./eq. resin	118	100	70	46	29

Table IV

Solvation of Silver Resinate in Dioxane–Water Solutions

Influent solution (wt. % dioxane)	0	25	50	75	100
Solvent uptake by resinate compn. (wt. % dioxane)	0	1.3	2.9	3.4	100
G. solv./eq. resin	118	123	80	55	29
Moles solv./eq. resin	6.6	6.8	4.3	3.0	0.3
Ml. solv./eq. resin	118	122	80	55	28

The equilibrium data for the exchange reactions are presented graphically in Figs. 1 and 2. The equilibrium quotient or selectivity coefficient, *k*, is calculated for each exchange reaction from the equation

$$k = \frac{M_{H^+}}{M_{Ag^+}} \times \frac{\text{Mole \% Ag Res.}}{\text{Mole \% H Res.}}$$

From these plots of equilibrium quotient *vs.* resin composition it may be observed that there is an over-all increase in affinity of the resin for silver ion when organic solvent is present. Moreover, the increase occurs to a greater extent when the resin is predominantly in the silver form. Since it has been noted that the presence of some organic solvent reduces the swollen volume of silver resinate and such is not the case from the hydrogen resinate, the possibility of a relationship between swelling and selectivity is indicated. This increase in selectivity may be due in part to increase in the activity coefficient ratio $f_{H\ Res}/f_{Ag\ Res}$ caused by an increase in the concentration of the resin phase. A similar

---

[3] The authors are grateful to Dow Chemical Company for supplying the resin used in these experiments.

[4] O. D. Bonner and V. Rhett, This Journal, 57, 254 (1953).

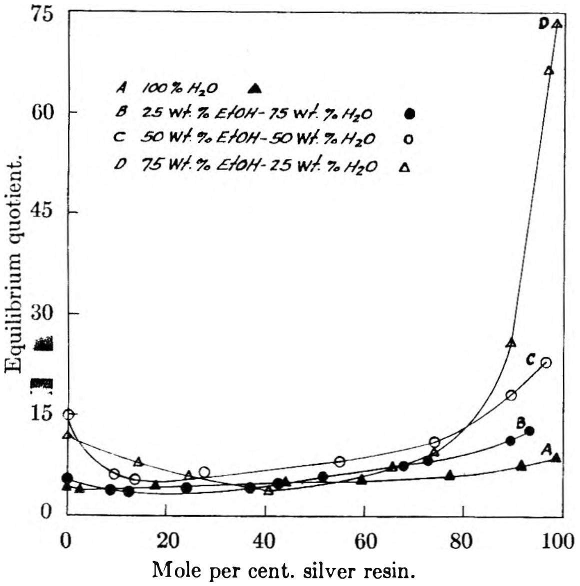

Fig. 1.—Silver–hydrogen exchange in ethanol–water media.

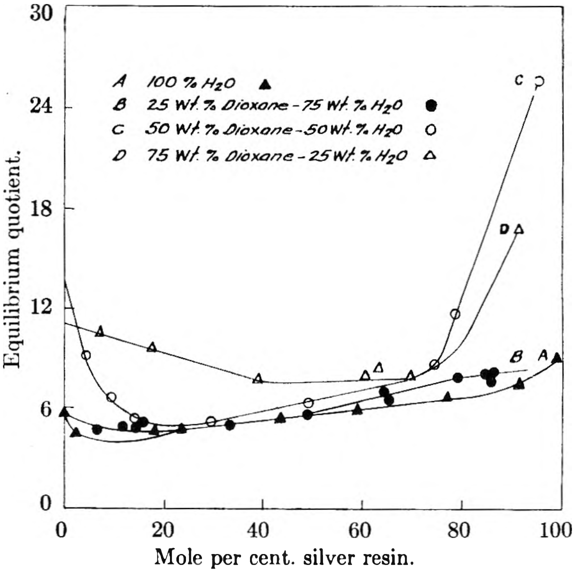

Fig. 2.—Silver–hydrogen exchange in dioxane–water media.

effect is observed for this system in aqueous media when the ionic strength of the external solution is increased,[5] thereby reducing the swollen volume of the resin. The selectivity coefficient is also increased at all resin compositions[4] for resins of higher DVB content, in which the swelling is inhibited to a greater extent. Since little is known concerning the behavior of silver ion in mixed solvents, it is difficult to predict the effect of the change in solvent composition in the resin phase with resin composition on the above activity coefficient ratio. The activity coefficient ratios of the ions in the external solution are likewise known only for aqueous media, and so the effect of this term on the selectivity coefficient cannot be quantitatively predicted. Theoretical considerations, other than those given above, therefore are not feasible.

[5] O. D. Bonner, W. J. Argersinger and A. W. Davidson, *J. Am. Chem. Soc.*, **74**, 1044 (1952).

THERMODYNAMIC DATA FOR THE ZINC–INDIUM SYSTEM OBTAINED FROM THE PHASE DIAGRAM

BY W. J. SVIRBELY

Department of Chemistry, University of Maryland, College Park, Maryland

Received March 4, 1954

Integral heats of mixing and the relative partial molal heat contents of zinc and indium in zinc–indium alloys at 700°K. have been determined from solubility data for the system by means of semi-empirical equations proposed by Kleppa. The relative partial molal heat contents of zinc have been used in turn to calculate the activities and partial molal entropies of zinc in zinc–indium alloys at 700°K. All calculated data have been compared with data in the literature. The results support Kleppa's equations as well as can be expected.

Introduction

Due to experimental difficulties, it is frequently impossible to apply either vapor pressure or electromotive force procedures to the determination of the thermodynamic properties of bimetallic systems. Consequently, attempts have been made to determine such properties through use of other available data, such as solubility data. Recently, Kleppa[1] has criticized some of the earlier attempts and he has presented a method which permits the separation of the calculated partial molal free energies along the liquidus into approximate heat and entropy terms. The method is restricted to a simple eutectic phase diagram with a steep liquidus displaced toward one extreme in composition.

The comparison of calculated heat data with experimental data made by Kleppa[1] does not lead to a satisfactory conclusion concerning the validity of Kleppa's method because of the lack of sufficient experimental data for the systems considered.

The phase diagram for the zinc–indium system[2,3] indicates that this system is subject to the above restrictions. Furthermore, the thermodynamic properties of the zinc–indium system have been determined recently.[4] There exist, therefore, in this case sufficient thermodynamic data for the checking of Kleppa's method.

Results

Thermal Calculations.—The data of Valentiner[2] and of Rhines and Grobe[3] were used in the cal-

[1] O. J. Kleppa, *J. Am. Chem. Soc.*, **74**, 6047 (1952)

[2] S. Valentiner, *Z. Metallkunde*, **35**, 250 (1943).

[3] F. N. Rhines and A. H. Grobe, *Am. Inst. Mining Met. Engrs., Inst. Metals Div.*, **156**, Tech. Pub. 1682 (1944).

[4] W. J. Svirbely and S. M. Selis, *J. Am. Chem. Soc.*, **75** 1532 (1953).

culations. Figure 1 shows a plot of log $N_{Zn(s)}$ in In(l) *vs.* $1/T$. From the slope and intercept of the limiting straight line, one obtains values for $\Delta\bar{H}$, the heat of solution for zinc, and log N_{Zn} at $1/T = 0$, respectively. Through use of equations 1 and 2

$$L^0_{Zn} = \bar{L}_1 = \Delta\bar{H} - \Delta H_f \qquad (1)$$

$$2.3R \log N_{1/T=0} - \Delta S_f = \Delta\bar{S}_1{}^{x0} \qquad (2)$$

values of $\bar{L}_1{}^0$, the relative partial molal heat content of zinc at high dilution, and $\Delta\bar{S}_1{}^{x0}$, the excess partial molal entropy of zinc at high dilution, were calculated to be 2675 cal./mole and 1.94 e.u., respectively. The heat of fusion of zinc was taken[5] to be 1765 cal./mole at 692.7°K.

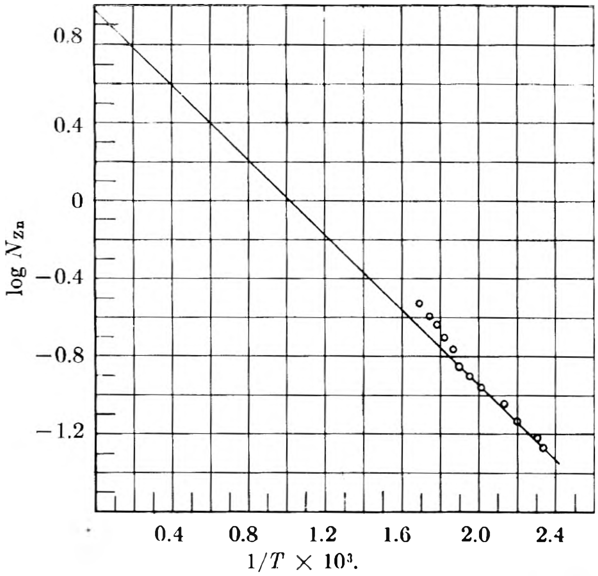

Fig. 1.—Solubility of Zn(s) in In(l).

Values of ΔH, the integral heating of mixing, $\bar{L}_1$, the relative partial molal heat content of zinc, and $\bar{L}_2$, the relative partial molal heat content of indium, can be calculated by equations 3, 4 and 5

$$\Delta H = N_1 N_2 \bar{L}_1{}^0 \qquad (3)$$

$$\bar{L}_1 = N_2{}^2 \bar{L}_1{}^0 \qquad (4)$$

$$\bar{L}_2 = N_1{}^2 \bar{L}_1{}^0 \qquad (5)$$

if one assumes the validity of the Baud–Heitler[6,7] equation for the heat of formation of one mole of solution. On the other hand, if one assumes the validity of the van Laar[8] equation for the integral heat of mixing, then ΔH, $\bar{L}_1$ and $\bar{L}_2$ can be calculated[1] by equations 6, 7 and 8

$$\Delta H = N_2 \frac{V_2}{V_1} \theta_1{}^2 \bar{L}_1{}^0 + N_1 \theta_2{}^2 \bar{L}_1{}^0 \qquad (6)$$

$$\bar{L}_1 = \theta_2{}^2 \bar{L}_1{}^0 \qquad (7)$$

$$\bar{L}_2 = \frac{V_2}{V_1} \theta_1{}^2 \bar{L}_1{}^0 \qquad (8)$$

In these equations, N, θ and V represent mole fraction, volume fraction and molar volume, respectively, for the designated component. All quantities calculated by use of mole fraction expressions (equations 3, 4, 5) and by use of volume fraction expressions (equations 6, 7, 8) are shown in Fig. 2 along with the experimental values for the same quantities. In the calculation of volume fractions, V_1 and V_2 were taken to be 9.2 and 15.7 cc. for zinc and indium, respectively,[9] over the complete temperature range. It should be emphasized that in this method of comparison one assumes that ΔH, $\bar{L}_1$ and $\bar{L}_2$ are independent of the temperature not only over the temperature range covered by the actual phase diagram but actually to 700°K., the temperature at which the experimental values were obtained.[4]

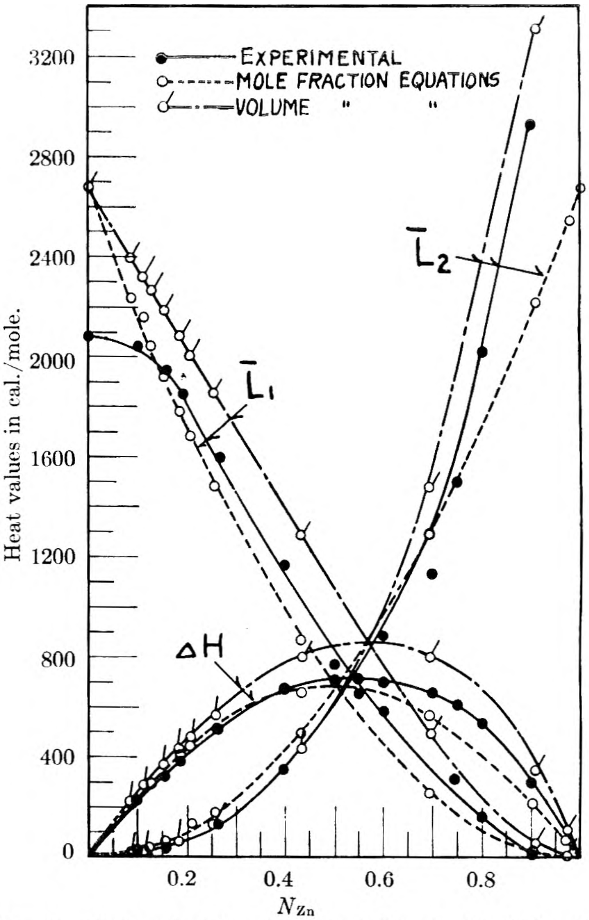

Fig. 2.—Heat values for zinc and indium in Zn–In liquid alloys at 700° K.

Activities.—In the calculation of the activities of components in a homogeneous bimetallic mixture from solubility data, one must remember that information obtained from the solubility diagram concerning equilibrium in the solid–liquid mixture is restricted to the temperature and composition along the liquidus. In such a case, N_1 is that mole fraction of zinc at each temperature in which

$$a_1{}^0(\text{s/l}) = a_1(\text{l/l}) \qquad (9)$$

where $a_1{}^0$(s/l) is the activity of pure solid zinc and a_1(l/l) is the activity of the zinc in the liquid alloy,

---

[5] K. K. Kelley, Bureau of Mines, Bulletin 476, p. 203.

[6] E. Baud, *Bull. soc. chim.*, [4] **17**, 324 (1915).

[7] W. Heitler, *Ann. Physik*, [4] **80**, 630 (1936).

[8] J. J. van Laar, "Thermodynamik der einheitlichen Stoffe und binäer Gemische," Groningen, 1935.

[9] J. H. Hildebrand and R. L. Scott, "The Solubility of Nonelectrolytes," 3rd ed., Reinhold Publ. Corp., New York, N. Y., 1950, p. 323.

both being referred to pure liquid zinc as the standard state. For the reaction Zn(s) → Zn(l), one can express the variation of the activity of liquid zinc with temperature by the usual equation, namely

$$R \ln a_1^0(\mathrm{l/s}) = \frac{\Delta H_f}{T} + C_1 \tag{10}$$

Similarly, one uses for the variation of the activity of zinc with temperature in each liquid alloy the equation

$$R \ln a_1(\mathrm{l/l}) = \frac{\bar{L}_1}{T} + C \tag{11}$$

Since $a_1^0(\mathrm{s/l}) = 1/a_1^0(\mathrm{l/s})$, then on applying the equality expressed by equation 9 to equations 10 and 11 one obtains

$$\frac{-\Delta H_f - \bar{L}_1}{T} = C_1 + C \tag{12}$$

Furthermore, since $F_l^0 - F_s^C = RT \ln a_1^0(\mathrm{l/s})$, then by equation 10

$$\frac{\Delta F^0 - \Delta H_f}{T} = C_1 \tag{13}$$

Combination of equations 12 and 13 yields

$$\frac{-\bar{L}_1 - \Delta F^0}{T} = C \tag{14}$$

Thus one can obtain C for each alloy of a fixed composition on the liquidus if both the ΔF^0 value for the melting of pure zinc and the $\bar{L}_1$ value for zinc in the alloy are available. Values of ΔF^0 at temperatures along the liquidus corresponding to the compositions for which $\bar{L}_1$ values had been obtained by Kleppa's method were calculated through use of equation[5] 15

$$\Delta F^0 = 852 - 4.951T \log T + 0.0012T^2 + 12.015T \tag{15}$$

The activity of zinc in an alloy of a fixed composition was next determined at 700°K. though use of equation 11 assuming constancy for $\bar{L}_1$ and C over the temperature range. The results of the calculations for zinc using values of $\bar{L}_1$ obtained by equations 4 and 7 are shown graphically in Fig. 3 along with the experimental values in the literature.[4]

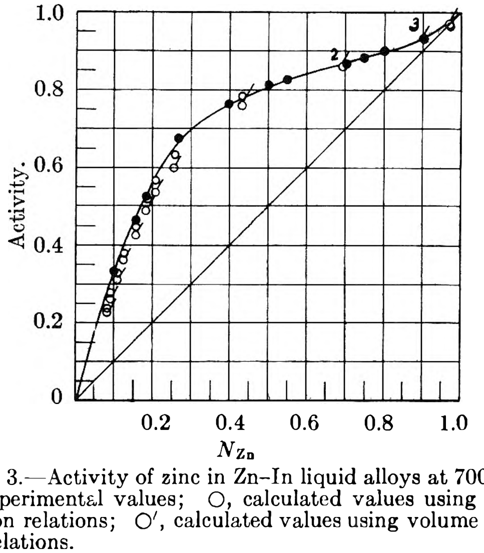

Fig. 3.—Activity of zinc in Zn–In liquid alloys at 700°K.: ●, experimental values; ○, calculated values using mole fraction relations; ○′, calculated values using volume fraction relations.

Entropies.—In liquid alloy, the partial molal entropy of a component may be expressed by equation 16, namely

$$\Delta \bar{S}_1 = \bar{L}_1/T - R \ln a_1(\mathrm{l/l}) \tag{16}$$

Using values of $\bar{L}_1$ and a_1 obtained by both mole fraction and volume fraction relations, values of $\Delta \bar{S}_1$ for zinc in the molten alloys were calculated at 700°K. and the results are shown in Fig. 4 along with the literature values.[4]

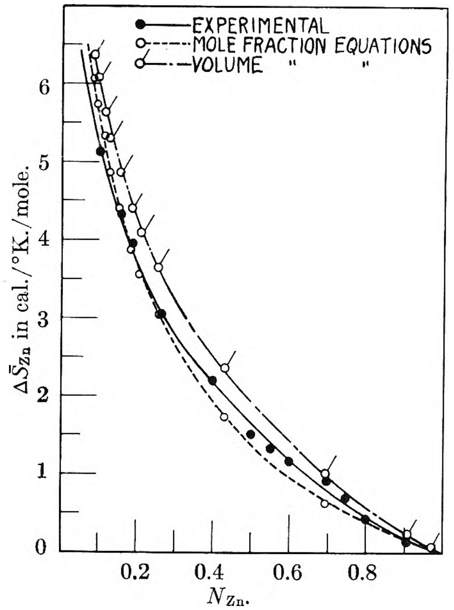

Fig. 4.—Partial molal entropy of zinc in Zn–In liquid alloys at 700°K.

Discussion.—Reference to Fig. 2 shows that neither the mole fraction nor the volume fraction expressions for ΔH, $\bar{L}_1$ and $\bar{L}_2$ are completely satisfactory for the accurate evaluation of those quantities over the entire concentration range of the zinc–indium system. However, the agreement is as good as can be expected considering the assumptions which were made in the derivation[1] of the equations. Moreover, consideration of the curves for all three quantities indicates that the mole fraction expressions lead to better agreement with experiment for the ΔH and $\bar{L}_1$ calculations than do the volume fraction expressions. However, the opposite appears to be true concerning the $\bar{L}_2$ results.

Reference to Fig. 3 shows that the calculated activities of zinc in the liquid alloys obtained by using the mole fraction values of $\bar{L}_1$ are in good agreement with the experimental activities. However, the calculated results obtained by using the volume fraction values of $\bar{L}_1$ are lower in the more dilute zinc alloys.

Reference to Fig. 4 shows that the partial molal entropies of zinc in alloys are reproduced as well as can be expected by use of $\bar{L}_1$ values obtained by either method.

In conclusion, it can be stated that while the results reported in this paper for the zinc–indium system support the semi-empirical relations proposed by Kleppa for certain restricted systems, nevertheless, one cannot choose definitely between the mole fraction or the volume fraction relations used.

SORPTION BY ATTAPULGITE. PART I. AVAILABILITY OF INTRACRYSTALLINE CHANNELS

By R. M. Barrer and N. Mackenzie

The Chemistry Department, The University of Aberdeen, Old Aberdeen, Scotland

Received March 8, 1954

Considerable doubt has existed as to the availability of the channels in attapulgite for intracrystalline sorption. A study of the kinetics and equilibria of sorption of N_2, O_2, CO_2, H_2O, NH_3, CH_3OH and C_2H_5OH has now been made which indicates some lattice penetration as well as substantial surface sorption by H_2O, NH_3, and to a lesser extent by the alcohols. Sorption of the other species is confined to the external surfaces of the crystallites, and possibly to some extra sites at the entrances to the channels. Curves of the differential quantities ΔH, ΔG and ΔS against the amount sorbed for N_2 and O_2 show that attapulgite is heterogeneous as a sorbent, and that the initial heat of sorption of nitrogen exceeds that of oxygen, as it does for several other polar sorbents. Possible reasons are given for this heterogeneity, for the small extent of hysteresis and for the failure of permanent gases to penetrate into the wide channels traversing the lattice of attapulgite.

The structure of attapulgite proposed by Bradley[1] presents this mineral as composed of lath-like crystallites with long double chains (Si_4O_{11}) running parallel to the long axis. The upper and lower parts of each double chain are joined together by a layer of Mg and Al atoms in 6-fold coördination, and to other chains by shared oxygen atoms along each edge. The chains thus form a network of strips presenting mainly oxygen atom surfaces. The strips are joined together only along edges so that a cross-section of the crystal normal to the strips would resemble a wall with every second brick removed. Accordingly there exist channels which run parallel to the crystal length and which normally contain water molecules. Half of these are believed to be closely coördinated to the outermost of the Mg cations sandwiched into the strips and half to be vagabond constituents of the crystal. If this latter group of water molecules were removed each channel should have an estimated free cross section of about 3.7 Å. by 6.0 Å. parallel to the long axis, since on dehydration the structure remains essentially intact. When the coördinated water is also removed the free cross-section would become approximately 3.7 Å. by 12 Å. Because of replacement by Al of some Si in tetrahedral and Mg in octahedral coördination within each aluminosilicate strip these strips develop a net anionic charge, neutralized by additional cations some of which are probably contained within the channels.[2] Only the Al-free Mg end member should be free of such cations. It should also be noted that although details of the structure of sepiolite have not been given it is possible that this mineral resembles attapulgite in structure,[3] differences being due as much to differences in chemical composition as to atomic configuration. Further work is required however before the true inter-relations can be established.

Clay minerals including attapulgus clay have become important as industrial sorbents[4,5] but considerable confusion exists regarding the nature of the sorption processes involved. Nederbragt and de Jong[6,7] thought that the intracrystalline channels in attapulgite might entrain *n*-paraffins but were too narrow to admit isoparaffins. McCarter and co-workers[5] also considered that sorption of nitrogen in the channels was possible. Granquist and Amero[8] on the other hand questioned the availability of the channels for nitrogen sorption. Bradley[9] observed a decrease in refractive index of attapulgite crystals when immersed in glycol, which might imply that channel water was removed without replacement by glycol. It was therefore of interest to carry out further studies of the sorbent properties of attapulgite, to try to establish whether sorption is intracrystalline or confined to external surfaces, or whether both types of sorption occur simultaneously. Migeon[10] has moreover made a study of sorption in sepiolite and has suggested that zeolitic sorption of oils and other species may occur. In view of this and because of the structural similarity that may exist between attapulgite and sepiolite some measurements of sorption were also made using this mineral.

Experimental

Sepiolite was supplied from the Department of Geology of this University. The attapulgite was supplied by the Royal Dutch Shell Co. An X-ray powder photograph showed that some quartz was also present. Both attapulgite and sepiolite were also examined by means of the electron microscope, and appeared as characteristic very fine lath-like crystallites.

Sorption isotherms were measured for less condensable gases in a volumetric apparatus, using helium to determine dead space. Helium, nitrogen and oxygen were obtained in the pure state from the British Oxygen Co. Ammonia was prepared by heating a mixture of calcium oxide and ammonium chloride previously degassed for six hours *in vacuo*. The ammonia evolved was passed through a column of freshly ignited quicklime, condensed and purified by repeated fractionation. Carbon dioxide of medical grade was obtained from the British Oxygen Co. It was bubbled through concentrated sulfuric acid, condensed and submitted to repeated fractionation. The sorption bulb in the volumetric apparatus was held at various constant temperatures by surrounding with constant temperature two-phase media: melting ice (0°); melting chloroform (−63.5°); and Dry Ice in acetone (−78°). Also liquid oxygen (−183°) and liquid nitrogen (−195°) were employed as refrigerants. Temperatures in the interval −183 to −195° were measured by means of an oxygen vapor pressure thermometer.

---

(1) W. F. Bradley, *Am. Mineralogist*, **25**, 405 (1940).

(2) C. E. Marshall and O. G. Caldwell, This Journal, **51**, 311 (1947).

(3) *Cf.* "X-Ray Identification and Structure of Clay Minerals," Mineralogical Soc., 1951, Chap. 8 and 9.

(4) C. L. Mantell, "Adsorption," McGraw-Hill Book Co., Inc., New York, N. Y., 1945, Chap. III.

(5) W. S. McCarter, K. A. Krieger and H. Heinemann, *Ind. Eng. Chem.*, **42**, 529 (1950).

(6) G. W. Nederbragt, *Clay. Min. Bull.*, **3**, 72 (1949).

(7) G. W. Nederbragt and J. J. de Jong, *Rec. trav. chim.*, **65**, 831 (1946).

(8) W. T. Granquist and R. C. Amero, *J. Am. Chem. Soc.*, **70**, 3265 (1948).

(9) W. F. Bradley, *Am. Mineralogist*, **30**, 704 (1946).

(10) G. Migeon, *Bull. soc. franc. mineral.*, **59**, 6 (1936).

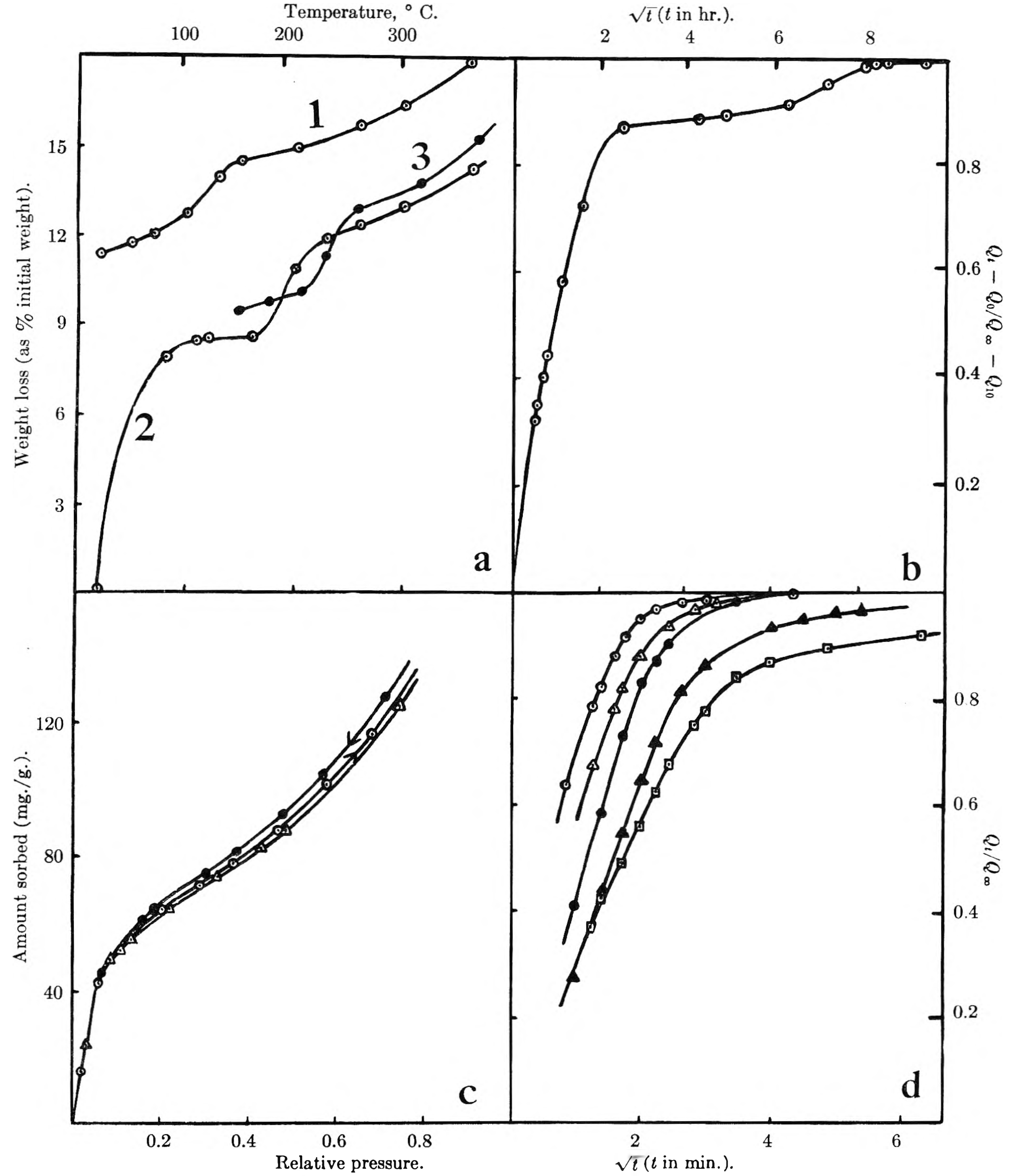

Fig. 1.—(a) Loss of volatile matter from attapulgite. Curve 1 refers to atmospheric conditions and curve 2 to vacuum. Results obtained by McCarter, *et al.*,[4] are also shown in Curve 3. (b) Rate of loss of volatile matter from attapulgite at room temperature *in vacuo*. (c) Water sorption on attapulgite outgassed at 70°: ⊙, ● are sorption and desorption points for an isotherm at 50°; △ are sorption points for an isotherm at 70°. (d) Rate of uptake of initial charge of water vapor at 50° by attapulgite samples outgassed at 50° (⊙), 102° (△), 124° (●), 175° (▲) and 215° (⊡).

The sorption of condensable vapors was measured by means of a modification of the McBain and Bakr silica spring balance. Silica springs were supplied by the Thermal Syndicate, Ltd. The springs gave a linear extension corresponding to ~15 cm. per g. with a maximum permissible load of ~1 g. They were calibrated in an air thermostat at several temperatures within the sorption range studied (10 to 70°). Extensions were independent of temperature in this range, and independent also of thermal treatments of the springs up to 360°. About 0.4 g. of sorbent was suspended from a spring in a glass bucket weighing about 0.1 g. Spring extensions were observed by means of a cathetometer reading to 0.001 cm., so that weight changes of 10^{-1} mg. per g. of sorbent could be measured with considerable accuracy. Corrections for buoyancy were made, but were usually very small. The cathetometer was used also to read the vapor pressures recorded by mercury manometers attached to the balance case of the silica spring balance.

The balance case was immersed in a water thermostat maintained within ±0.05° at any desired temperature 10 to 70°. Temperatures between 10 and 20° were reached by circulating cold water through a U-tube immersed in the thermostat. The liquid sorbate was maintained in a second thermostat similarly regulated. It was retained by mercury cut-offs in place of taps, and was kept at temperatures

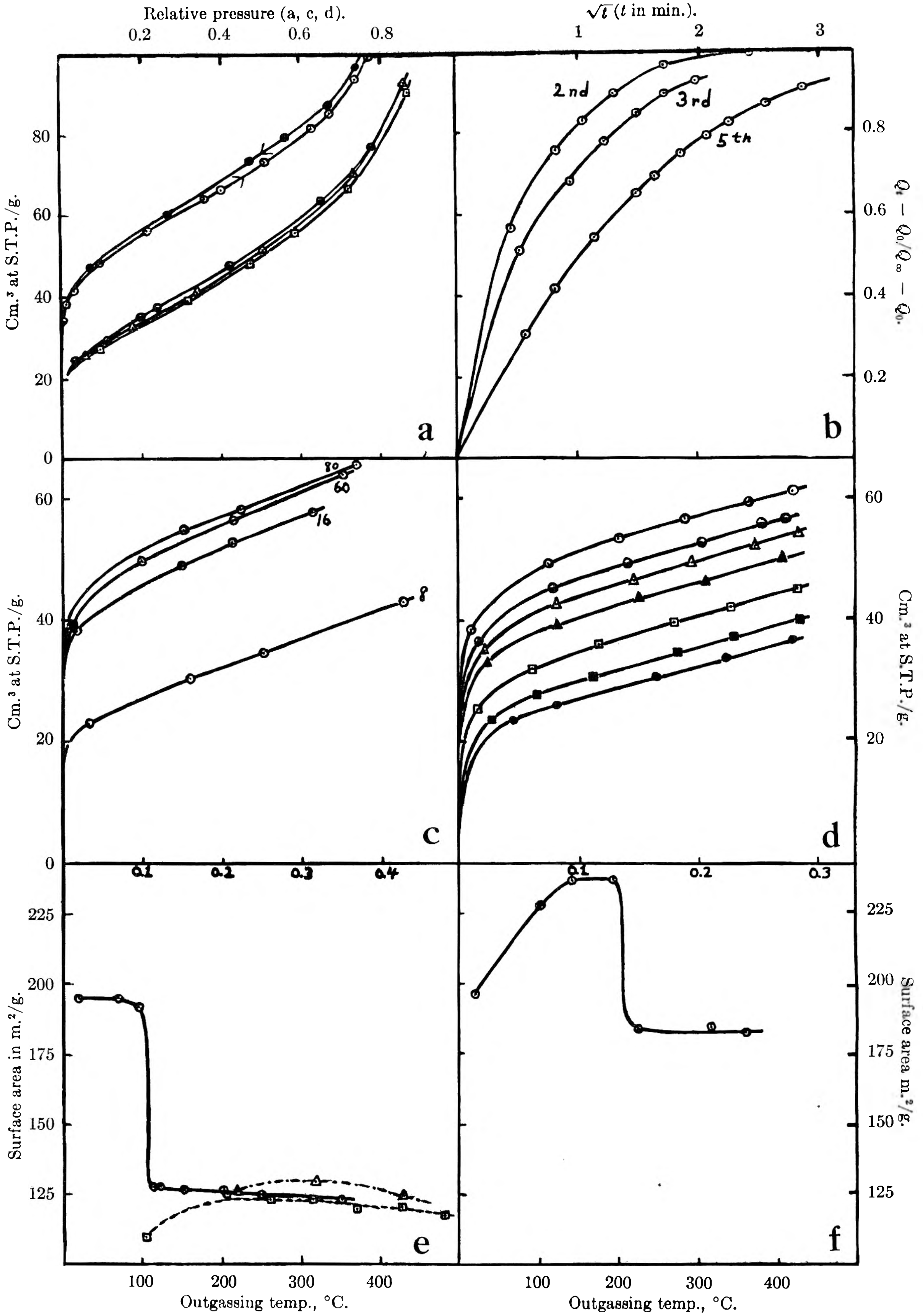

Fig. 2.—(a) Isotherms for N_2 on attapulgite at −194°. Sorption (⊙) and desorption (●) on sorbent outgassed at 20°; ⊖, sorbent outgassed at 115°; △, sorbent outgassed at 250°; ⊡, sorbent outgassed at 350°. (b) Kinetics of N_2 sorption at −194°. p/p_0 = 0.28, 0.46 and 0.75 for 2nd, 3rd and 5th charges, respectively. (c) Effect of outgassing time at room temperature upon N_2 sorption at −194°. Outgassing times are indicated on the isotherms in hours. (d) N_2 sorption.

at −194° showing regeneration of attapulgite with saturated water vapor, after initial outgassing at 145° (◒), 220° (△), 285° (▲), 320° (⊡) and 350° (■). For comparison N_2 isotherms are also shown on samples outgassed at 20° (⊙) and 145° (●) without subsequent treatment with water vapor. (e) Effect of outgassing temperature on surface area of attapulgite. This investigation (⊙); Granquist and Amero (△); McCarter, Krieger and Heinemann (⊡). (f) Effect of outgassing temperature on surface area of sepiolites.

equal to or below that in the thermostat containing the balance case. The connecting tube between the sorbate and sorbent was heated electrically. By opening the appropriate mercury cut-off any desired dose of sorbate vapor could be admitted to the sorbent in the balance case, and the sorbate then sealed off again. The condensable sorbates used were twice-distilled water, and methanol and ethanol of AnalaR grade. Various pure hydrocarbons were also studied in this apparatus as described in Part II.

To outgas the minerals at temperatures above 70° the water was run out of the thermostat in which the balance case and silica spring were placed, and a tubular furnace supported by vertical guide rails was slid down over the balance case. This furnace was operated up to 360°.

The electron microscope used in examination of the crystal form of attapulgite was a Metrovick EM3 instrument. X-Ray photographs of the crystals were taken with a Hilger HRX Unit, using filtered Cu Kα radiation at 39 kv.

Sorption of Water.—It was early apparent that the sorptive properties of attapulgite toward other species were linked with its water content. Accordingly the sorption process for water was investigated. The dependence of water loss upon the temperature is shown in Fig. 1a. For each point the crystals were left for as long as 70 hours at the experimental temperature. There is obviously a very marked difference when water loss is effected under exposure to the atmosphere, and when the water is removed under vacuum (curves 1 and 2). However our curve 1 and that of McCarter, *et al.*,[4] also for water removal under atmospheric conditions but allowing only 30 minutes for equilibration of each point, correspond satisfactorily. Water loss also has been investigated by Longchambon.[11] Fig. 1b shows the rate of evolution of the water during outgassing of attapulgite crystals at room temperature.

When crystals of attapulgite are bathed in water vapor the sorption isotherms are sigmoid in form (Fig. 1c) and if the crystals had been outgassed initially at rather low temperatures close to those of the subsequent sorption there was only a very slight hysteresis. Equilibration times increased with the amount sorbed and were rather longer for desorption than for adsorption. The small temperature coefficient of sorption shows that the heat of transfer from liquid water to adsorbed film is quite small.

As the initial outgassing temperatures increased the sorption equilibrium in subsequent low temperature isotherms was established with increasing slowness. This is shown in Fig. 1d, for the rate of approach to equilibrium on admitting a first charge of water to the crystals initially outgassed at 55, 102, 124, 175 and 215°. Many days were eventually required for the intermediate and later parts of the isotherms. Water isotherms obtained at 50° after high temperature outgassing of attapulgite are not necessarily completely equilibrated, although such equilibria must have been rather closely approached. Monolayer values, v_m, did not vary greatly, however, whatever the outgassing temperature. To some extent this may be associated with a chance balance between two opposing influences: a decrease in external surface area (as found with N_2, O_2 and CO_2 (*e.g.*, Fig. 2d)); and an increase in the number of available intracrystalline sites as more intracrystalline water is removed by initial outgassing at increasing temperatures (Fig. 1a). Two processes do appear to be involved in sorption of water, firstly adsorption upon external surfaces, which is a rapid process; and secondly a slow penetration into the crystals, becoming evident only when some intracrystalline water has been removed.

Sorption of Nitrogen.—Correlation was sought between the behavior of nitrogen and oxygen as sorbates, and the water content of the crystals of attapulgite. Isotherms of nitrogen and oxygen at −195 and −183° were sigmoid in form (Fig. 2a) just as were the water isotherms of Fig. 1c. These isotherms under all conditions showed only a very slight but definite hysteresis. The rates of sorption for the three permanent gases were always rapid, and though these rates tended to decrease as the charge of gas increased (Fig. 2b), the much slower processes observed with water were not noted.

The progressive removal of water, by degassing attapulgite crystals at room temperature, results in a corresponding increase in the sorption of nitrogen (Fig. 2c). When the initial removal of water from attapulgite occurred over a period of as much as 70 hours but at progressively higher temperatures, the attapulgite crystals showed interesting changes in the high surface area as revealed by nitrogen sorption at −183° (Fig. 2e). With outgassing in the range 20–95° there was little change in the v_m values for nitrogen; between 95 and 115° a rapid decrease in v_m occurred; and between 115 and 350° the magnitude of v_m and so of derived surface areas remained nearly constant. On Fig. 2e are also given the curves of surface area *vs.* "activation" (*i.e.*, water removal) temperatures as obtained by Granquist and Amero[8] and by McCarter, *et al.*[5] Neither of these groups of workers observed the very large areas obtained by degassing below 95°, presumably because they did not study low activation temperatures. Our numerical values of v_m and of surface area are given, in relation to outgassing temperature, in Table I.

TABLE I

OUTGASSING TEMPERATURE AND SURFACE AREA OF ATTAPULGITE (BY N_2 SORPTION AT −183°)

Outgassing temp., °C.	Mean v_m value, cm.^{3} at S.T.P./g.	Derived surface area, m.^{2}/g.	Outgassing temp., °C.	Mean v_m value, cm.^{3} at S.T.P./g.	Derive surface area, m.^{2}/g.
20	46.85	195	150	30.59	127
70	46.85	195	200	30.59	127
95	46.09	192	250	30.06	125
115	30.85	128	350	29.54	123
120	30.85	128			

A study of nitrogen sorption at −183° in sepiolite also showed a close correlation between the temper-

---

[11] *E.g.*, H. Longchambon, *Compt. rend.*, **204**, 55 (1937).

ature of water removal and the surface area (Fig. 2f). As with attapulgite, nitrogen equilibrated quickly to give a copious sorption, the isotherm again being of type 2 in Brunauer's classification. The area available for N_2 sorption at first increased with outgassing temperature, from 196 m.^{2}/g. at 20° to 236 m.^{2}/g. at 140°. This area then remained constant up to 185°. Next, between 185 and 225° a rapid drop in area occurred, but between 225 and 360° the area again stayed constant at $\sim$184 m.^{2}/g. While there are quantitative differences in behavior between attapulgite and sepiolite there are also very striking qualitative similarities.

The rapid establishment of equilibrium, and changes in sorption with outgassing temperatures suggest that nitrogen does not show significant intracrystalline penetration in attapulgite. Had penetration occurred, the sorption of nitrogen should have increased as the water was more completely removed from intracrystalline positions, and so provided more sites for nitrogen uptake. Instead Fig. 2c and Table I show that v_m decreases as the water is more completely removed. Evidently this water loss does not open up the intracrystalline channels for nitrogen. The same behavior was also observed in attapulgite with the somewhat smaller molecule of oxygen. The initial rise in v_m and derived surface area in the case of sepiolite (Fig. 2f) may be associated with improved but very limited access to the mouths of channels (see Discussion).

The various specimens of attapulgite which had been outgassed at 115–145, 220, 285, 320 and at 350° were then exposed to saturated water vapor at room temperature and once more outgassed, but this time at a low temperature ($\sim$20°). When the nitrogen sorption at $-183°$ was again examined it was found that the high surface areas associated with low temperature outgassing were largely or partially regenerated. Recovery was almost complete for the crystals initially outgassed in the range 115 to 145°, and was less and less complete when the crystals had been initially outgassed at progressively higher temperatures than this, as shown in Fig. 2d.

The behavior which has been described indicates that there are two stages in the loss of surface area associated with higher temperature water removal. There is first a sudden change in area coupled with water removal at 95–115°, but not with its removal below this range. This change is reversible merely by treatment with saturated aqueous vapor. The second stage in the process is the fixation of the low surface area configuration. This is a slow reaction which becomes progressively accelerated as the temperature rises. These changes are not demonstrably coupled with intracrystalline lattice alterations since X-ray powder photographs remained those of attapulgite. Following from the crystal structure given by Bradley,[1] the surface of the crystals should consist of corrugations on a molecular scale. The changes coupled with water removal from 95° upwards may be connected with surface changes in these corrugations.

Sorption of Polar Vapors.—The sorption of the polar molecules ammonia, methanol, ethanol and carbon dioxide was studied in order to find to what extent lattice penetration could be observed among species which vary considerably both in size and polarity.

Ammonia.—While the behavior of other sorbates followed the same general pattern, ammonia sorption on attapulgite was characterized by a considerable hysteresis loop in the initial isotherm, by a long equilibration time and by a marked dependence on outgassing temperature and sorptive history. In an isotherm determined at 100° after an initial removal of water at 150° ammonia was still being sorbed, although very slowly, after four days. Sorption rates at 100° increased as the temperature of initial removal of water increased, and in general desorption was slower than sorption. Such slow processes are associated with lattice penetration.

Isotherm points at $-63.5°$ were read after an hour because of the difficulty of maintaining this temperature for very long periods. Isotherm points at 0 and 100° were read after four hours on the sorption run and after eight hours on desorption. Thus the isotherm shown in Fig. 3 may not represent true equilibrium. Such isotherms should however be in correct relative positions.

The substantial hysteresis observed at higher temperatures (Fig. 3a) is associated with non-equilibrium states of sorption due to slow lattice penetration. The hysteresis became less and less in each successive sorption–desorption cycle until finally it was very slight. At higher temperatures only isotherms on much used samples were repeatable. The performance of the sorbent degassed at 200° and used at 100° was improved by preliminary repeated ammonia sorption with outgassing at room temperature (Fig. 3d); on the other hand the performance at $-63.5°$ decreased with usage when the outgassing temperature between runs was 20° (Fig. 3c). Finally, when sorption at 100° was studied in relation to the outgassing temperature of a much used sample of attapulgite, the results of Fig. 3b were obtained. Sorption of ammonia is not greatly changed for outgassing temperatures of 100, 200 and 250°, but drops sharply between 250 and 300°. There is little further change between 300 and 350°.

It is seen from the foregoing results that sorption phenomena associated with ammonia are complex. They can however be correlated with slow lattice penetration coupled with surface sorption. Also a connection between water loss and ammonia sorption exists here as for the adsorption of nitrogen and oxygen although in a different range of temperatures.

Alcohols.—Isotherms of methanol and ethanol resembled those of nitrogen in giving sigmoid isotherms with little hysteresis (Fig. 4a). Unlike water and ammonia but similarly to nitrogen, v_m decreased when the initial removal of water from attapulgite was in the range 95–115°. Nevertheless for higher initial outgassing temperatures of the crystals a slow process was observed requiring many days for its completion and superposed upon the usual rapid adsorption. Hysteresis loops allowing finite time for each isotherm point now became more marked and presumably reflect non-

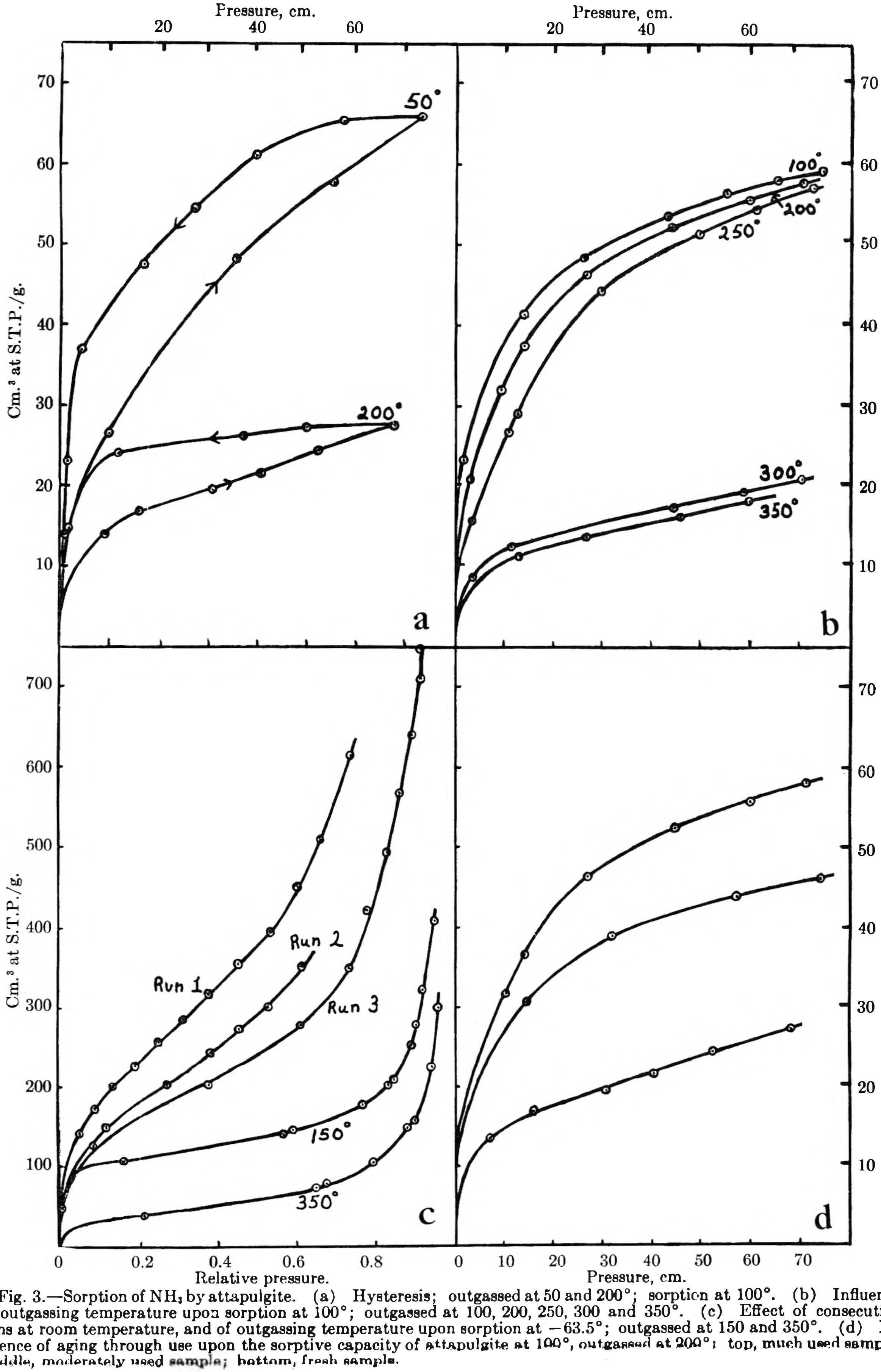

Fig. 3.—Sorption of NH_3 by attapulgite. (a) Hysteresis; outgassed at 50 and 200°; sorption at 100°. (b) Influence of outgassing temperature upon sorption at 100°; outgassed at 100, 200, 250, 300 and 350°. (c) Effect of consecutive runs at room temperature, and of outgassing temperature upon sorption at −63.5°; outgassed at 150 and 350°. (d) Influence of aging through use upon the sorptive capacity of attapulgite at 100°, outgassed at 200°; top, much used sample; middle, moderately used sample; bottom, fresh sample.

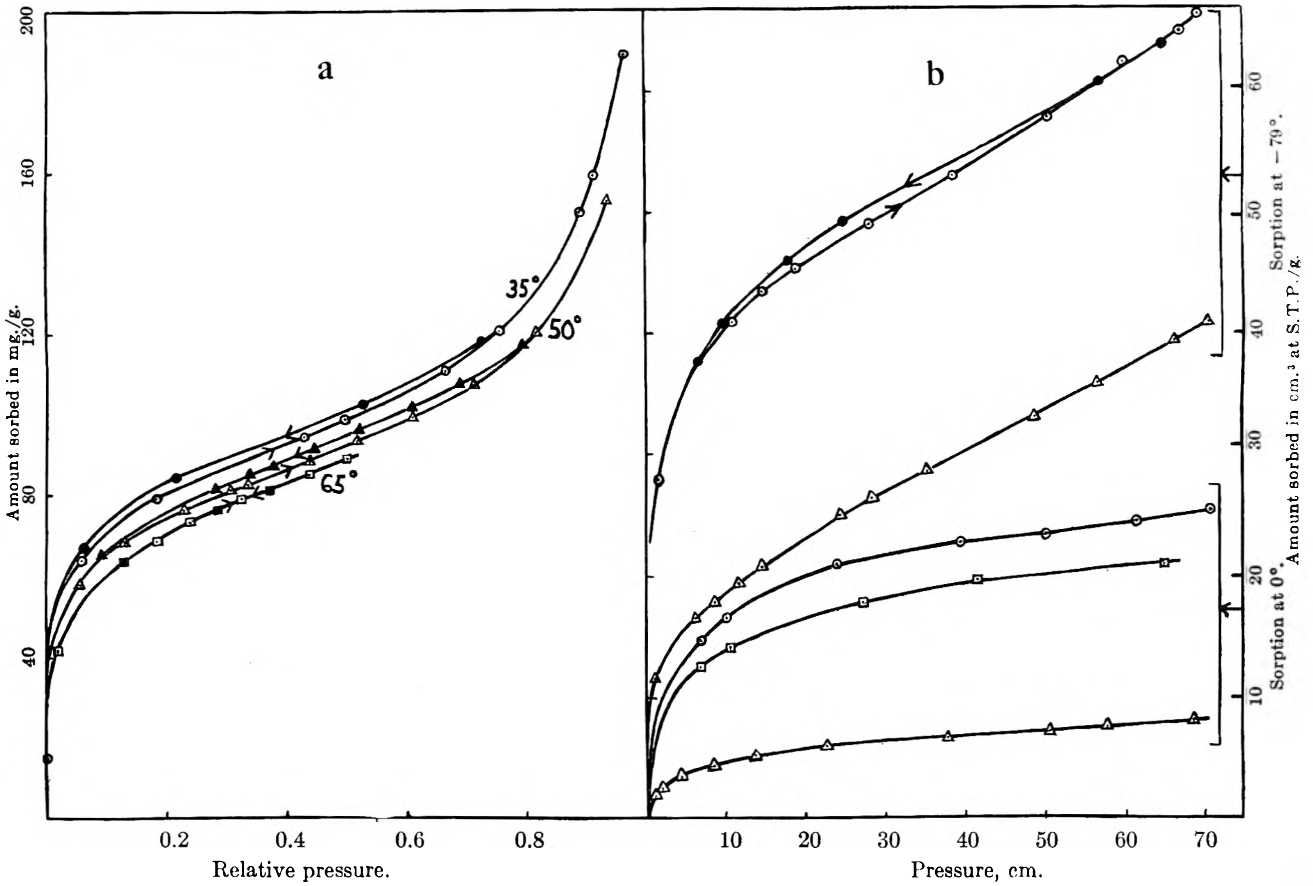

Fig. 4.—(a) Sorption-desorption cycles for CH_3OH on attapulgite outgassed at 70°. (b) Sorption of CO_2 on attapulgite: ●, ⊙, after outgassing at 20°; △, after outgassing at 150°; ⊡, after outgassing at 150°, followed by treatment with saturated water vapor and a second outgassing at 20°.

equilibrium states of the system. Complete removal of the sorbate required a period of five to six days *in vacuo* at the sorption temperature.

The results suggest, as with water and ammonia, that when the original intracrystalline water has been at least partly removed simple alcohol molecules may very slowly enter the crystals and take its place. The penetration process is however less marked, possibly because it occurs more slowly.

Carbon Dioxide.—Carbon dioxide, which is intermediate in physical properties between the readily condensable alcohols and the permanent gases, was found to follow in all respects the nitrogen pattern. Typical isotherms are shown in Fig. 4b. The amount of carbon dioxide sorbed fell sharply between outgassing temperatures of 20 and 150°, but regeneration with water vapor after outgassing at 150° very largely restored the high activity characteristic of the crystals when degassed at room temperature. No slow sorption was observed, and lattice penetration was therefore discounted.

Surface Areas.—Monolayer values, v_m, were determined by means of the appropriate linear plots for various isotherm models, based on equations of BET,[12] Huttig[13] and Barrer, Mackenzie and MacLeod.[14] The degree of variation in v_m determined by means of these extrapolation formulas is shown for nitrogen at 78°K. in Table II. Not all of the equations fit the experimental isotherm equally well. Isotherms[14] H, K_1, K_2 and K_3 are in very satisfactory agreement with the isotherm, and all give closely corresponding v_m values. As pointed out earlier[14] the most consistent v_m values in general follow from the best fitting extrapolation formulas.

Table II

v_m Values for N_2 at 78°K. Using Various Extrapolation Formulas

Isotherm designation[a]	v_m, cm.³ at S.T.P./g.	Isotherm designation[a]	v_m, cm.³ at S.T.P./g.
BET	43.81	F	56.07
Huttig	47.19	H	46.31
A	46.66	K_1	47.34
B	40.62	K_2	47.81
D	40.05	K_3	46.62

[a] Isotherms A to K_3 correspond to the notation of Barrer, Mackenzie and MacLeod.[14]

From the v_m values one may obtain "surface" areas for the crystals of attapulgite outgassed at various temperatures. The results for two extreme outgassing temperatures, 20 and 350° are shown in Table III. This table includes, for purposes of comparison, data for *n*-heptane, isoöctane and the isomeric pentanes, the sorption of which will be considered in another paper.[15] Where only the re-

---

(12) S. Brunauer, "Physical Adsorption of Gases and Vapors," O.U.P., 1945, Chap. 6.

(13) G. F. Huttig, *Monatsh.*, **78**, 177 (1948).

(14) R. M. Barrer, N. Mackenzie and D. M. MacLeod, *J. Chem. Soc.*, 1736 (1952); 4184 (1953).

(15) R. M. Barrer, N. Mackenzie and D. M. MacLeod, in preparation.

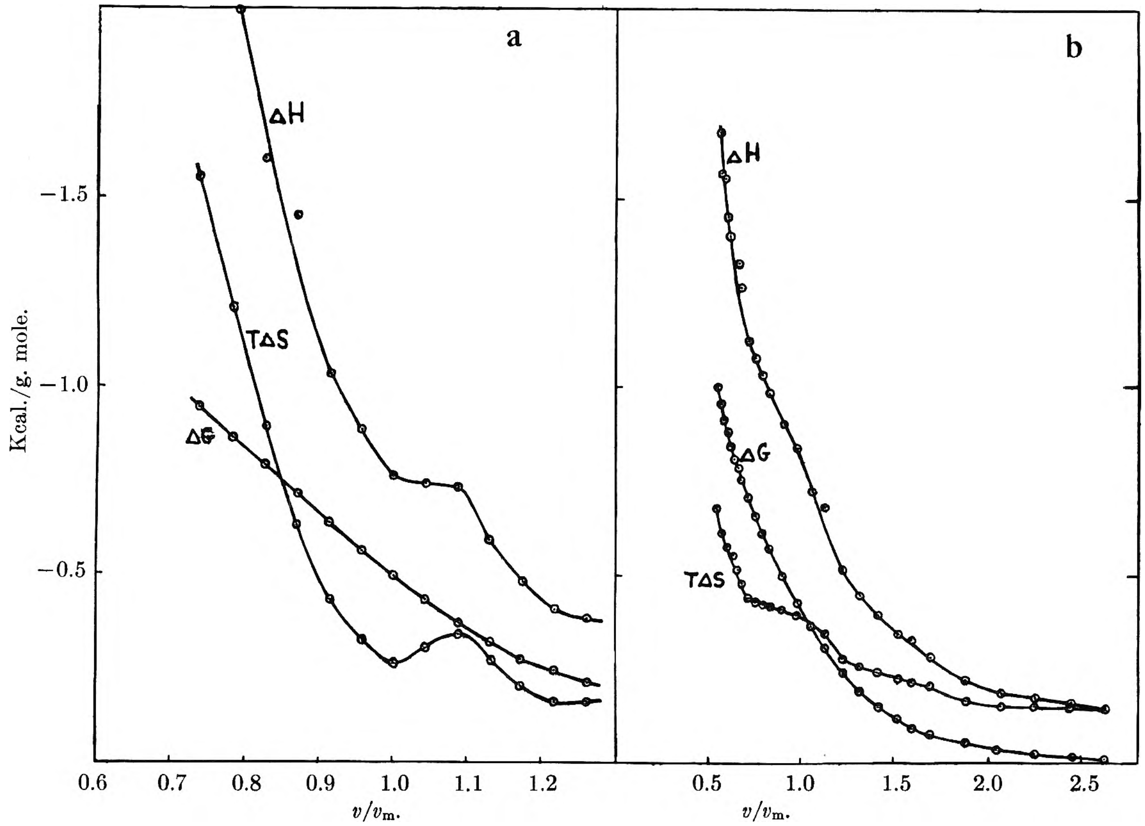

Fig. 5.—Thermodynamic functions for sorption of N_2 (left) and O_2 (right) by attapulgite, determined from isotherms at 79.25 and 89.45°K.

TABLE III

AVERAGE SURFACE AREAS FOR ATTAPULGITE CRYSTALS

Outgassing temp., °C.	Sorbate	Area assumed per molecule, Å.²	Isotherm equation used in getting av. v_m	Av. v_m, cm.³ at S.T.P./g.	Surface area, m.²/g.
20	N_2	15.4	11	46.85	195
	O_2	14.6	3	53.25	210
	NH_3	12.6	11	201.78	685
	CO_2	19.5	3	36.57	193
	H_2O	11.0	3	70.30	209
	CH_3OH	18.5	3	43.15	216
	C_2H_5OH	23.4	2	31.50	199
	n-Heptane	59.4	12	9.67	152
	Isoöctane	57.8	12	6.85	107
	n-Pentane	49.7	9	12.79	172
	Isopentane	50.4	9	11.38	155
	Neopentane	45.5	9	9.10	112
350	N_2	15.4	4	29.54	123
	NH_3	12.6	11	36.36	123
	CO_2	19.5	3	17.77	94
	n-Pentane	49.7	9	7.06	95
	Isopentane	50.4	9	7.54	103
	Neopentane	45.5	9	7.55	93

sults of a small number of isotherms are averaged these were the best fitting among the equations of Table II and the Chu Liang[16] formula. The surface areas with the exception of the value for ammonia are of the same order as the area of 150 m.²/g. estimated by Endell[17] from geometric considerations. However, with some vapors a fraction of the sorbate is taken into the lattice, and this process presumably accounts for the abnormally large initial sorption of ammonia. The areas in Table III will be high when measurable lattice penetration occurs.

For molecules which do not penetrate appreciably the attapulgite lattice there is a considerable variation between surface areas, which is outside any likely error in the area per molecule of sorbate (*cf.* Table III, column 3). It seems for example that the topography of the crystal surface when outgassed at 20° is such that isoöctane packs badly in the monolayer as compared with *n*-heptane. This is considered elsewhere.[15]

Thermodynamic Functions.—The differential thermodynamic functions ΔH, ΔG and ΔS associated with transfer of liquid sorbate to the adsorbed film on attapulgite outgassed at room temperature were evaluated for nitrogen and oxygen, with a view to obtaining additional information regarding the sorption process. Isotherms for nitrogen were determined at 79.25 and 89.45°K., and ΔH calculated from these isotherm data using the integrated Clapeyron–Clausius equation. ΔG was found from the relation $\Delta G = -RT \ln p_0/p$, and ΔS from the expression $\Delta H - T\Delta G = T\Delta S$. The results are shown in Fig. 5a. Figure 5b shows the analogous curves for oxygen.

Attapulgite is seen from Fig. 5 to show a very pronounced heterogeneity toward both sorbates. This heterogeneity could at least partially be associated with the surface corrugations following from the Bradley[1] structure. The oxygen and nitrogen molecules will then occupy preferentially the valleys

---

[16] S. Chu Liang, THIS JOURNAL, **55**, 1410 (1951).

[17] J. Endell, *Z. Naturforsch.*, **1**, 646 (1946).

between parallel ridges. The top of each ridge will tend to be covered later when each valley has been largely occupied by sorbate molecules.

As in the case of several other polar sorbents[18,19] the heat of sorption of nitrogen is initially appreciably higher than that of oxygen. This is also true of the initial entropy decrease following sorption.

Discussion

It now appears that in addition to substantial adsorption upon external surfaces H_2O, NH_3 and possibly (although to a lesser extent) CH_3OH and C_2H_5OH may enter the intracrystalline channels in attapulgite. These channels are not however equally available to N_2, O_2 or CO_2. Thus polarity rather than molecular dimensions governs the effect. A rather similar behavior is found with the zeolites analcite or harmotome, which accommodate only small polar species. Sorption is measurable within a crystal only if there is a free energy decrease when occlusion occurs. Even in channels so narrow that appreciable molecular distortion must result from sorption the endothermic nature of this distortion may be exceeded by the exothermic interaction between polar molecule and polar environment, and the net value of ΔG is still negative for the polar species while it is positive for a non-polar molecule.[20]

However, the channels in attapulgite are, as noted in the introduction, of considerable dimensions, and in a perfect crystal should be able to accommodate small non-polar species. Imperfections of the crystal structure[2] nevertheless result in additional cations being sparsely distributed along the channels, which, together with water molecules, provide high energy barriers opposing diffusion. Moreover, unlike those in many zeolites, the channels in attapulgite are not interconnected. Where this situation occurs the high energy barriers may, even if few in number, largely or almost wholly inhibit entry into the crystal, by reducing the diffusion rate to a negligible value.[21] Sorption of non-polar molecules (N_2, O_2) and of CO_2 may nevertheless occur at or just within the entrance points to channels, before the first barrier is encountered, but this, while providing some extra sites, does not amount to real lattice penetration.[15]

Throughout the isotherm measurements a very small but sometimes reproducible hysteresis was observed. The slight extent of hysteresis is almost certainly associated with the physical texture of the crystals. These are in the form of thin lath-like crystals, often in parallel, twinned configurations as compact crystal clusters, but also in loose aggregates. With such a texture wedge-shaped capillaries will be common which will fill and empty reversibly. Substantial hysteresis will be found not with materials such as sepiolite or attapulgite, which both have the same texture, but rather with spongy xerogels (porous glass,[22] and some silica gels[23]). Flaky crystals such as montmorillonite should tend to be intermediate in behavior between attapulgite and porous glass.

[18] L. E. Drain and J. A. Morrison, *Trans. Faraday Soc.*, **49**, 654 (1953).

[19] R. M. Barrer, *ibid.*, **40**, 555 (1944).

[20] R. M. Barrer, "Colloques internationaux du CNRS," No. 19, "Adsorption et Cinetique heterogene," 1949, p. 27.

[21] R. M. Barrer and L. V. Rees, in preparation.

[22] *E.g.*, R. M. Barrer and J. A. Barrie, *Proc. Roy. Soc.* (*London*), **213A**, 250 (1952).

[23] *E.g.*, "Advances in Catalysis," Vol. 4, Academic Press, New York, N. Y., 1952, p. 87, *et seq.*

SORPTION BY ATTAPULGITE. PART II. SELECTIVITY SHOWN BY ATTAPULGITE, SEPIOLITE AND MONTMORILLONITE FOR *n*-PARAFFINS

BY R. M. BARRER, N. MACKENZIE AND (IN PART) D. M. MACLEOD

The Chemistry Department, The University of Aberdeen, Old Aberdeen, Scotland

Received March 8, 1954

A study has been made of the sorption of *n*-heptane, isoöctane and *n*-, iso- and neopentane on attapulgite; and of the pentanes on montmorillonite and sepiolite. Attapulgite and montmorillonite show selective sorption in the direction *n*-heptane > isoöctane; and *n*-pentane > isopentane > neopentane. Sepiolite outgassed at 20 or 140° sorbed *n*- and isopentane equally strongly, but neopentane less strongly. In the case of attapulgite selectivity has been investigated as a function of outgassing temperature, and has been found to decrease and disappear when the degassing occurs above about 88°. Selectivity reappears to an extent dependent upon the initial outgassing temperature on treatment with saturated water vapor at room temperature. An analysis of the isotherms for attapulgite has been made in terms of changes in v_m values and of affinity constants C, and in terms of free energies, heats and entropies of sorption. v_m and C drop sharply for *n*-heptane and *n*-pentane when outgassing occurs above 88°, but are little dependent upon outgassing temperature for neopentane and isoöctane. Curves of ΔG, ΔH and ΔS against amount sorbed show the sorbent to be heterogeneous, and that all these quantities are initially greater in numerical magnitude for *n*-paraffins than for branched chain paraffins. The selectivity has been discussed in terms of these observations.

When mixtures of saturated *n*-paraffins such as *n*-hexadecane and *n*-tetracosane with analogous branched chain paraffins were dissolved in pentane and passed through a column of attapulgite, Nederbragt and de Jong[1,2] found that the *n*-paraffin constituents were preferentially retained by the crystals, while the isoparaffins were carried through. It was suggested by them that the *n*-paraffins might be entrained in the channels present in attapulgite[3,4] but that the branched chain paraffins were not. However, the results of the previous paper[4] indicate that even quite small non-polar molecules

[1] G. W. Nederbragt and J. J. de Jong, *Rec. trav. chim.*, **65**, 831 (1946).

[2] G. W. Nederbragt, *Clay Min. Bull.*, **2**, 72 (1949).

[3] *Cf.* "X-Ray Identification and Structure of Clay Minerals," Mineralogical Soc., London, 1951, Chap. 9 and p. 237.

[4] R. M. Barrer and N. Mackenzie, THIS JOURNAL, **58**, 560 (1954).

such as nitrogen and oxygen are not appreciably occluded within crystals of attapulgite. The sorption of single pure *n*- and isoparaffins has accordingly been studied to determine what measure of selectivity arises among their sorption isotherms and to find if possible what factors govern such selectivity.

Experimental

The gravimetric apparatus of Part I[4] was used, according to the procedure there described. The same attapulgite and sepiolite crystals were employed, and also crystals of montmorillonite obtained from the Macaulay Institute for Soil Research. The montmorillonite had a base exchange capacity of about 100 meq. per 100 g. The main exchangeable cation was sodium, but there was also about 15% of calcium. Before use the attapulgite and sepiolite were outgassed at various temperatures, while the montmorillonite was outgassed at 50°, a temperature adequate for removal of practically all the inter-laminar water.[5]

The sorbates studied were *n*-heptane (from hevea pine, of engine test standard), isoöctane (2,2,4-trimethylpentane) of the same standard; and also *n*-, iso- and neopentane. The latter three hydrocarbons were first obtained as Phillips research grade pure chemicals and ultimately from the Chemical Research Laboratory, Teddington. The purity was then above 99.5%.

Sorption of *n*-Heptane and Isoöctane.—Although the boiling points of *n*-heptane and of isoöctane are nearly the same it was soon apparent that *n*-heptane showed the greater affinity for attapulgite. Figures 1a and b give the isotherms of *n*-heptane and of isoöctane at 50 and 65° on attapulgite initially outgassed at 70°. There is not a large temperature coefficient in the sorption, so that the heat of transfer from liquid *n*-heptane or isoöctane to the surface of the crystals is small. Equilibrium was established quickly as with nitrogen or oxygen,[4] and hysteresis was only slight. Last traces of *n*-heptane were less easily removed than were those of isoöctane.

The isotherm curves at 50° were thoroughly investigated in a comparative manner, using various theoretical isotherms as extrapolation formulas to obtain the monolayer values v_m and the affinity constant C, both these quantities being defined just as in the BET theory.[6] The results are seen in Table I and show that v_m and C are both larger for the *n*-paraffin than for the isoöctane.

TABLE I

Isotherm designation[a]	*n*-Heptane v_m, cm.^{3} at S.T.P./g.	*n*-Heptane C	Isoöctane v_m, cm.^{3} at S.T.P./g.	Isoöctane C
BET[6]	8.90	68	5.86	11.6
Huttig[7]	9.88	40	7.43	8.1
A	9.65	45	6.51	9.7
B	7.86	100	4.92	13.8
D	9.09	64	4.76	13.0
H	9.55	42	6.43	9.3
K	10.51	24	7.15	7.5
Theimer[8]	10.80	24	8.08	6.6
Chu Liang[9]	8.99	..	5.43	..

[a] Isotherms A to K are those correspondingly designated by Barrer, Mackenzie and MacLeod.[10]

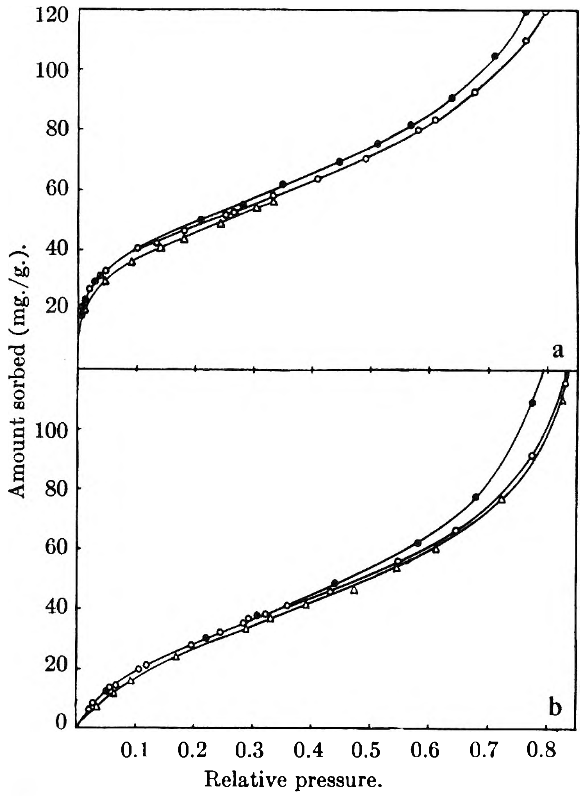

Fig. 1.—Sorption isotherms of (a) *n*-heptane and (b) isoöctane on attapulgite outgassed at 70°: ⊙, sorption at 50°; ●, desorption at 50°; △, sorption at 50°.

The area per molecule of sorbed heptane has been given as 64[11] and as 59[12] sq. Å. Using scale models, areas of 54 sq. Å. for *n*-heptane and 52.5 sq. Å. for isoöctane were obtained. Such areas tend to be low; multiplying each by 1.1 gives an area of 59.4 sq. Å. for *n*-heptane (in line with Livingston's figure[12]) and 57.8 sq. Å. for isoöctane. These areas are very similar, and the marked differences in v_m in Table I therefore suggest that a larger surface is available for *n*-heptane than for isoöctane, owing to some configurational peculiarity of the surface. Apart from this the C constants of Table I show that *n*-heptane molecules in the first layer have the greater affinity for the crystals. Two factors therefore increase the selectivity toward the *n*-paraffin.

The Pentane Isomers.—The sorption of the three pentane isomers confirmed the results obtained with *n*-heptane and isoöctane, the order of selectivity in sorption being *n*-pentane > isopentane > neopentane, provided the initial outgassing was carried out below 88° (see below). If however the crystals were outgassed at higher temperatures the selectivity was reduced almost to nothing (Fig. 2a). It also was found that the same order of selectivity occurred when montmorillonite (outgassed at 50°) was used as sorbent at 50° (Fig. 2b). The quantity of each isomer sorbed is however very much smaller, corresponding to a much reduced surface of the sorbent.

When sepiolite was the sorbent, whether water removal had occurred by outgassing at 20° or at

---

(5) R. M. Barrer and D. M. MacLeod, in preparation.

(6) S. Brunauer, "Physical Adsorption of Gases and Vapors," O.U.P., 1945, Chap. 6.

(7) G. F. Huttig, *Monatsh.*, **78**, 177 (1948).

(8) O. Theimer, *Trans. Faraday Soc.*, **48**, 326 (1952).

(9) S. Chu Liang, THIS JOURNAL, **56**, 1410 (1951).

(10) R. M. Barrer, N. Mackenzie and D. M. MacLeod, *J. Chem. Soc.*, 1736 (1952); 4184 (1953).

(11) E. H. Loeser and W. D. Harkins, *J. Am. Chem. Soc.*, **72**, 3427 (1950).

(12) H. K. Livingston, *J. Colloid Sci.*, **4**, 447 (1949).

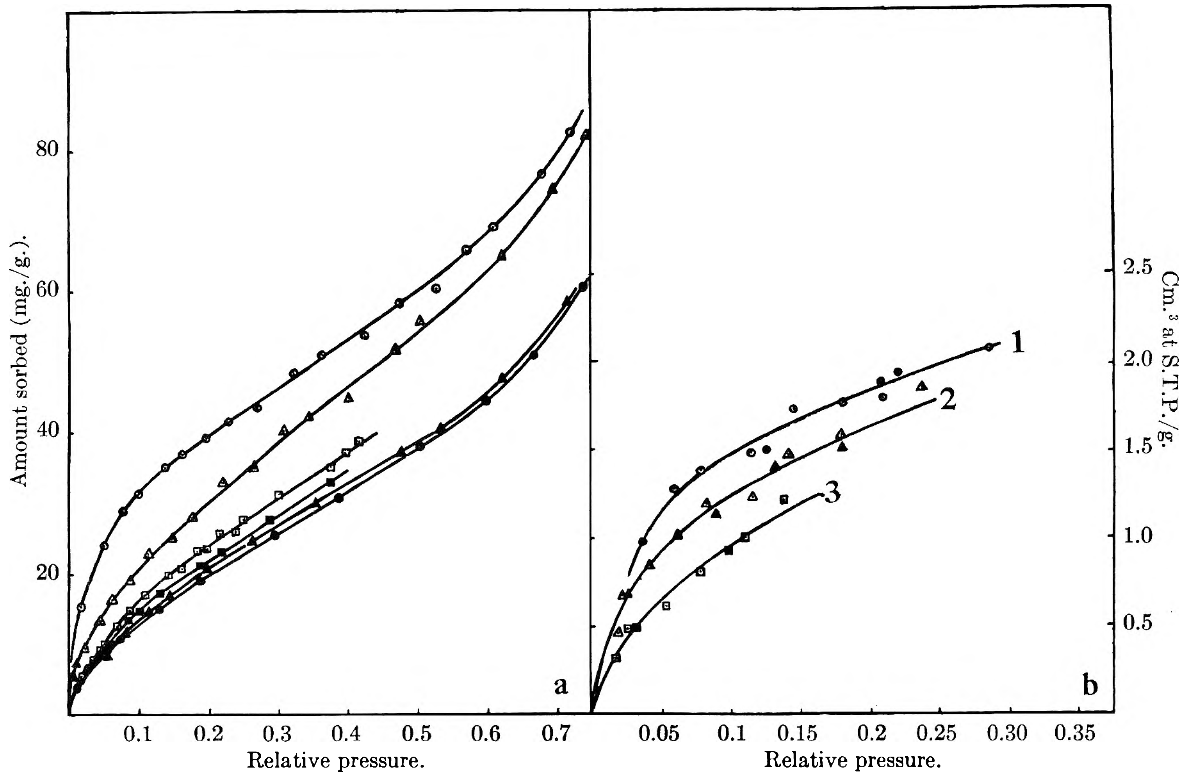

Fig. 2.—(a) n-C_5H_{12} (⊙), iso-C_5H_{12} (△) and neo-C_5H_{12} (⊡) at 20° on attapulgite outgassed at 70°. Also n-C_5H_{12} (●), iso-C_5H_{12} (▲) and neo-C_5H_{12} (■) at 20° on attapulgite outgassed at 215°, showing loss of selectivity. (b) Sorption of isomeric pentanes at 50° on montmorillonite outgassed at 50°. ⊙, △ and ⊡, sorption points; ●, ▲ and ■, desorption points. 1, n-C_5H_{12}; 2, iso-C_5H_{12}; 3, neo-C_5H_{12}.

140°, the isotherms showed no selectivity as between n- and isopentane, but both these paraffins were at given p/p_0 more copiously sorbed than neopentane. Sorption equilibria were rapidly established, suggesting that, as with nitrogen,[4] lattice penetration was not important. The amounts sorbed were however large, as with attapulgite.

Sorption and Outgassing Temperatures.—Sorption isotherms of each pentane isomer were measured at 20° on the attapulgite crystals outgassed at 20, 70, 88, 110, 124, 130, 260 and 360°, a selection of the data being given in Fig. 2a. Surface areas were next determined from all the isotherms using the BET linear plot to find v_m and C for each isomer (Table II). In these calculations the surface areas used were 49.7 sq. Å. (n-pentane), 50.4 sq. Å. (isopentane) and 45.5 sq. Å. (neopentane). Scale models of each molecule were used to find the relative molecular areas, and then each area was multiplied by the factor required to bring the n-pentane area up to the value of 49.7 sq. Å., as given by Corrin.[13] According to Table II there is a sharp drop in the area available for sorption of n-pentane and of isopentane, but not in that available to neopentane, for outgassing temperatures between 88 and 110°. This is paralleled by changes in the affinity constant, C, for n- and isopentanes.

TABLE II

EFFECT OF OUTGASSING TEMPERATURE ON SURFACE OF SORBENT

Outgassing temp., °C.	n-Pentane Area, m.²/g.	C	Isopentane Area, m.²/g.	C	Neopentane Area, m.²/g.	C
20	172	60	155	21.4	112	14.8
70	170	58	153	16.8	105	14.9
88	170	39	154	18.3	104	13.6
110	114	18.0	115	12.6	98	13.1
124	109	9.6	110	10.1	97	10.4
130	109	10.5	111	11.5	92	13.5
260	100	11.6	107	9.7	95	11.8
360	95	11.1	103	8.2	93	9.9

The close relationship between the temperature coefficient of water loss, affinity constants C, surface areas and amounts sorbed at relative pressures of 0.1 is brought out in Fig. 3, where each of these quantities is shown in relation to outgassing temperature. It is only the low temperature stage of water loss which is coupled with marked changes in the other quantities. Similar behavior was also observed when the sorbates were N_2, O_2 and CO_2 (Part I[4]). Moreover, as shown in Fig. 4, the attapulgite recovered its selectivity if crystals initially degassed above 88° were exposed to saturated water vapor and then again degassed at a temperature below 88°. The extent of recovery was less the higher the initial outgassing temperature above 88°.

Thermodynamic Functions.—The differential thermodynamic functions ΔG, ΔH and ΔS for transfer of hydrocarbons from the liquid to the sorbed state were calculated as in Part I.[4] The relationships between these functions and the surface coverage on attapulgite crystals are shown in Fig. 5 for n-heptane and isoöctane, and in Fig. 6 for the isomeric pentanes. The sorbent was here outgassed below 88°.

---

(13) M. L. Corrin, THIS JOURNAL, 55, 612 (1951).

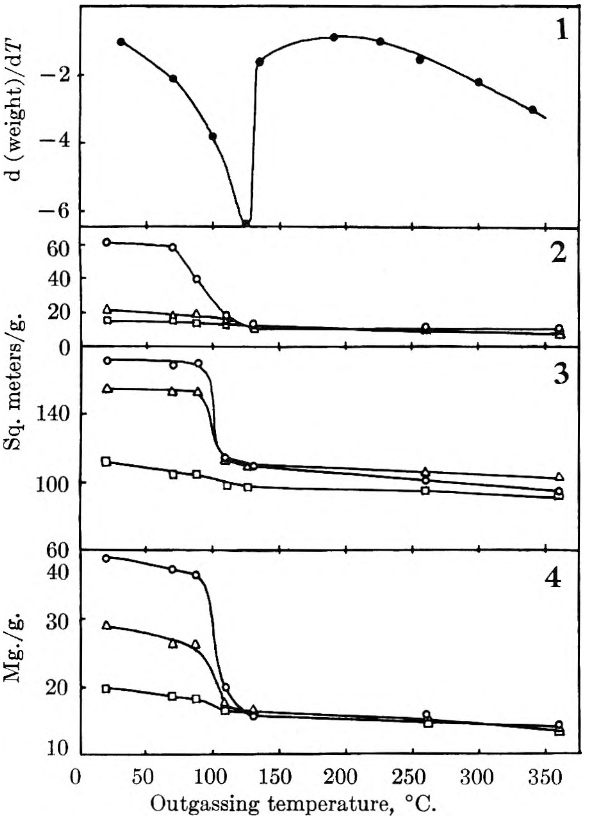

Fig. 3.—Correlation of various properties in pentane sorption with outgassing temperature: ⊙, n-C_5H_{12}; △, iso-C_5H_{12}; ⊡, neo-C_5H_{12}: 1, water loss from attapulgite; 2, C value; 3, surface area; 4, amount sorbed at relative pressure 0.1.

The free energy, heat and entropy changes on sorption are clearly much greater for n-heptane than for isoöctane. In particular the entropy decrease on transferring isoöctane from liquid to adsorbed film is very small, while the corresponding decrease for n-heptane is initially extremely large. This suggests that for n-heptane the configurations of the molecule on the surface may be very restricted. This will be the case if the n-heptane molecule closely fits its environment in the surface. Large initial heat, entropy and free energy changes are associated also with the uptake of n-pentane. On the other hand for iso- and neopentanes, like isoöctane, the three thermodynamic functions are initially smaller. The branched chain molecules studied have fewer possible configurations in liquid or vapor states than have their more flexible straight chain counterparts. If all molecules when sorbed are constrained to one configuration the entropy decrease for the n-paraffin will on this count exceed that for the branched chain species. However the constraint on sorption of branched chain molecules does not in fact seem very large, as shown for instance by the small entropy change for isoöctane. It seems therefore that the first n-paraffin molecules sorbed in the process lose a relatively greater fraction of their already more numerous gaseous and liquid phase configurations than do branched chain paraffins.

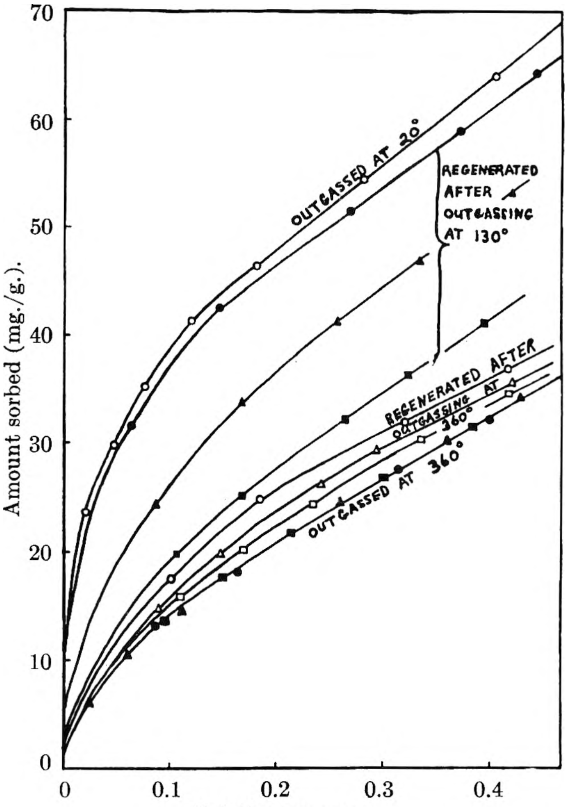

Fig. 4.—Regeneration of selectivity in sorption of pentanes at 20° by treatment of attapulgite outgassed at 130 and 360° with saturated water vapor at 20°. For comparison the isotherm of n-C_5H_{12} on a fresh sample outgassed at 20°, and isotherms of the three pentanes on a sample outgassed at 360°, are shown: ⊙, ●, n-pentane; △, ▲, isopentane; ⊡, ■, neopentane.

Discussion

The loss of selectivity when the crystals of attapulgite are outgassed above 88° is a process associated with decreasing v_m and C for n-pentane, but with little change in these quantities for neopentane, while isopentane behaves in an intermediate manner (Fig. 3). A reason for the higher energy and greater entropy decrease on sorption of n-paraffins as well as of the decrease in v_m and C may be sought in terms of the structure of the crystals. These according to Bradley's model[14] should have surface corrugations[4] of molecular dimensions, in which it may be that only n-paraffins may fit closely provided the crystals are degassed below 88°. Moreover, a very limited entry into the mouths of the intracrystalline channels may be possible for simple non-polar molecules and for n-paraffins thereby providing some additional energetically sorbing sites for these species, whereas more globular branched chain molecules cannot avail themselves of these sites. Such a process of entry would be limited to positions just at or very near the surface because of permanent adventitious cations,[3] arising from crystal defects and causing barriers in the channels. The entrance points to channels have then to become blocked to n-paraffins and the availability of corrugations also be impaired if outgassing is above 88°. This could result from a process of surface sintering and reaction, for example if some hydroxyl water were eliminated and caused

---

(14) W. F. Bradley, *Am. Mineralogist*, **25**, 405 (1940).

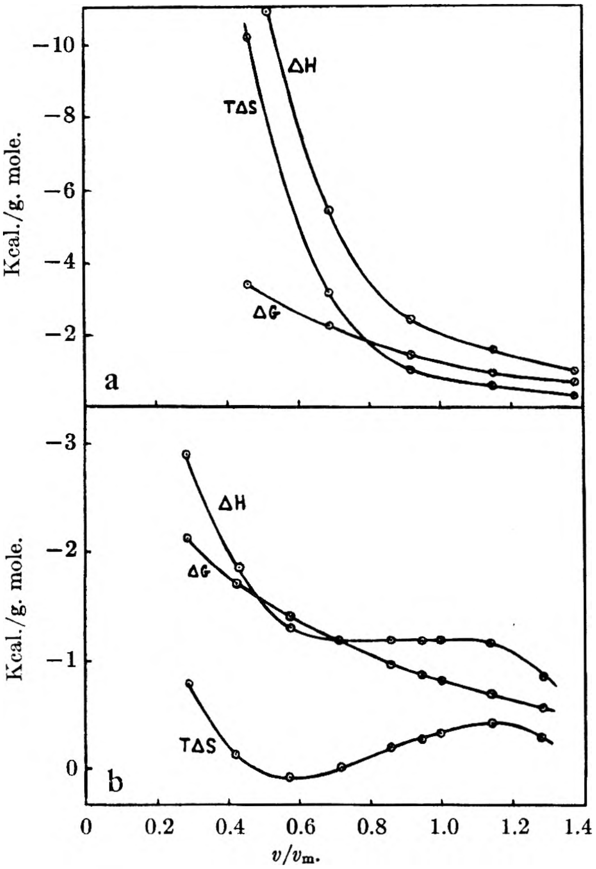

Fig. 5.—Some thermodynamic functions for (a) n-heptane and (b) isoöctane, calculated from isotherms at 50 and 65°.

Si–O–Si bonds to form across the narrow dimensions of the channels or corrugations (~3.7 Å. across). Nevertheless such a process must be partially reversed on treatment with water. Although objections can be raised to some aspects of the above view it seems to offer the best interpretation so far of Fig. 3 and of the thermodynamic data.

Selectivity shown by the layer lattice crystals of montmorillonite toward the n-pentane cannot be explained in similar terms. However it is to be expected that if flattened on to the basal surfaces of montmorillonite the center of gravity of n-pentane will be nearest and that of neopentane farthest from these surfaces. This means that n-pentane will tend to be sorbed with the greatest heat and decrease in entropy. The same order of selectivity among the pentanes has been observed for carbon[15] and for some ion-exchanged montmorillonites.[5] In the former case a similar explanation to that above has been offered. The difficulty which this view encounters as an interpretation also for the data obtained with attapulgite is the drop in this case in v_m and C for n-pentane on outgassing above 88°, while there is *no* appreciable change in v_m or C for neopentane, so that selectivity vanishes. According to arguments based only on the distance from the surface of molecular centers of gravity the selectivity would always remain.

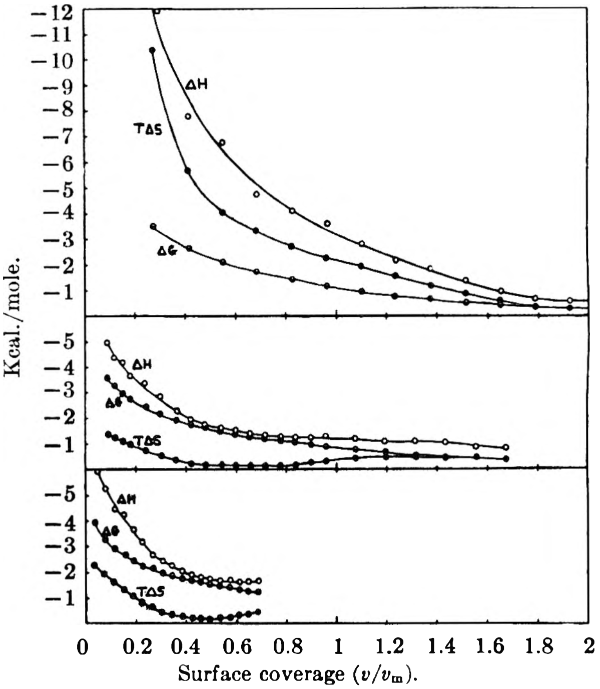

Fig. 6.—Thermodynamic functions for the sorption of the pentane isomers on attapulgite outgassed at 70°, calculated from sorption isotherms at 20 and 30°: top, n-C_5H_{12}; middle, iso-C_5H_{12}; bottom, neo-C_5H_{12}.

The order of selectivity in sepiolite (n-pentane $\simeq$ isopentane > neopentane) also cannot be related simply to distances of molecular centers of gravity from the sorbing surface, because n-pentane and isopentane are not differentiated by this sorbent. The possible structural similarity between attapulgite and sepiolite[4,3] may mean that an explanation in terms of surface corrugations must be sought also for sepiolite. It may be concluded that one general explanation of the influence of molecular structure upon selectivity toward isomeric paraffins is not possible for attapulgite, montmorillonite and sepiolite.

---

[15] R. A. Beebe, G. Kington, M. H. Polley and W. R. Smith, *J. Am. Chem. Soc.*, **72**, 40 (1950).

NOTES

POTENTIOMETRIC DETERMINATION OF FORMATION CONSTANTS OF ACETYLACETONATES BY A DISPLACEMENT REACTION

By Burl E. Bryant

School of Chemistry and Physics, The Pennsylvania State College, State College, Pa.

Received August 6, 1953

The formation constants of the copper, beryllium and uranyl acetylacetonates have been determined potentiometrically by a procedure involving the displacement of nickel ion from its complex. The constants for uranyl acetylacetonate determined by displacement of zinc ion were in excellent agreement with those determined by displacement of nickel ion. The values obtained for the copper and beryllium compounds agreed well with those determined by another method.

The work of Plumb, *et al.*,[1] on spectrophotometric determinations of the displacement series in metal complexes suggested that such displacements might be followed by other methods. The most direct method would be to observe the release of one metal ion from its complex upon addition of a second metal ion. In cases where a suitable electrode is available, the displacement could be followed readily. In the absence of such an electrode, the displacement can be followed by having present an excess of the chelating agent and considering the equilibria involving the chelating ion, the metal ions and hydrogen ion. Although the displacement of one metal ion by another is not pH dependent, in the presence of excess chelating agent the equilibrium involving hydrogen ion will be displaced by addition of a second metal ion. The displacement can then be followed indirectly with the glass electrode.

Since the system MCh$_x$–HCh constitutes a buffer system, it is possible to adjust, within limits, the pH at which the displacement is to be observed. The extensive hydrolysis of the uranyl ion in solutions of intermediate pH makes it necessary to study the equilibrium $UO_2Ch^+ \leftrightarrows UO_2^{++} + Ch^-$ in the low pH region. By the use of two different buffer systems, in which the concentrations of free Ch$^-$ can be calculated with reasonable accuracy, calculations of formation constants can be cross-checked. If the results are consistent, there is some assurance that hydrolysis effects have been minimized.

The idea was first checked by the use of systems for which constants were already known. In the experiment described, the chelating agent was acetylacetone, and copper ion was allowed to displace nickel from its complex.

The solvent used was 50% aqueous dioxane. To 100 ml. of this solvent was added *ca.* 1.2×10^{-3} mole of acetylacetone, 1×10^{-3} mole of tetramethylammonium hydroxide, and 4×10^{-4} mole of $Ni(NO_3)_2$. This solution was titrated with a standard solution of $Cu(NO_3)_2$.

The formation constants for the nickel complexes of acetylacetone were measured by the conventional methods. Found: $\log k_1 = 6.91$, $\log k_2 = 5.17$. Mellor and Maley[2] report $\log k_1 = 6.82$, $\log k_2 = 5.24$.

The acid dissociation constant for acetylacetone was found to be 2×10^{-10}. The concentration of un-ionized acetylacetone was assumed to be the total original concentration less the sum of the concentrations of $N(CH_3)_4^+$ and H^+. From the concentrations of H^+ and HCh, the expression for the acid dissociation constant can be solved to yield the concentration of free Ch$^-$. By difference, the total coördinated ion can then be calculated.

From the known concentration of total nickel ion, the calculated concentration of free Ch$^-$, and the two expressions for the formation constants of the nickel complexes, the total Ch$^-$ bound to nickel can be calculated. The difference between total Ch$^-$ bound to metal ion and Ch$^-$ bound to nickel ion is a measure of Ch$^-$ bound to copper ion. All the quantities necessary for the calculation of formation constants are then available.

Actual calculations were done by the method of Block and McIntyre.[3] Six calculations were made for the copper complex. The values determined were: $\log (\text{average } k_1) = 9.55$, $\log (\text{average } k_2) = 8.13$, $\log k_1k_2 = 17.68$. Calvin and Wilson[4] report $\log k_1k_2 = 17.4$.

Two determinations for the beryllium acetylacetonate were made by this method. The values found were: $\log k_1 = 9.16, 9.16$; $\log k_2 = 7.75, 7.74$. By conventional methods, the values found were: $\log k_1 = 9.06$, $\log k_2 = 7.62$.

No values have been reported in the literature for the formation constants of the uranyl complexes of acetylacetone. The values determined by the displacement of nickel were: $\log k_1 = 9.32$, $\log k_2 = 7.60$. Those determined by displacement of zinc were: $\log k_1 = 9.32$, $\log k_2 = 7.62$.

Acknowledgment.—This work was supported by the United States Atomic Energy Commission through Contract AT (30-1)-907.

---

[1] R. C. Plumb, A. E. Martell and F. C. Bersworth, This Journal, **54**, 1208 (1950).

[2] D. P. Mellor and L. Maley, *Nature*, **159**, 370 (1947).

[3] B. P. Block and G. H. McIntyre, Jr., *J. Am. Chem. Soc.*, **75**, 5667 (1953).

[4] M. Calvin and K. Wilson, *ibid.*, **67**, 2003 (1945).

EXTREME PRESSURES. I. A NEW PRESSURE–VOLUME RELATIONSHIP

By Leonard S. Levitt

Department of Chemistry, Stevens Institute of Technology, Hoboken, N. J.

Received November 13, 1953

Boyle's Law is a limiting law, in that it is applicable and theoretically sound only at the extreme low-pressure end of the pressure range. Its applicability is, in fact, like the volume, inversely proportional to the pressure. Only those empirical equations of the power series type like the Onnes equation, which involve at higher and higher pressures a larger and larger number of empirical constants (virial coefficients), adequately describe the pressure–volume relationship at the higher pressures. These equations, however, are unsatisfactory at high pressures not only from the mathematical and theoretical standpoint, but also from what might be called the aesthetic or philosophical standpoint. On the other hand, Boyle's Law is a satisfying, as well as a satisfactory, expression of the relationship at low pressure because it is simple, because it makes good sense, and because it works.

The purpose of this paper is to present a functional relationship between pressure and volume which is quite simple in form and is valid at both moderately and extremely high pressures. In fact this relationship, it will be seen, actually becomes more strictly applicable the higher the pressure, and in this sense it may be thought of as a limiting law at the upper end of the pressure range (to 100,000 kg./cm.^{2}). In addition, the author has discovered that the new relationship is valid not only for gases under high pressure, but also for a great variety of liquids and of solid elements and solid compounds under very high pressure. The view has been widespread[1,2] that the pressure–volume relationship, after passing through an intermediate anomalous phase, should, at extreme pressures, revert again to the simple Boyle's Law hyperbolic equation. It appears, however, that such is not the case.

The new limiting law, at constant temperature and high pressures, is given by the exponential equation

$$p = Ce^{B/v} \qquad (1)$$

in which B and C are constants characteristic of the particular substance. It should be emphasized that this expression has not been deduced, but is a simple and accurate statement of empirical fact at high pressure, just as Boyle's Law is for low pressure. According to this equation, a plot of log p *vs.* either $1/v$ or density should be a straight line. That such is the case is immediately apparent from the accompanying logarithmic plots (Figs. 1–6) for

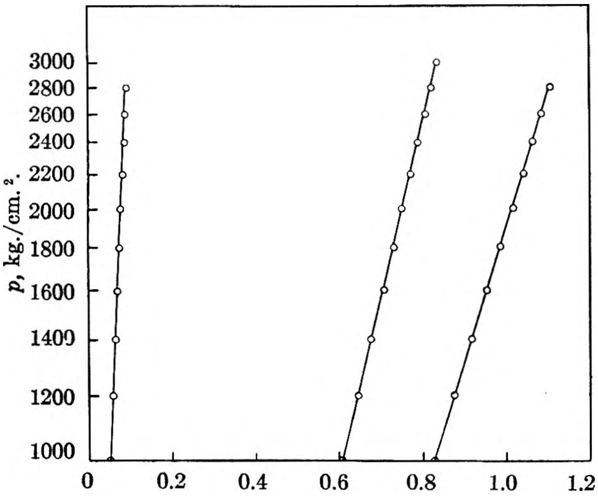

Fig. 1.—Compression of gases at 0°, left to right: H_2, N_2, O_2

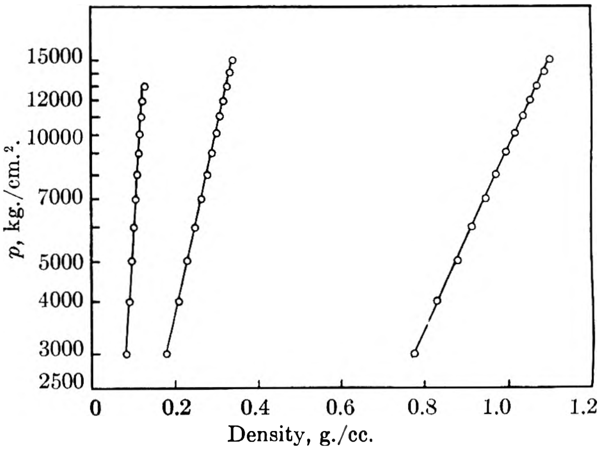

Fig. 2.—Compression of gases at 65°, left to right: H_2, He, N_2 (N_2 at 68°).

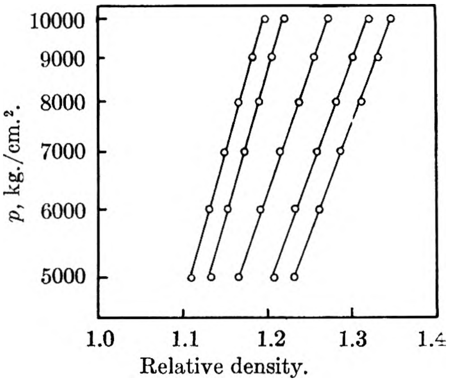

Fig. 3.—Compression of liquids, left to right: H_2O (95°), H_2O (50°), C_2H_5OH (80°), $(C_2H_5)_2O$ (80°), n-C_5H_{12} (95°).

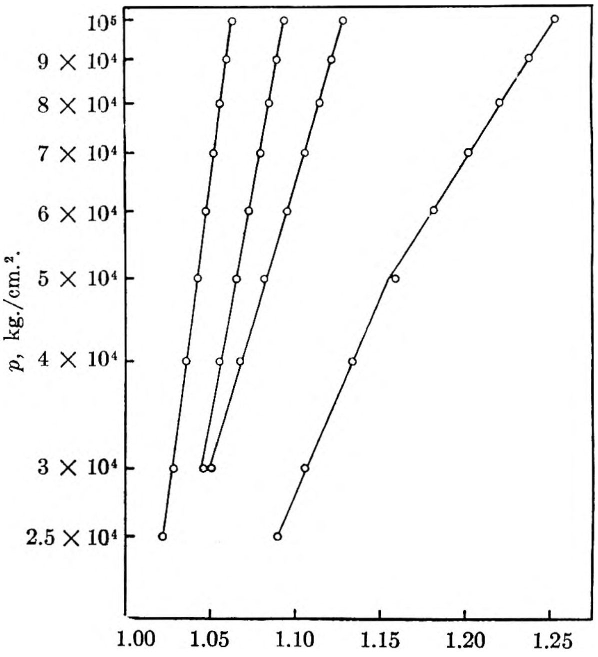

Fig. 4.—Compression of heavy metals, left to right: U, Mn, Th, La.

---

[1] P. W. Bridgman, "The Physics of High Pressure," G. Bell & Sons, London, 1949, pp. 177, 183.

[2] H. Jensen, *Z. Physik*, **111**, 373 (1938).

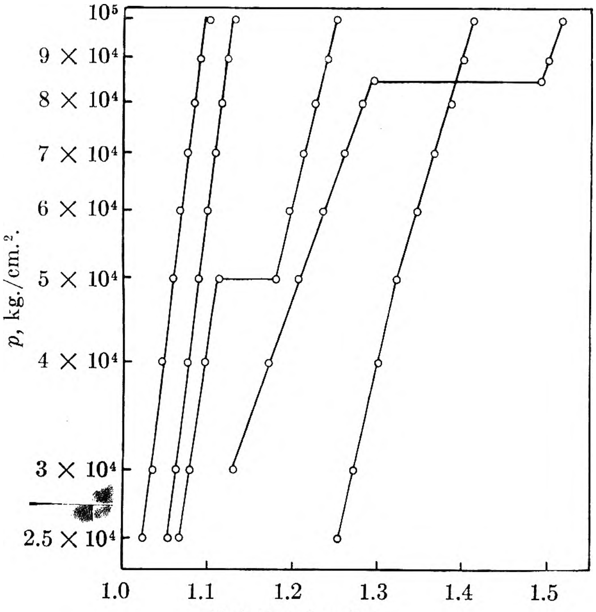

Fig. 5.—Compression of other solid elements, left to right (at bottom): Zr, C, black P, red P, Ce.

various gases[3,4] up to 15,000 kg./cm.², for various liquids[5] up to 12,000 kg./cm.², and for a wide variety of solids[6,7] up to 100,000 kg./cm.². (These were the highest pressure ranges for which the author was able to find data.)

It is interesting to note that the relationship becomes valid for gases at 1,000 kg./cm.² or lower, for liquids at about 5,000 kg./cm.² and for solids only above 25,000 kg./cm.².

In addition to showing such obvious and previously recognized polymorphic transitions (represented by abrupt discontinuities), such as occurs at 50,000 kg./cm.² with black phosphorus (Fig. 5) and with PbTe at 45,000 kg./cm.² (Fig. 6), some of these plots reveal rather sharp points of inflection never before brought to light. These do not appear to be gradual curvatures, but actually quite abrupt changes in slope. For example, La and Ce (Figs. 4, 5), as well as all the alkali metals, seem to undergo a change in compressibility at around 45,000 to 55,000 kg./cm.². In all cases the change is toward a more compressible form. On the conventional curvilinear plot of volume or compressibility *vs.* pressure, however, these changes cannot be detected.

If Eq. (1) be differentiated with respect to volume, one obtains

$$\frac{dp}{dv} = \frac{-BCe^{B/v}}{v^2} = \frac{-Bp}{v^2} \tag{2}$$

which may also be written

$$\frac{d \ln p}{dv} = \frac{-B}{v^2} \tag{2}$$

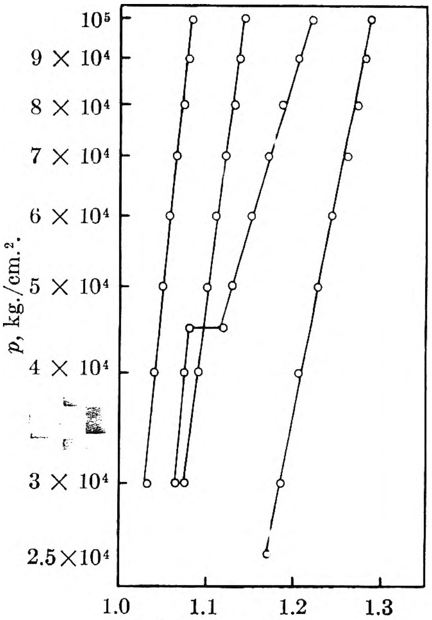

Fig. 6.—Compression of solid compounds, left to right (at bottom): ZnS, PbTe, PbS, HgSe.

This expression, on integration between the limits v_1 and v_2, becomes

$$\ln \frac{p_2}{p_1} = B\left(\frac{1}{v_2} - \frac{1}{v_1}\right) \tag{4}$$

Setting the density, ρ, equal to m/v, and converting to common logarithms, we may write

$$\log \frac{p_2}{p_1} = \frac{B}{2.3m}(\rho_2 - \rho_1) \tag{5}$$

By means of Eq. (5) densities at high pressures may be calculated, provided, of course, that the density at one pressure is known and the value of B (the slope of the plot of $\ln p$ *vs.* $1/v$) is known. The compressibility, α, is defined by the equation

$$\alpha = \frac{-(\partial v/\partial p)}{v} \tag{6}$$

An exact expression for the compressibility of any substance at high pressures may readily be obtained by inverting Eq. (2)

$$\frac{dv}{dp} = \frac{-v^2}{Bp} \tag{7}$$

and multiplying through by $-1/v$ to give

$$-\frac{1}{v}\left(\frac{dv}{dp}\right) = \alpha = \frac{v}{Bp} \tag{8}$$

It is evident from Eq. (8) that the compressibility at high pressure varies directly with the volume and inversely with the pressure, in accord with all experimental experience. It is to be noted that the greater the value of the constant B for a given substance, the smaller is its compressibility, a fact which is obvious, of course, from the logarithmic plots (Figs. 1–6).

Equation (8) can be differentiated with respect to p to give the decrease in compressibility with increasing pressure. Thus

$$-\frac{d\alpha}{dp} = \frac{v}{Bp^2} + \left(\frac{v}{Bp}\right)^2 = \frac{v}{Bp^2}\left(1 + \frac{v}{B}\right) \tag{9}$$

---

[3] "International Critical Tables," McGraw-Hill Book Co., Inc., New York, N. Y., pp. 5, 8, 17.

[4] P. W. Bridgman, *Proc. Am. Acad.*, **59**, 173 (1924).

[5] P. W. Bridgman, "The Physics of High Pressure," G. Bell and Sons, London, 1949, pp. 128–130.

[6] *Ibid.*, pp. 149–188.

[7] P. W. Bridgman, *Proc. Am. Acad.*, **76**, 4, 63, 66 (1945–1948).

Since $v/Bp = \alpha$, it is seen that Eq. (9) is equivalent to

$$-\frac{d\alpha}{dp} = \frac{\alpha}{p}(1 + \alpha p) = \frac{\alpha}{p}\left(1 + \frac{v}{B}\right) \quad (10)$$

which may also be expressed in the form

$$-\frac{1}{\alpha}\left(\frac{d\alpha}{dp}\right) = \frac{-d \ln \alpha}{dp} = \frac{1}{p} + \alpha = \frac{1}{p}\left(1 + \frac{v}{B}\right) \quad (11)$$

or

$$-\frac{d \ln \alpha}{d \ln p} = 1 + \alpha p = 1 + \frac{v}{B} \quad (12)$$

Finally, one obtains the following expression for the change of compressibility with volume at extreme pressures by differentiating Eq. (8) with respect to v

$$\frac{d\alpha}{dv} = \frac{1}{p}\left(\frac{1}{v} + \frac{1}{B}\right) = \frac{1}{pv}\left(1 + \frac{v}{B}\right) \quad (13)$$

SOLUBILITY OF CUPRIC STEARATE IN WATER AND BENZENE AT 25°[1]

By Alan Dobry

Westinghouse Research Laboratories, East Pittsburgh, Pa.

Received March 30, 1954

In the course of some thermodynamic calculations, values for the solubility of cupric stearate in water and benzene were required. Daniel[2] has published a value of 1.4×10^{-4} g./ml. for the solubility of cupric stearate in benzene at 23°, but this value seemed much too large. Determination of these solubilities at 25° gave values of $7 \pm 2 \times 10^{-9}$ g./100 g. of water and $8 \pm 2 \times 10^{-7}$ g./100 g. of benzene.

Experimental

Cupric stearate was prepared by treating sodium stearate (made from stoichiometric amounts of reagent grade sodium hydroxide and reagent grade stearic acid) in water with the stoichiometric amount of reagent grade $CuSO_4 \cdot 5H_2O$. The precipitated soap was recrystallized twice from benzene and dried.

Anal. Calcd. for $C_{36}H_{70}O_4Cu$: C, 68.68; H, 11.19; Cu, 10.08. Found: C, 68.62, 68.68; H, 11.42, 11.42; Cu, 9.81, 9.82.

Mixtures of excess copper stearate with the respective solvents (reagent grade benzene or doubly distilled water) were boiled in flasks with ground glass joints. The flasks were tightly stoppered and shaken, along with similar mixtures which had not been boiled, for several days at room temperature. The flasks were then kept overnight at 25° and the mixtures filtered through S. and S. No. 507 filter paper. The benzene filtrates were extracted with 10% H_2SO_4 and the acid solutions analyzed for copper; the aqueous solutions were analyzed directly. Analysis was carried out by a colorimetric method employing sodium diethyl dithiocarbamate.[3]

---

[1] This work is taken from a paper presented before the 9th Meeting of the American Society of Lubrication Engineers, April, 1954, and is Scientific Paper No. 1812 from the Westinghouse Research Laboratories.

[2] S. G. Daniel, *Trans. Faraday Soc.*, **47**, 1351 (1951).

[3] E. B. Sandell, "Colorimetric Determination of Traces of Metals," 2nd ed., Interscience Publishers, Inc., New York, N. Y., 1954, p. 309.

COLLECTIVE NUMERICAL PATENT INDEX

to

Volumes 31–40 of CHEMICAL ABSTRACTS

- Contains more than 143,000 entries, classified by countries in numerical order.
- Index references give volume, page and location of patent abstract in CHEMICAL ABSTRACTS.
- Classification by patent number is an enormous timesaver.
- Cloth bound, 182 pages, 7½″ x 10″ overall, 8 columns of listings per page covering all patents abstracted in CHEMICAL ABSTRACTS from 1937–46, inclusive.

PRICE $6.50 POSTPAID

Send orders and inquiries to:
Special Publications Dept.

American Chemical Society
1155 Sixteenth St., N.W., Washington 6, D. C.

STRUCTURAL CHEMISTRY OF INORGANIC COMPOUNDS

By Walter Huckel

A systematic treatise on inorganic chemistry written by one of the foremost authorities. It presents a system of inorganic chemistry based on the structure and constitution of compounds and not on the conventional classification of elements. It succeeds in giving an integrated and consistent picture of the "inorganic" state of matter, bringing into focus the similarities and analogies of compounds rather than their individualities. It is valuable as an advanced text and is important for everyone engaged in synthetic or analytical work in inorganic chemistry, crystallography and mineralogy.

The specialist will consult the excellent index on his own subjects, and see how many fresh ideas emerge when a rich collection of diverse but selected data is viewed from an original angle. "It will undoubtedly become a valuable reference book, and all inorganic chemists should own a copy." *Chemistry & Industry.* "This work represents a most important contribution to chemical literature." *J. of the Royal Institute of Chemistry*

Vol. I. 438 pp., 50 illus. $10.00. Vol. II, 656 pp., 124 illus., $13.50.

Available on 10 day free approval

ELSEVIER PRESS INC.
1603 Oakdale Street Houston 4, Texas

CHEMICAL NOMENCLATURE

Number eight of the Advances in Chemistry Series
Edited by the staff of *Industrial and Engineering Chemistry*

A collection of papers comprising the Symposium on Chemical Nomenclature, presented before the Division of Chemical Literature at the 120th meeting—Diamond Jubilee—of the American Chemical Society, New York, N. Y., September 1951

Paper bound $2.50

Published August 15, 1953, by
AMERICAN CHEMICAL SOCIETY
1155 Sixteenth Street, N.W.
Washington, D. C.

CONTENTS

Introduction 1
Letter of Greeting 3
Some General Principles of Inorganic Chemical Nomenclature 5
Nomenclature of Coordination Compounds and Its Relation to General Inorganic Nomenclature 9
Problems of an International Chemical Nomenclature 38
Chemical Nomenclature in Britain Today 49
Chemical Nomenclature in the United States 55
Basic Features of Nomenclature in Organic Chemistry 65
Organic Chemical Nomenclature, Past, Present, and Future 75
Work of Commission on Nomenclature of Biological Chemistry 83
Nomenclature in Industry 95
Development of Chemical Symbols and Their Relation to Nomenclature 99
The Role of Terminology in Indexing, Classifying, and Coding 106

COLLOID SCIENCE

By H. R. Kruyt

The line of thought underlying this book is that this branch of science has to do with large kinetic units. Emphasis is placed on the harmony which exists between classical colloid science and the domain of macromolecular systems which has developed so rapidly in the last 20 years.

The subjects treated are classified according to general phenomena and not according to substances or systems. Examples are used only to illustrate the phenomena involved. Detailed treatment and the many experimental data that are presented bring to the English-speaking reader a vast sum of knowledge hitherto found largely in the German monographs. This book is a guide to research in the colloid science and all investigators will find it indispensible.

Vol. I, Irreversible Systems, 389 pp., 222 illus., $11.00.
Vol. II, Reversible Systems, 754 pp., 475 illus., $11.50.

Available on 10 day free approva

ELSEVIER PRESS INC.
1603 Oakdale Street **Houston 4, Texas**

No. 6 of the

ADVANCES IN
CHEMISTRY
SERIES

AZEOTROPIC
DATA

- 247-page table of binary systems
- 41-page formula index
- 17-page table of ternary systems
- 107 charts

329 pages . . . . cloth bound $4.00

American Chemical Society
1155 Sixteenth St., N. W. Washington 6, D. C.

New Reprints

CHEMICAL ABSTRACTS

Volume 4, 1910, paper bound in 5 volumes, $75.00
Volume 5, 1911, paper bound in 5 volumes, $75.00

Also Available:

AMERICAN CHEMICAL SOCIETY: JOURNAL

Volumes 1–25
(Proceedings 2 vols., Journal Vols. 1–25, 1879–1903;
General Index to vols. 1–20)
Cloth bound in 37 volumes, $600.00
Both reprints have been undertaken with the permission
of the original publishers.

Address inquiries and orders to

JOHNSON REPRINT CORPORATION
125 East 23rd Street, New York 10, N. Y.